U.PORTO

Mestrado em Controlo da Qualidade

Fármacos e plantas medicinais

Design and development of potential CBD nanodelivery systems for the treatment of anxiety

Sara Raquel Marques Pinto

M

2026

U.PORTO

FACULDADE DE FARMÁCIA
UNIVERSIDADE DO PORTO

mesosystem®

Design and development of potential CBD nanodelivery systems for the treatment of anxiety

Sara Raquel Marques Pinto

Dissertação do 2º Ciclo de Estudos Conducente ao Grau de Mestre em Controlo da Qualidade

Trabalho realizado sob a orientação de: Doutor Javier Fidalgo, Doutor Hugo Almeida e Professora Doutora Beatriz Oliveira

Julho de 2026

DECLARAÇÃO DE REPRODUÇÃO

É AUTORIZADA A REPRODUÇÃO INTEGRAL DESTA DISSERTAÇÂO APENAS PARA EFEITOS DE INVESTIGAÇÃO, MEDIANTE DECLARAÇÃO ESCRITA DO INTERESSADO, QUE A TAL SE COMPROMETE.

ACKNOWLEDGMENTS

I would like to express my sincere gratitude to my supervisors, Dr. Hugo Almeida, Professor Maria Beatriz Oliveira and Dr. Javier Fidalgo, for their guidance, support and invaluable advice throughout this project. Their expertise and encouragement were essential to the completion of this dissertation. I would also like to thank Dr. Ana Casas for the opportunity to develop my project at Mesosystem.

I am grateful to the team at Mesosystem for all their help and encouragement throughout this internship and for making it such a positive experience. In particular, I would like to thank Rita, Tiago, Juliana, both Dianas and Fátima for all their assistance and support during this time.

I would also like to express my gratitude to Asal for her assistance in obtaining the TEM images and to Nelson for his help with the MTT assays.

I would especially like to thank my parents for their unwavering love and kindness throughout all these years, for making my dream of pursuing a master's degree possible and for being my greatest supporters.

To my family, thank you for always being present during life's most important moments.

To Bruna and Josefina, thank you for your unwavering friendship and support, which I deeply cherish.

To, Barbara, Diana and Margarida, I am truly grateful for your friendship throughout this journey, which made the experience so enjoyable.

To Louis, thank you for always being by my side, for your constant encouragement, and for constantly reminding me that I can achieve anything I set my mind to. Thank you for believing in me.

ABSTRACT

This dissertation focused on the development and characterisation of cannabidiol (CBD)-loaded nanocarriers, with the aim of overcoming the limitations such as poor aqueous solubility, low oral bioavailability, and extensive first-pass metabolism. Therefore, this work aimed to develop and characterize nanotechnology-based delivery systems, namely polymeric nanomicelles and self-nanoemulsifying drug delivery systems (SNEDDS), to improve CBD delivery.

Different excipients, including Labrafil® M 1944 CS, Labrasol®, Labrafac™ Lipophile WL 1349, Capryol® 90, Transcutol® HP, sodium deoxycholate and sodium alginate, were evaluated through solubility, miscibility and formulation studies. The physicochemical properties of the formulations were evaluated by Dynamic Light Scattering (DLS), while Transmission Electron Microscopy (TEM) was used to assess particle morphology. Encapsulation efficiency was determined, and *in vitro* cytotoxicity studies were performed in Caco-2 and SH-SY5Y cell lines using the MTT assay. Accelerated stability studies at 40 ºC were also carried out for two formulations.

The developed formulations exhibited particle sizes ranging from approximately 17 to 55 nm, moderate PDI values (around 0.250), and zeta potential values between approximately -16 and +2 mV depending on formulation composition and dispersion medium. Labrasol® - based formulations generally produced smaller particles than their Labrafil® counterparts. TEM analysis confirmed the formation of predominantly spherical nanostructures with good agreement with DLS measurements. Encapsulation efficiencies above 98% were achieved for SNEDDS and selected polymeric nanomicelles, while *in vitro* studies demonstrated good biocompatibility at lower concentrations, particularly in SH-SY5Y cells.

Overall, the developed nanoformulations showed suitable physicochemical characteristics, high encapsulation efficiencies and acceptable *in vitro* biocompatibility within the experimental conditions evaluated. Although these findings provide preliminary evidence supporting the use of polymeric nanomicelles and SNEDDS as potential carriers for CBD, further studies are required to improve the robustness of the results and to better assess the stability, reproducibility and biological performance of these systems.

Keywords: Cannabidiol, nanoformulations, dynamic light scattering, nanotechnology, physicochemical properties.

RESUMO

Esta dissertação focou-se no desenvolvimento e caracterização de nanotransportadores carregados com canabidiol (CBD), com o objetivo de superar limitações como a sua baixa solubilidade, reduzida biodisponibilidade oral e metabolismo extensivo de primeira passagem. Este trabalho teve como objetivo desenvolver e caracterizar sistemas de libertação, nomeadamente nanomicelas poliméricas e sistemas auto-nanoemulsionantes de libertação de fármacos (SNEDDS), para melhorar a libertação de CBD.

Diferentes excipientes, incluindo Labrafil® M 1944 CS, Labrasol®, Labrafac™ Lipophile WL 1349, Capryol® 90, Transcutol® HP, desoxicolato de sódio e alginato de sódio, foram avaliados através de estudos de solubilidade, miscibilidade e formulação. As propriedades físico-químicas das formulações foram avaliadas por Espalhamento Dinâmico de Luz (DLS), enquanto a Microscopia Eletrónica de Transmissão (TEM) foi utilizada para determinar a morfologia das partículas. Foi determinada a eficiência de encapsulamento e realizados estudos de citotoxicidade *in vitro* nas linhas celulares Caco-2 e SH-SY5Y utilizando o ensaio de MTT. Foram também efetuados estudos de estabilidade acelerada a 40 ºC.

As formulações desenvolvidas apresentaram partículas com tamanhos entre aproximadamente 17 e 55 nm, valores de PDI moderados (~0.250) e potenciais zeta compreendidos entre aproximadamente -16 e + 2 mV, dependendo da composição da formulação e do meio de dispersão. As formulações baseadas em Labrasol® produziram, geralmente, partículas de tamanhos menores do que as suas homólogas com Labrafil®. A análise por TEM confirmou a formação de nanoestruturas predominantemente esféricas, em concordância com as medições de DLS. Foram alcançadas eficiências de encapsulamento superiores a 98% para os SNEDDS e para uma formulação de nanomicelas poliméricas, enquanto os estudos *in vitro* demonstraram uma boa biocompatibilidade em concentrações mais baixas, particularmente nas células SH-SY5Y.

Globalmente, as nanoformulações apresentaram características físico-químicas adequadas, elevadas eficiências de encapsulamento e uma biocompatibilidade *in vitro* aceitável dentro das condições experimentais avaliadas. Apesar dos resultados obtidos, são necessários estudos adicionais para melhorar a robustez dos resultados e para avaliar melhor a estabilidade, reprodutibilidade e desempenho biológico destes sistemas.

Palavras-chave: canabidiol, nanoformulações, espalhamento de luz dinâmico, nanotecnologia, propriedades físico-químicas.

INDEX

LIST OF FIGURES

LIST OF TABLES

LIST OF EQUATIONS

LIST OF ABBREVIATIONS AND SYMBOLS

2-AG	2-Arachidonoylglycerol
5-HT1A	5-Hydroxytryptamine (Serotonin) Receptor 1A
ACM	Autorização de colocação no mercado
AEA	Anandamide
ALT	Alanine aminotransferase
API	Active pharmaceutical ingredient
AST	Aspartate aminotransferase
AUC	Area under the curve
BCS	Biopharmaceutical Classification System
Ca^{2+}	Calcium ion
Caco-2	Human colorectal adenocarcinoma cell line
CBCA	Cannabichromenic acid
CBC	Cannabichromene
CBD	Cannabidiol
CBDA	Cannabidiolic acid
CBGA	Cannabigerolic acid
CBG	Cannabigerol
CBN	Cannabinol
CBR1	Cannabinoid receptor type 1
CBR2	Cannabinoid receptor type 2
CBT	Cognitive behavioural therapy
CHMP	Committee for Medicinal Products for Human Use
CMC	Critical micellar concentration
Cmax	Maximum plasma concentration
Cu	Copper
CYP	Cytochrome P450 enzyme family
CYP2C9	Cytochrome P450 2C9
CYP2D6	Cytochrome P450 2D6
CYP3A4	Cytochrome P450 3A4
D	Translational diffusion coefficient
Da	Dalton

DEGEE	Diethylene glycol monoethyl ether
d_H	Hydrodynamic diameter
DLS	Dynamic light scattering
DMEM	Dulbecco's Modified Eagle's Medium
DMSO	Dimethyl sulfoxide
ECS	Endocannabinoid system
EE (%)	Encapsulation efficiency
ELS	Electrophoretic light scattering
EMA	European Medicines Agency
EP	European Pharmacopoeia
EPR	Enhanced permeability and retention
FDA	Food and Drug Administration
GAD	Generalised anxiety disorder
GGT	Gamma-glutamyl transferase
GI	Gastrointestinal
g	Gram
g/L	Grams per litre
GRAS	Generally recognised as safe
h	Hour
HCl	Hydrochloric acid
HLB	Hydrophilic-lipophilic balance
LC_{50}	Median lethal concentration
INFARMED	Portuguese National Authority of Medicines and Health Products
k_B	Boltzmann constant
kg	Kilogram
kV	Kilovolt
LCTs	Long-chain triglycerides
LFCS	Lipid formulation classification system
log P	Octanol/water partition coefficient
MCTs	Medium-chain triglycerides
mL	Millilitre
mM	Millimolar
mg	Milligram
mg/kg	Milligrams per kilogram

mg/kg/day	Milligrams per kilogram per day
mg/L	Milligrams per litre
min	Minute
MTT	3-(4,5-Dimethylthiazol-2-yl)-2,5-diphenyl-2H-tetrazolium bromide
mV	Millivolt
µg/mL	Micrograms per millilitre
µL	Microlitre
µM	Micromolar
n	Number of replicates
NaDC	Sodium deoxycholate
NAD(P)H	Reduced nicotinamide adenine dinucleotide (phosphate)
nm	Nanometre
OCD	Obsessive-compulsive disorder
O/W	Oil-in-water
PB	Phosphate buffer
PDI	Polydispersity index
PEG	Polyethylene glycol
pH	Hydrogen potential
pKa	Acid dissociation constant
PN	Polymeric nanomicelles
PPARγ	Peroxisome proliferator-activated receptor gamma
PTSD	Post-traumatic stress disorder
R^2	Coefficient of determination
s	Second
SA	Sodium alginate
SAD	Social anxiety disorder
SEDDS	Self-emulsifying drug delivery systems
SH-SY5Y	Human neuroblastoma cell line
SMEDDS	Self-microemulsifying drug delivery systems
SNEDDS	Self-nanoemulsifying drug delivery systems
T	Transmittance
TEM	Transmission electron microscopy
THC	Δ^9-Tetrahydrocannabinol
THCA	Tetrahydrocannabinolic acid

Tmax	Time to maximum plasma concentration
TMS	Transcranial magnetic stimulation
TPGS	D-α-Tocopheryl polyethylene glycol 1000 succinate (Vitamin E TPGS)
TRPV1	Transient receptor potential vanilloid 1
USP	United States Pharmacopeia
USP–NF	United States Pharmacopeia–National Formulary
UV	Ultraviolet
w/v	Weight/volume percentage
w/w	Weight/weight percentage

1. INTRODUCTION

1.1. Anxiety and its disorders

Anxiety is an emotional state associated with the anticipation of future adversity, distinguished from fear by its prolonged duration and focus on non-specific threats. It is characterized by a combination of psychological apprehension and physiological strain, typically manifesting through accelerated heart rate and physical tension as the organism prepares for an upcoming threat (1).

Anxiety comprises a group of mental health disorders characterized by excessive fear, nervousness, worry and apprehension, which can significantly impair a person's general well-being. When anxiety becomes frequent, interferes with daily functioning, persists after the situation is over or it is out of proportion to a situation, it can indicate an anxiety disorder (2). The main types of anxiety disorders, summarized in Table 1, include generalized anxiety disorder (GAD), panic disorder, agoraphobia, specific phobia, social anxiety disorder (SAD), separation anxiety disorder, and selective mutism (3). Post-traumatic stress disorder (PTSD), although often classified separately as a trauma-related disorder, shares overlapping features with anxiety disorders and is frequently considered in this context (4). The referred disorders are the conditions for which CBD-related research is most prevalent. GAD is characterized by excessive and uncontrollable worry across multiple life domains, such as academic or occupational performance, lasting for months or years (5). Panic disorder involves recurrent, unexpected panic attacks accompanied by persistent concern about future attacks or maladaptive avoidance behaviours, persistent for at least 1 month (3). Agoraphobia is characterized by fear of situations such as crowds or public transport where escape might be difficult. Specific phobia involves intense fear of circumscribed objects like animals or heights (6). SAD involves a fear or avoidance of social interactions where an individual might be the focus of attention or scrutiny by others, patients often fear negative judgment, embarrassment or rejection (7). Separation anxiety disorder consists in the inappropriate fear regarding the loss of attachment figures. Selective mutism is defined as a consistent failure to speak in specific social settings despite being able to speak in others (3). PTSD develops following exposure to a traumatic event, and it's distinguished by symptoms such as intrusive memories, avoidance, negative alterations in mood and cognition; and panic attacks or distress triggered by reminders of the trauma (8).

Table 1. Classification of Anxiety Disorders and Brief Definitions.

Disorders	Definitions	Key Symptoms	Ref
GAD	Entail excessive and persistent worry about different periods of life, which can be challenging to control.	Restlessness, sleep disturbances, irritability, easily fatigued.	(3,5)
Panic Disorder	Known for sudden and intense moments of fear and terror, designated panic attacks.	Chest pains, shortness of breath, worry about future attacks, sweating.	(3)
Agoraphobia	Fear of being in situations from which it might be hard to escape or get help in case of a panic attack or other unwanted situations.	Fear/avoidance of public transport, open spaces or being outside alone.	(6)
Specific Phobia	Involves irrational and intense fear of specific situations or objects.	Intense anxiety and active avoidance of triggers such as animals, blood, or enclosed places.	(6)
SAD	Persistent fear or anxiety in social situations where there is a potential for scrutiny by others.	Trembling, fear of rejection, and avoidance of speaking or eating in front of others.	(7)
Separation anxiety disorder	Excessive fear regarding separation from attachment figures.	Nightmares, physical symptoms of distress, and reluctance to leave home.	(3)
Selective mutism	Consistent failure to speak in specific social settings.	Failure to speak where speech is expected, persisting for at least one month.	(3)
PTSD	It presents itself after going through a traumatic event and frequently comorbid with anxiety.	Flashbacks, nightmares, panic attacks associated with exposure to traumatic reminders.	(8)

GAD, Generalized Anxiety Disorder; **SAD**, Social Anxiety Disorder; **PTSD**, Post-Traumatic Stress Disorder.

In addition to the anxiety disorders described above, several other clinically recognized conditions are relevant but currently lack sufficient research regarding the therapeutic potential of CBD. These include obsessive-compulsive disorder (OCD) and related disorders, acute stress disorder, adjustment disorder with anxiety, substance/medication-induced anxiety disorder, anxiety disorder due to another medical condition and unspecified anxiety disorder.

In 2019, an estimated 301 million people around the world were affected by anxiety disorders. However, current treatments for these situations are often associated with limited response rates, residual symptoms, and adverse effects, indicating an unmet clinical need (9).

1.1.1. Current therapeutic approaches

Current approaches to managing anxiety disorders involve a variety of psychological and pharmacological interventions, reflecting the multifaceted nature of these conditions. Cognitive behavioural therapy (CBT) and pharmacotherapy are regarded as the primary therapeutic option for anxiety disorders, with emerging alternatives gaining traction. CBT employs strategies like exposure therapy to reduce symptoms (10). Pharmacological options include antidepressants, most notably selective serotonin reuptake inhibitors and serotonin-norepinephrine reuptake inhibitors, which are widely prescribed and have demonstrated efficacy in managing anxiety disorders (10,11). Benzodiazepines can also provide symptom relief, but their side effects and limitations, have encouraged a search for alternative methods (10). Among these, approaches such as transcranial magnetic stimulation (TMS) and mindfulness practices are being explored for their potential to expand therapeutic options beyond traditional therapies (12). Nonetheless, significant barriers, including stigma and limited access to care, continue to restrict the effectiveness and accessibility of these treatment strategies in broader populations.

1.2. Cannabidiol (CBD)

1.2.1. The endocannabinoid system and anxiety regulation

The endocannabinoid system (ECS) is a widespread physiological signalling network composed of cannabinoid receptors, endogenous lipid-based ligands called endocannabinoids, and the enzymes responsible for their synthesis and degradation (13). The primary cannabinoid receptors include cannabinoid receptor 1 (CBR1) and cannabinoid receptor 2 (CBR2), which interact with both endogenous ligands as well as plant-derived cannabinoids such as THC. The CBR1 is mainly located in the brain and central nervous system, whereas the CBR2 are predominantly expressed in the immune system and peripheral tissues (14). Endocannabinoids such as anandamide (AEA) and 2-arachidonoylglycerol (2-AG) are synthesized and degraded by specific enzymatic systems. The ECS acts as a homeostatic regulator by producing endocannabinoids on demand, allowing them to act locally at cannabinoid receptors to modulate neuronal and immune activity. Through this signalling, the ECS contributes to the regulation of synaptic

transmission, stress responses, emotional processing, and several other physiological functions (13). Different classes of phytochemicals can interact with the ECS. Plant-derived cannabinoids such as Δ9-tetrahydrocannabinol (THC) and CBD are the most well-known, but other phytocannabinoids, including cannabigerol (CBG), cannabichromene (CBC) and cannabinol (CBN), can also influence ECS signalling. In addition, certain terpenes and flavonoids found in Cannabis have also been suggested to interact with cannabinoid signalling pathways, although their precise mechanisms remain under investigation (14).

The ECS has been implicated in the regulation of stress and anxiety-related processes due to its role in modulating neural and neuroendocrine signalling pathways associated with stress responses. Compounds such as CBD, and in some cases low doses of THC, have been investigated for their potential anxiolytic effects. However, current clinical evidence remains inconsistent. The therapeutic use of cannabinoids in anxiety disorders is limited by mixed findings in human studies, such as the psychoactive and the dose-dependent anxiogenic effects of THC, as well as the lack of approved cannabinoid-based treatments for anxiety disorders (15).

1.2.2. Cannabinoids and phytochemicals

Cannabis sativa L. (Cannabaceae) contains a chemically diverse assortment of phytochemicals, most notably cannabinoids. These are produced predominantly in the glandular trichomes of *Cannabis sativa*. The predominant cannabinoids in most chemovars are THC and CBD, which are typically present in the plant mainly as their acidic precursors, tetrahydrocannabinolic acid (THCA) and cannabidiolic acid (CBDA). The biochemical pathway begins with the central precursor, cannabigerolic acid (CBGA), being converted into THCA, CBDA, and cannabichromenic acid (CBCA) by the key oxidocyclase enzymes-THCA synthase, CBDA synthase, and CBCA synthase, respectively (16). Upon exposure to heat, light or prolonged storage, these acidic forms undergo non-enzymatic decarboxylation, being transformed into their corresponding neutral cannabinoids: THC, CBD and CBC, respectively (Figure 1) (16).

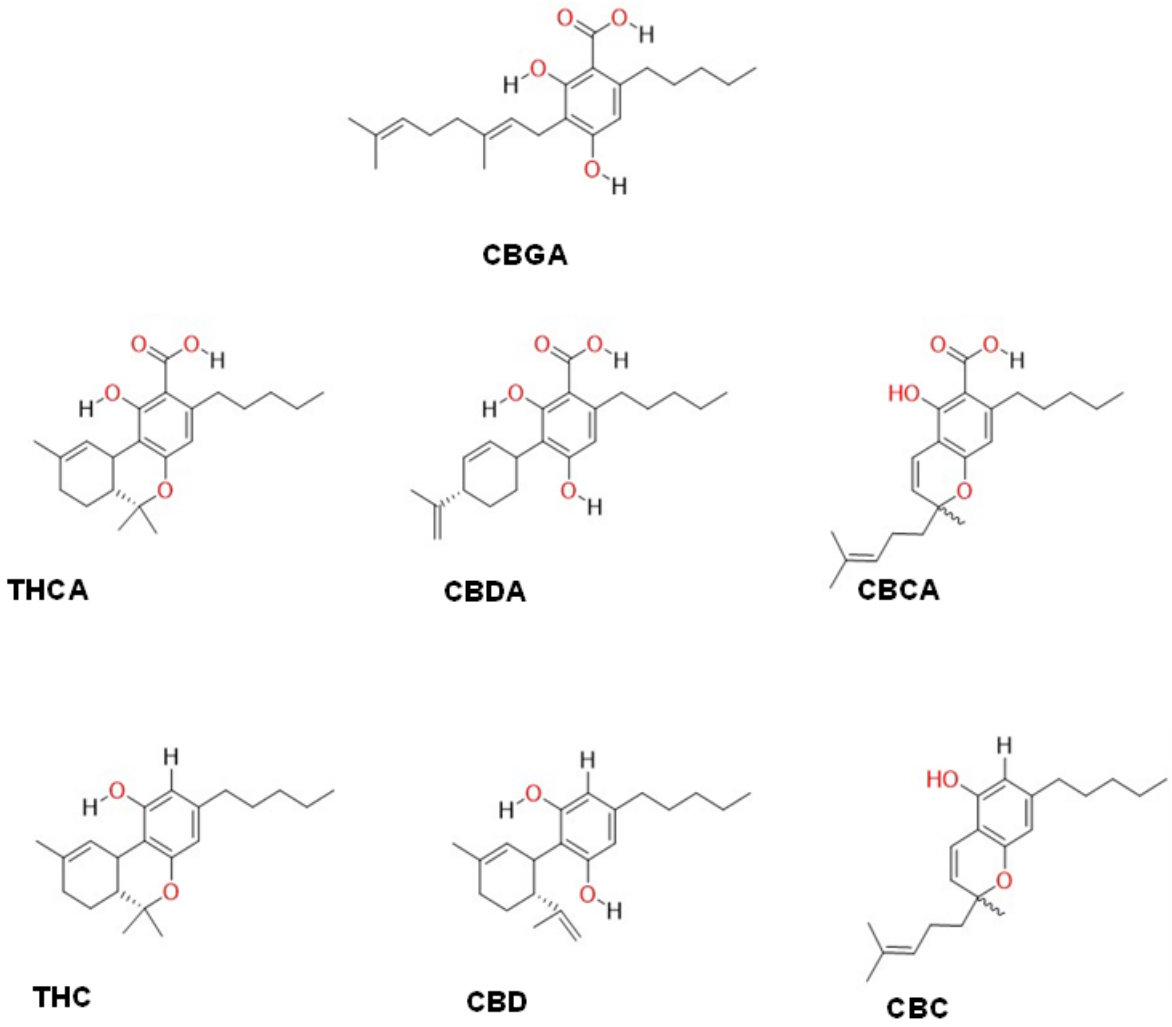

Figure 1. Conversion of CBGA to THCA, CBDA and CBCA, and their subsequent decarboxylation (CO2 release) to THC, CBD and CBC, respectively. **CBGA**, cannabigerolic acid; **THCA**, tetrahydrocannabinolic acid; **CBDA**, cannabidiolic acid; **CBCA**, cannabichromenic acid; **THC**, tetrahydrocannabinol**; CBD,** cannabidiol**; CBC,** cannabichromene**.**

This mechanism explains why the Cannabis plant contains predominantly acidic cannabinoids in their raw state. Despite sharing the same molecular formula ($C_{21}H_{30}O_2$) and similar molecular weight (~314.5 g/mol or Da), THC and CBD differ structurally. THC features a closed cyclic ring, while CBD has an open-ring structure with a different spatial arrangement of its hydroxyl groups, which makes CBD a bicyclic compound while THC is a tricyclic (17). CBD appears as a white crystalline substance and demonstrates poor water solubility, with an aqueous solubility of around 1 mg/L. Based on the Biopharmaceutical Classification System (BCS), CBD is categorized as a class II compound due to its limited solubility combined with high permeability characteristics (17). Beyond THC and CBD, other major-to-minor phyrocannabinoids contribute to the plant´s chemical complexity. CBC exhibits a chromene (benzopyran) scaffold, representing a separate structural class of

cannabinoids. In contrast, CBN is not produced enzymatically but arises primarily through oxidative aromatization of THC (16). All major cannabinoids are characterized by having a high lipophilicity and a very low aqueous solubility, consistent with their terpenoid-derived hydrophobic skeletons. CBD has a high partition coefficient (log P) of approximately 6 and a pKa around 9.1 (18,19). These characteristics contribute to its poor water solubility and its sensitivity to environmental factors such as pH, heat, oxygen and light. Beyond cannabinoids, Cannabis also contains other predominant phytochemical families, particularly terpenes and flavonoids, which may influence aroma and biological activity and are often considered when describing the overall chemical profile of the plant.

1.3. CBD in anxiety disorders

1.3.1. Mechanisms of action in anxiety modulation

CBD is a major non-psychoactive phytocannabinoid derived from *Cannabis sativa* that exhibits complex pharmacological and biological activity. It has been investigated for its potential therapeutic effects in a range of conditions, including, chronic pain, anxiety, cardiovascular diseases, cancer, and neuropsychiatric disorders (20). Current evidence suggests that CBD interacts with various neurobiological targets, including the ECS and a range of non-cannabinoid targets, ultimately modulating neurotransmission, neuroinflammation, and neural circuits (20,21).

CBD does not behave as a conventional agonist of CBR1 and CBR2. Instead, it has been reported to function as a negative allosteric modulator of CBR1 and as a CBR2 inverse agonist (20). CBD may also influence retrograde signalling, a mechanism in which the endocannabinoids such as AEA and 2-AG are synthesized on demand in the postsynaptic neuron in response to increased neuronal activity and intracellular Ca^{2+} levels. These endocannabinoids diffuse retrogradely across the synaptic cleft and activate CBR1 located on the presynaptic neuron. The activation of CBR1, inhibits voltage-gated calcium channels, reducing the release of excitatory and inhibitory neurotransmitters (Figure 2). This action results in decreased synaptic transmission and reduced neuronal excitability (15). In addition, CBD interacts with several non-cannabinoid molecular targets, notably the serotonin receptors (such as the 5-Hydroxytryptamine (Serotonin) Receptor 1A (5-HT1A)), where it has been described as an agonist and a positive allosteric modulator (20). CBD also activates several transient receptor potential channels, including transient receptor potential vanilloid 1 (TRPV1), initiating a cycle of activation followed by desensitization, which contributes to reductions in excitatory transmission and neuroinflammatory signalling (20,21). Another relevant molecular mechanism includes the activation of peroxisome

proliferator-activated receptor gamma (PPARγ), through which CBD may promote anti-inflammatory and neuroprotective effects (20).

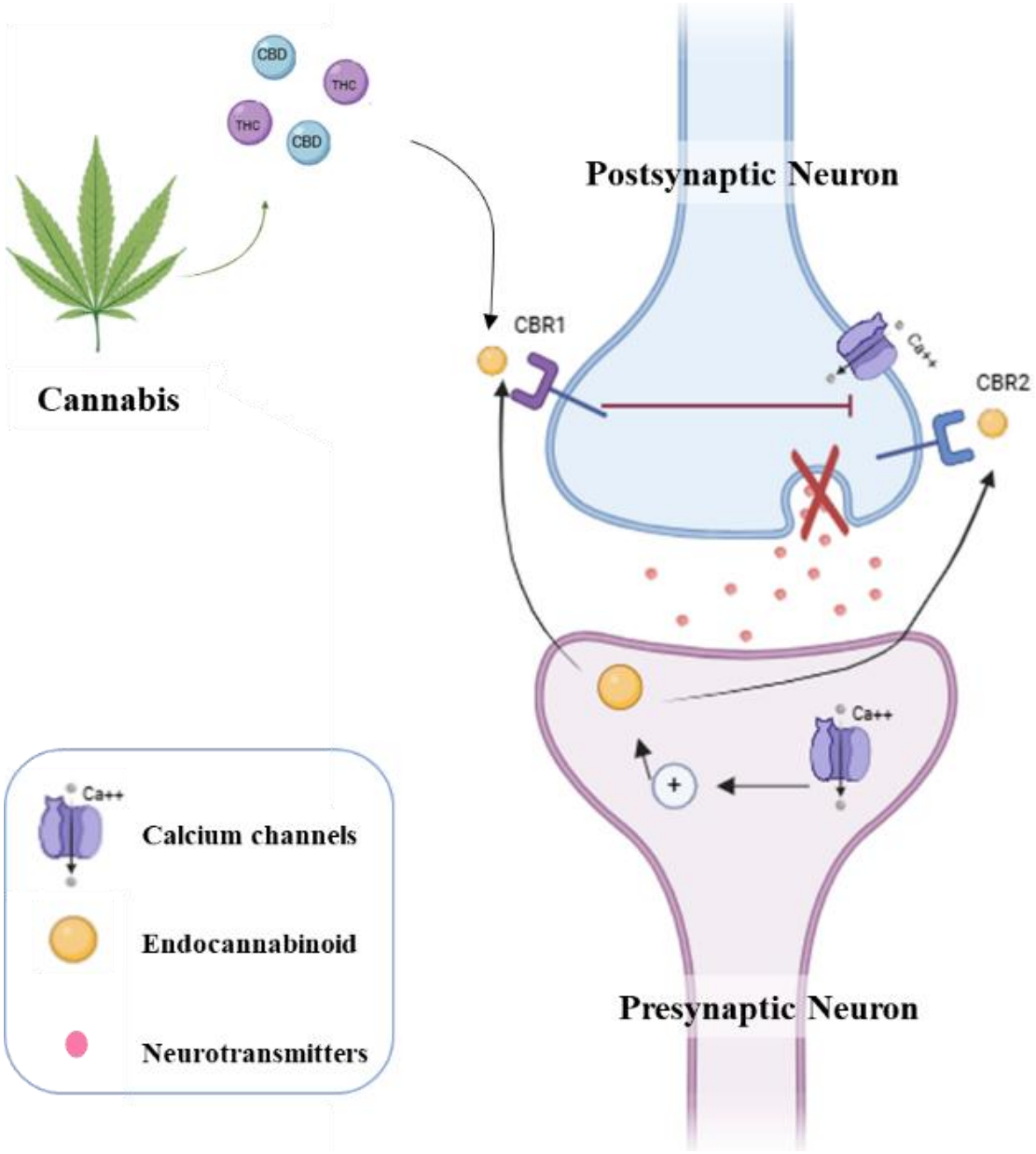

Figure 2. Schematic representation of retrograde synaptic signalling mediated by the endocannabinoid system.

These diverse interactions highlight CBD's complex pharmacological profile and its potential for modulating anxiety-related pathways beyond the ECS (20). Neuroimaging and behavioural studies indicate that CBD can reduce amygdala-related activation and modulate responses associated with fear and stress. These effects appear to depend in part on 5-HT1A signalling, since pharmacological blockade of this receptor attenuates CBD-induced anxiolysis (21,22). Despite promising mechanistic and behavioural findings, substantial limitations remain regarding the understanding of CBD's anxiolytic effects.

Reviews focusing on the ECS indicate that although endocannabinoid signalling plays an essential role in mood and anxiety regulation, the quality of clinical evidence supporting cannabinoid use in anxiety disorders is still weak and often methodologically inconsistent, particularly concerning sample size, dosing heterogeneity, and long-term outcomes (15,22). Systematic evaluations also highlight that although increasing endocannabinoid tone tends to correlate with reduced anxiety-like behaviour, the translation of these findings to clinical recommendations is limited, and large, rigorously designed human studies are still required to clarify the therapeutic relevance and safety of CBD in anxiety disorders (15). As showed, CBD´s engagement with multiple cellular pathways, explains its broad therapeutic potential, however, more clinical trials are necessary to establish its prolonged safety and effectiveness (21).

1.3.2. CBD efficient and productive dosages

Scientific evidence shows a complex view of CBD dosing for anxiety, with findings suggesting that the optimal dose may not follow a simple linear progression. Research indicates a dose-response curve with an inverted U-shape (23). For instance, in a simulated speech performance test involving healthy volunteers, it was found that the administration of 300 mg of CBD led to a significant reduction in anxiety symptoms, whereas doses of 150 mg and 600 mg were less effective (24). This dose-response pattern indicates that an intermediate dose may be more effective than lower or higher doses for certain forms of anxiety. Furthermore, evidence suggests a potential entourage effect where the combination of multiple compounds found in Cannabis, including CBD, other cannabinoids and terpenes, may result in greater therapeutic benefits compared to isolated CBD (25). This may explain why lower doses of full- spectrum extracts sometimes appear to achieve similar or better results when compared with higher doses of CBD in some studies. In participants with generalized SAD, research has provided evidence that higher doses (~400 mg), have been associated with reductions in subjective anxiety and alterations in brain activity in regions of anxiety regulation (26). These findings are further supported by a systematic review of clinical trials reporting that single oral doses of CBD between 300 and 600 mg consistently produced anxiolytic effects in human experimental models (24). In addition, a systematic review of clinical research investigating CBD´s impact on various medical conditions, including anxiety, reported improvements in primary outcomes where it was observed daily doses from below than 1 mg/kg to 50 mg/kg (27). Consistently, a retrospective real-world case series observed that moderate daily doses of CBD administered over months led to reductions in anxiety symptoms in adults with unspecified anxiety disorders, supporting the potential utility of sustained treatment in clinical practice

(28). Preclinical studies conducted in animal models have further supported CBD´s anxiolytic potential, with anxiety reduction observed at doses between 2.5 mg/kg and 10 mg/kg (23). However, translating these findings to humans remains challenging due to interspecies differences in drug metabolism and response.

1.3.2.1. CBD dosage in the different anxiety disorders

CBD has emerged as a promising compound for the treatment of anxiety disorders, although available clinical evidence reveals considerable variability in dosing, study designs, and therapeutic outcomes. Across the literature, CBD dosing is frequently reported in milligram per day or expressed relative to body weight (mg/kg/day), allowing for more precise comparison across individuals. Fixed oral doses commonly used in research can be translated into mg/kg/day estimates for adults weighing 50-100 kg. For example, a low daily dose of 6 mg corresponds to approximately 0.06-0.12 mg/kg/day, whereas single doses of 300 mg and 400 mg represent roughly 3-8 mg/kg/day depending on body weight. Higher doses, such as 800 mg, are equivalent to approximately 8-16 mg/kg/day. Evidence shows that specific dosages of CBD could exhibit greater efficacy depending on the type of anxiety. A recent review of randomized controlled trials reported consistent evidence that CBD reduces anxiety symptoms compared with placebo, particularly in studies using moderate oral doses between 300 and 400 mg (~3-8 mg/kg for adults weighing 50-100 kg) (29). Several trials in SAD showed significant reductions in anxiety following acute administration of 300-400 mg, aligning with earlier findings summarizing the benefits of moderate acute dosing in SAD (29,30). Additionally, one clinical trial demonstrated favourable outcomes with a daily 300 mg regimen administered for four weeks in young adults with SAD, suggesting that both single-dose and repeated-dose protocols may be effective (29). Evidence for GAD spans a broader dose range. Lower daily doses, such as 25-75 mg, have been associated with clinically meaningful reductions in anxiety symptoms, corresponding to approximately 0.25-1.5 mg/kg, depending on body weight (30). These findings are consistent with previous systematic reviews, although other studies also support the effectiveness of 300-400 mg in experimentally induced anxiety and GAD-related symptomatology (29,30). A recent meta-analysis reported that CBD produced a significant overall anxiolytic effect across GAD, SAD, PTSD, noting a moderate effect size but substantial heterogeneity, partly due to large variations in dose and treatment duration (31). CBD has also been investigated for its potential in PTSD, although the evidence base remains more limited. Small clinical trials have evaluated acute 300 mg doses (~3-6 mg/kg), reporting reductions in anxiety and intrusive symptoms (31). These findings suggest that CBD may offer benefits either as an adjunctive therapy or as a stand-alone intervention for

PTSD, although larger controlled studies are still required to confirm these preliminary observations (30,32). Current evidence indicates that moderate doses (300-400 mg) may be particularly relevant for individuals with moderate to severe anxiety, while lower daily doses may be suitable for milder presentations or longer-term symptom management (29,32). Taken together, across multiple recent reviews, effective CBD dosages for anxiety disorders appear to range widely - from low daily doses (~25-75 mg) to moderate acute doses (300-400 mg) - depending on the disorder, symptom severity, and treatment context. Acute higher doses have been examined primarily in SAD, whereas lower chronic regimens appear promising for GAD and adjunctive PTSD treatment. Despite encouraging results, all reviews emphasize the need for larger, well-controlled trials with standardized dosing protocols, as dose-response relationships and long-term safety profiles remain insufficiently defined.

1.3.3. Side effects of CBD

CBD has acquired widespread popularity due to increasing public interest, and the Food and Drug Administration (FDA) approval of Epidiolex® for the treatment of refractory epilepsy (21). Although CBD is frequently described as having a favourable safety profile, research suggests that different side effects may occur, especially at higher doses or when combined with other medication (33).

The most reported adverse effects arise from studies using oral administration. Gastrointestinal disturbances, like changes in appetite, nausea and diarrhoea, have appeared consistently across adult epilepsy trials. Somnolence and sedation are also frequent and occur in a dose-dependent manner. These effects are often potentiated when CBD is co-administered with central nervous system depressants, including clobazam, valproate and alcohol (33,34). Hepatic effects represent one of the most clinically relevant concerns. High levels of liver transaminases (mostly ALT, AST, and GGT) have been widely documented, particularly in patients receiving CBD with valproate (34). CBD also exhibits potential drug-drug interactions. It inhibits several hepatic enzyme systems, thereby increasing plasma concentrations of co-administered substances and potentially enhancing their toxicity (33). This pharmacokinetic profile necessitates careful clinical monitoring when CBD is used alongside antiepileptics and other medicines with narrow therapeutic indices. Taken together, current data suggest that while CBD is generally well tolerated, clinically meaningful adverse effects may occur - particularly hepatic abnormalities, sedation, gastrointestinal symptoms, and drug–drug interactions. Importantly, long-term safety data remain limited, and further research is required to clarify the consequences of chronic exposure (33,34).

1.4. Challenges in CBD delivery

CBD has attracted significant attention due to its therapeutic potential across a wide range of conditions; however, its clinical implementation remains challenging due to several physicochemical and pharmacokinetic limitations. One of the main challenges is related to its intrinsic physicochemical properties, which significantly complicate formulation development and drug delivery. In particular, the poor physicochemical characteristics of CBD have been identified as a major barrier to its successful clinical application and pharmaceutical development (35). Another limitation of CBD is its low bioavailability. Pharmacokinetic studies have demonstrated that CBD exhibits a highly inconsistent absorption profile following oral administration, with substantial variability across individuals and formulation. This variability is further increased by the complex pharmacokinetic profile of CBD, influenced by various physiological and formulation-related factors, making dose-exposure relationships difficult to predict (36). Moreover, studies have shown that CBD oral bioavailability follows a nonmonotonic pattern, with an inverted U-shaped curve between dose and systemic exposure, further complicating dose optimization (37). Another major factor contributing to its low oral bioavailability is its extensive first-pass metabolism. Following oral administration, a significant quantity of CBD is metabolized before reaching systemic circulation, thereby limiting the amount of active compound available for therapeutic action (37). This effect has been consistently identified as a key limitation of oral delivery, significantly reducing its pharmacological efficiency (38). As a result, only a fraction of the administered dose reaches the systemic circulation, necessitating higher or repeated dosing strategies. The variability in CBD pharmacokinetics is also influenced by external factors such as food intake and physiological conditions. For instance, the presence of food has been shown to significantly increase systemic exposure, while conditions such as hepatic impairment can further alter bioavailability and pharmacokinetic profiles (37). These factors introduce an additional unpredictability and complicate the establishment of standard dosing.

Collectively, these limitations represent significant challenges in the development of effective CBD-based therapies. These issues highlight the need for advanced formulation strategies aimed at improving the delivery, stability and performance of CBD.

1.5. Nanotechnology-based delivery systems

Nanotechnology-based drug delivery systems have emerged as a promising strategy to improve the performance of drugs with unfavourable properties, particularly those with variable pharmacokinetic profiles, low bioavailability, and low water solubility.

These systems are design to enhance the drug solubilisation, stability and absorption, therefore improving overall therapeutic efficiency (35,39). In this context, nanoscale delivery systems offer advantages due to their nanoscale particle size, high surface area and ability to modulate drug release and distribution profiles (39). Among the various nanotechnology-based approaches, lipid-based and self-assembling systems have gained considerable attention for the delivery of hydrophobic compounds. These systems facilitate drug incorporation into nanostructures that improve dispersion in aqueous environments and promote interactions with biological membranes, which can enhance absorption and bioavailability. In addition, delivery systems can protect the encapsulated drug from degradation and contribute to more consistent pharmacokinetic profiles (35,39).

1.5.1. Polymeric nanomicelles

Polymeric nanomicelles represent advanced nanoscale drug delivery platforms, typically ranging from 10 to 100 nm in diameter, which are generated through the thermodynamic self-assembly of amphiphilic polymers (40). These systems are characterized by a core-shell structure, in which the hydrophobic core enables the incorporation of lipophilic compounds, while the hydrophilic outer shell ensures dispersion and stability in aqueous media (Figure 3). This self-organisation occurs specifically when the amphiphilic surfactants or polymers concentration exceeds the critical micellar concentration (CMC), resulting in a distinctive core-shell architecture (41-43).

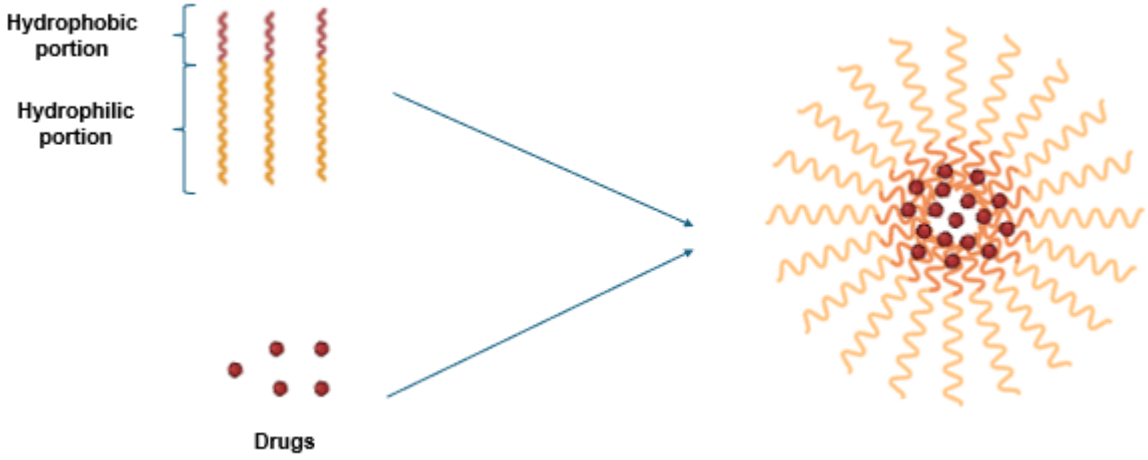

Figure 3. Schematic representation of the self-assembly of amphiphilic polymers and drug molecules into polymeric nanomicelles. Adapted from (43).

The distinctive core-shell architecture of polymeric nanomicelles is particularly advantageous for drug delivery, as it facilitates the sequestration of poorly water-soluble compounds within a protected hydrophobic inner core whilst maintaining stable colloidal dispersion in aqueous environments (41,44). As a result, these nanostructures are highly effective in improving the apparent solubility of lipophilic drugs, which represent a major limitation in conventional formulations (45). In addition to enhancing solubility, polymeric nanomicelles contribute to the protection of the encapsulated compound from degradation, thereby improving its stability in biological environments (41,42). This protective effect is particularly relevant in biological systems, where drug degradation and clearance can significantly reduce therapeutic efficacy. These nanostructures also exhibit favourable physicochemical properties that support their role as drug delivery systems. Their stability is influenced by thermodynamic and kinetic factors, including the CMC, which determines the conditions under which micelles form and remain stable in solution. This stability allows polymeric nanomicelles to maintain their structural integrity under physiological conditions and ensures that the drug remains encapsulated until reaching the target site (42,46). Furthermore, the small size and high surface area of these systems facilitate enhanced interaction with biological membranes, which can improve drug transport and absorption (47). Their nanoscale dimensions also enable improved tissue penetration and the potential for passive targeting through mechanisms such as enhanced permeability and retention (EPR), leading to increased drug accumulation at specific sites (45,47). Another important advantage these systems is their capacity for high drug loading and controlled drug release. The hydrophobic core allows efficient incorporation of lipophilic compounds, while the micellar structure can be engineered to respond to environmental stimuli such as pH, temperature, or redox conditions, enabling controlled and sustained drug release (47).

Overall, these nanostructures represent a versatile and efficient nanotechnology-based drug delivery platform. Their ability to enhance solubility, improve stability, facilitate drug transport, and enable controlled release makes them particularly suitable for the delivery of lipophilic compounds such as cannabidiol, where conventional delivery approaches remain limited.

1.5.2. Self-nanoemulsifying drug delivery systems (SNEDDS)

SNEDDS are isotropic mixtures composed of oils, surfactants, and co-surfactants that spontaneously form oil-in-water (O/W) nanoemulsions upon dilution in aqueous media under mild agitation conditions, such as those present in the gastrointestinal tract. SNEDDS, according to the lipid formulation classification system (LFCS), are considered

class III compositions (48). This spontaneous emulsification process results in the formation of nano-sized droplets with a large interfacial surface area, which facilitates drug dispersion and enhances dissolution (48,49) (Figure 4).

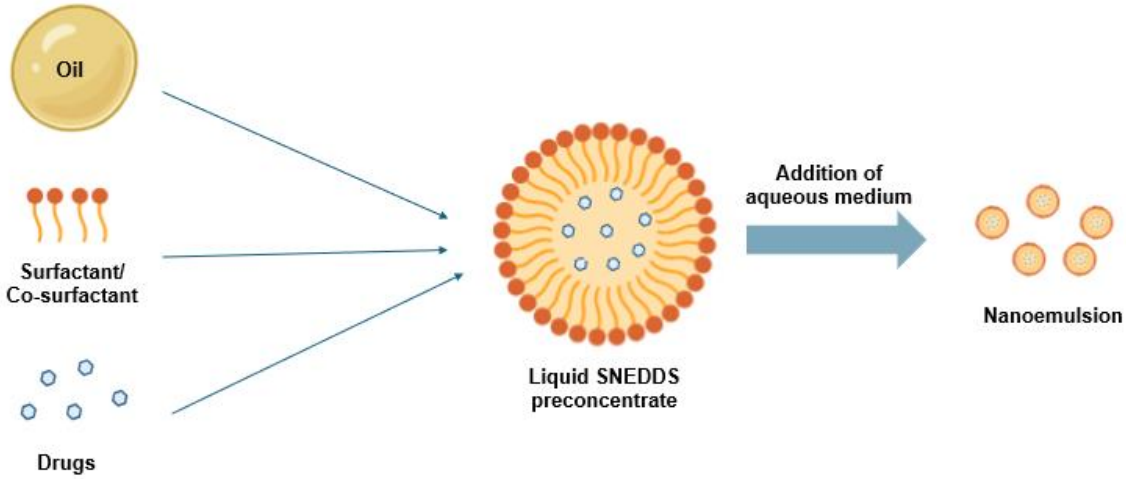

Figure 4. Schematic illustration of SNEDDS and nanoemulsion formation after dispersion in aqueous medium. Adapted from (50).

SNEDDS are particularly suitable for the delivery of poorly water-soluble compounds (50), as they maintain the drug in a solubilised state within the lipid phase prior to administration. Upon contact with the gastrointestinal fluids, the formulation forms a nanoemulsion in which the drug remains dissolved, improving its dissolution rate and promoting more efficient absorption (51). This characteristic is especially relevant for lipophilic molecules, whose oral bioavailability is typically limited by low aqueous solubility. In addition to this, SNEDDS have been shown to improve oral bioavailability through multiple mechanisms. These include increased surface area for drug absorption, improved interaction with the gastrointestinal membrane, and potential enhancement of lymphatic transport, which may reduce the extent of first-pass metabolism (51,52). Another important advantage of SNEDDS is their ability to reduce variability in drug absorption. By maintaining the drug in a pre-dissolved state, these systems minimize the influence of physiological factors such as gastrointestinal pH, motility, and food intake, improving the predictability of drug absorption (48). Recent advances have also focused on the development of modified SNEDDS formulations, including solid SNEDDS, which aim to overcome limitations associated with liquid systems, such as stability and handling issues. These solidified systems retain the self-emulsifying properties while offering improved physical stability and greater suitability for large-scale manufacturing and patient compliance (53).

Despite their advantages, these systems present formulation challenges that must be carefully addressed. The selection and optimisation of oils, surfactants, and co-surfactants are critical to ensure efficient self-emulsification, adequate drug loading, and system stability. Additionally, high concentration of surfactants may raise concerns related to toxicity and gastrointestinal irritation, highlighting the need for careful formulation design (48,49). Overall, SNEDDS represent a versatile and effective nanotechnology-based strategy for improving the solubility, absorption, and bioavailability of poorly water-soluble compounds. Their ability to maintain drugs in a solubilised state, enhance absorption and mechanisms, and reduce pharmacokinetic variability makes them particularly suitable for the delivery of lipophilic compounds such as CBD.

1.6. Routes of administration

The route of administration significantly influences CBD´s pharmacokinetics, systemic bioavailability, and therapeutic potential. Oral administration remains the most studied route in clinical research due to its convenience and established dosage forms, yet it suffers from substantial first-pass metabolism and variable absorption. Because of this, other routes of administration are being studied, such as sublingual administration.

1.6.1. Oral administration

Oral delivery of CBD, using pharmaceutical forms such as capsules, oils, or self-emulsifying systems, represents the most common method investigated in clinical trials. The physicochemical properties of CBD - including poor aqueous solubility and extensive first-pass metabolism - pose challenges for consistent systemic absorption, resulting in generally low and variable bioavailability profiles. Optimization of oral formulations has therefore been a major focus of pharmaceutical research to enhance plasma concentrations and therapeutic effect. It is essential to highlight that the oral bioavailability of CBD is relatively low, generally estimated between 6% and 19% (54). This indicates that a substantial portion of the orally ingested CBD may not reach the systemic circulation. For example, randomized trials have demonstrated that oil-based oral formulations achieve higher plasma concentrations than powder formulations of identical doses, indicating that the pharmaceutical vehicle can significantly influence absorption kinetics and systemic exposure (55). Recent advances in formulation science aim to improve oral CBD's bioavailability. Biodegradable self-emulsifying drug delivery systems (SEDDS) incorporating lipid cores and optimized emulsifiers have shown absolute bioavailability to marketed oil products, with numerically higher plasma concentrations, though these

differences did not reach statistical significance. Such approaches leverage enhanced mucosal permeability and lipid-based transport to mitigate the impact of first-pass metabolism on CBD absorption (56). Collectively, these findings highlight that while oral administration remains the predominant and most convenient route for human CBD use, formulation strategies are critical determinants of pharmacokinetic behaviour. Improved bioavailability through sophisticated lipid and emulsion-based systems could enhance therapeutic consistency, yet intersubject variability and the metabolic impact of the gastrointestinal tract remain important considerations.

1.6.1.1. Oral delivery of CBD and its limitations

The oral administration of CBD is fundamentally constrained because of its poor aqueous solubility, extensive first-pass metabolism, and instability under gastrointestinal conditions. These factors when put together, produce low and inconsistent bioavailability. These limitations have motivated the development of micro- and nanocarrier systems designed to enhance CBD stability and absorption.

In a recent study, researchers addressed CBD´s susceptibility to acidic degradation and its limited intestinal permeability by producing flexible zein nanoparticles capable of improving molecular adaptability and protecting CBD during gastrointestinal transit. They prepared the CBD-loaded nanoparticles and evaluated, in rats, physicochemical characteristics, *in vitro* gastrointestinal release, and *in vivo* pharmacokinetics. This formulation was able to improve gastric stability, delay release in acidic conditions, and enhanced intestinal delivery, resulting in increased maximum plasma concentration (Cmax) and area under the curve (AUC) values of approximately 1.7-fold relative to conventional zein nanoparticles, demonstrating a significant enhancement in oral bioavailability (57). A second major limitation of conventional oral CBD is the inability to consistently reach therapeutic plasma concentration due to CBD´s high lipophilicity and dependence on dietary fat for optimal absorption. To overcome this issue, a study developed biodegradable SEDDS optimized for oral delivery. Several CBD-loaded SEDDS formulations were generated, using different emulsifiers. Their emulsification performance, stability, and *in vivo* pharmacokinetic were assessed against a marked CBD formulation. Results showed rapid self-emulsifying, high CBD loading efficiency, and substantially improved oral absorption, with some formulations exhibiting greater Cmax (numerically) and comparable absolute bioavailability relative to the reference product. These findings confirmed that rationally designed self-emulsifying systems can substantially improve systemic exposure following oral CBD administration (56). A third limitation that motivates the use of nanocarriers is the significant degradation of CBD during processing, storage and biological exposure, which

compromises therapeutic consistency. A recent review of CBD-loaded nanocarriers highlighted that these delivery systems enhance solubility and protect CBD against enzymatic degradation, while specific formulations - such as zein nanoparticles and nanoemulsions - have demonstrated additional protection against thermal, photolytic, and light-induced degradation. The review also reported improvements in absorption and therapeutic performance across preclinical models of inflammation and pain, Table 2 (58).

Table 2. Examples of CBD nanoencapsulation systems and associated administration routes used to overcome limitations of oral delivery.

Systems	Administrative route	Target disorder	Main findings	Ref
Lipid-based nanoparticles	Oral	Anxiety; epilepsy	Enhanced physicochemical stability and bioavailability; reduced oxidative and photochemical degradation; sustained release and higher plasma levels compared to free CBD.	(58)
Zein-based nanoparticles	Oral	Anxiety; inflammatory diseases	Improved aqueous solubility and mucosal absorption; faster onset of action and increased bioavailability.	(57)
Solid/lipid nanoparticles	Oral/ Intranasal	Neurodegenerative disorders	Increased stability under gastrointestinal conditions; sustained release and enhanced anti-inflammatory and anxiolytic efficacy versus non-encapsulated CBD.	(58)
Self-emulsifying drug delivery systems (SEDDS)	Oral	Anxiety; general therapeutic applications	Rapid self-emulsification; high CBD loading efficiency; substantially improved oral absorption; increased Cmax and absolute bioavailability compared to commercial CBD formulation.	(56)

Cmax, maximum plasma concentration.

Despite these technological advances, oral delivery of CBD continues to exhibit significant limitations in both preclinical and clinical settings. A growing number of evidence demonstrates that CBD can exert anxiolytic effects through interactions with the ECS and serotonergic signalling pathways, clinical outcomes remain highly variable due to inconsistent absorption and pharmacokinetics. Recent data from a phase 3 clinical trial, involving a nanodispersible oral CBD formulation, reported improvements in anxiety scores and sleep quality, with plasma concentrations showing expected interindividual variability and a marked food effect (Cmax approximately 1.5-fold and AUC approximately 3-fold higher in the fed state) (9). Another thing to consider is the fact that CBD can affect certain drug metabolisms by interacting with some of the CYP family of enzymes (CYP 2D6, CYP 2C9, CYP 3A4) so interfering with the normal metabolism of Ibuprofen, benzodiazepines and some antidepressants, among others (e.g., fluoxetine) (59). A recent systematic review of human pharmacokinetic studies showed that the formulation plays a critical role in determining CBD absorption parameters. Nanotechnology-based formulations consistently demonstrated lower Tmax values than conventional formulations such as Epidiolex, indicating a faster onset of action. The review also showed that factors like dose and route of administration influence key parameters including Cmax and AUC. These pharmacokinetic differences are summarised in Table 3, showing that nanoencapsulation improves systemic exposure in comparison to non-encapsulated CBD by reducing the time to maximum plasma concentration (Tmax) and increasing Cmax and AUC (36). These findings are consistent across preclinical and new clinical data.

Overall, the evidence supports nanoencapsulation as a promising strategy to optimise CBD oral delivery. Across multiple studies, encapsulated CBD demonstrated improved solubility, stability, and bioavailability, enhancing controlled release, improved absorption, and prolonged therapeutic efficacy.

Table 3. Comparative pharmacokinetic profile of nanoencapsulated versus non-encapsulated CBD.

Parameter	Free CBD	Nanoencapsulated CBD	Ref
Solubility	It has a very low aqueous solubility, since it depends on dietary fat for absorption.	It improves solubility in aqueous medium, regardless of diet, facilitating intestinal absorption.	(56)
Stability	It is sensitive to light, heat, oxidation and GI degradation.	It has better physicochemical and GI stability.	(58)
Tmax	It is delayed, normally hours after oral intake.	It is reduced, having a faster peak plasma concentration of CBD.	(36)
Cmax	It is moderate and variable.	Increased and more consistent plasma peak levels.	(36,56)
AUC	It has lower exposure.	It increases when in comparison with non-encapsulated CBD.	(36)
Absorption	It has a high inter-individual variability.	It has a reduced variability because of controlled delivery.	(36)
First-pass metabolism	It is high, even more in oral formulations.	It reduces substantially.	(56)

AUC, area under the curve; **Tmax**, time to maximum plasma concentration; **Cmax**, maximum plasma concentration.

1.6.2. Sublingual administration and bioavailability

Sublingual administration is widely regarded as a promising strategy to improve the systemic delivery of CBD, since it allows the compound to bypass hepatic metabolism, resulting in faster systemic absorption and enhanced bioavailability compared to traditional oral formulations. This theoretical advantage aligns with the wider pharmacokinetic principles described in recent reviews. They highlighted CBD´s limited performance after oral ingestion, strongly shaped by its physicochemical characteristics and extensive first-pass metabolism. In this context, delivery routes capable of easing absorption through the oral mucosa (such as the sublingual pathway), offer the potential for more direct entry into the systemic circulation and a reduction in metabolic loss, an approach identified as promising to improve CBD exposure (35). However, human data also shows important nuances. A recent controlled study comparing sublingual drops with orally ingested

capsules found that both routes produced broadly similar systemic pharmacokinetic profiles, suggesting that the real-world sublingual performance may depend significantly on formulation characteristics and the user´s ability to maintain the compound in contact with the mucosa long enough for meaningful absorption to occur (60). These findings indicate that the full potential of this delivery method may not be realized under standard conditions and highlight the need for optimized formulations designed specifically to enhance mucosal uptake. Taken together, evidence from both pharmacokinetic research and theoretical delivery-systems, support the idea that sublingual administration remains a strategically advantageous alternative to conventional oral ingestion.

1.7. CBD products approved for anxiety by regulatory authorities

Currently, the best-characterized CBD medicine is the oral solution Epidiolex (marketed as Epidyolex in Europe), originally developed by GW Pharmaceuticals. In the United States, Epidiolex is marketed by Greenwich Biosciences (GW Pharmaceuticals' U.S. subsidiary) and is now under Jazz Pharmaceuticals. It received initial FDA approval on 25th June of 2018, for seizures associated with Lennox-Gastaut syndrome and Dravet syndrome (with subsequent label expansions for additional seizure indications) (21). In Europe, Epidyolex received European Commission marketing authorisation in 2019, and the marketing authorisation holder/applicant is GW Pharma (International) B.V. In parallel, CBD is widely consumed through non-approved commercial products whose composition and bioavailability may be uncertain, reinforcing the need for well-controlled, adequately powered trials to establish efficacy for anxiety, determine optimal dosing, and characterize long-term safety.

In Portugal, cannabis-based medicinal products are regulated under a specific legal framework established by Dec.-Lei No. 8/2019, which defines the conditions for the medicinal use of cannabis-based preparations and substances and establishes the Portuguese National Authority of Medicines and Health Products (INFARMED) as the competent regulatory body (61). Currently, several ACM-approved cannabis preparations containing different proportions of CBD and THC are available in Portugal. However, the approved therapeutic indications are mainly limited to conditions such as chronic pain, epilepsy-related disorders, multiple sclerosis-associated spasticity, chemotherapy-induced nausea and vomiting, and appetite stimulation in palliative care, with no specific approval for anxiety disorders reported to date (62).

Despite the growing interest in CBD for a range of clinical applications, no regulatory authority, including the FDA or the European Medicines Agency (EMA), has approved any cannabidiol-based medicinal product for the treatment of anxiety disorders. Within the

European regulatory framework, the only product with CBD in its composition that has formal authorization is Epidyolex, and it is approved use is strictly limited to specific forms of epileptic conditions. The EMA has not endorsed CBD for indications such as psychiatric or anxiety, as current evidence is considered insufficient to meet the standards required for approval of a dedicated therapeutic indication. Although preclinical and certain clinical studies have shown promise regarding CBD´s anxiolytic properties, the current body of evidence remains insufficient to meet the standards required for regulatory approval for a specific indication such as anxiety (21). It is worth noting that the Committee for Medicinal Products for Human Use (CHMP) has initiated an analysis of Stresam (etifoxine), a non-cannabinoid medicine, for the treatment of anxiety disorders (63). This reflects an ongoing interest in addressing anxiety treatments within the regulatory framework; however, CBD-based products are not the current focus of approval for this indication. As no CBD-based medicinal products are approved by the FDA for anxiety, no official dosage guidelines exist for this condition. The current support for many CBD-related claims is derived mainly from its broad range of biological targets rather than from well-controlled clinical trials. While CBD is widely available in unapproved over-the-counter products with variable composition, Epidiolex® is the main formulation supported by rigorous pharmacokinetic and clinical evaluation and is approved by the U.S. FDA for severe childhood-onset seizure disorders. For other indications, the evidence remains limited and often methodologically weak, and the quality control and bioavailability of commercial CBD products can be uncertain (21).

2. OBJECTIVES OF THE RESEARCH WORK

The main objective of this research was to design and develop novel nanotechnology-based delivery systems with CBD for potential application in the treatment of anxiety disorders. Considering the limitations associated with CBD, particularly its low aqueous solubility and variable bioavailability, this work aimed to improve its physicochemical and biological performance through advanced formulation strategies. To achieve this, preliminary solubility and miscibility studies were conducted to identify suitable excipients and optimise formulation conditions. Based on these findings, nanotechnology-based systems, namely SNEDDS and polymeric nanomicelles, were developed. The formulations were subsequently characterised in terms of their physicochemical properties, including particle size, PDI and surface charge, using Dynamic light scattering (DLS). Selected formulations were further analysed by transmission electron microscopy (TEM) and evaluated for encapsulation efficiency. Finally, the safety and biological performance of the developed systems were assessed through *in vitro* cell viability studies using MTT assays in Caco-2 intestinal epithelial cells and SH-SY5Y neuroblastoma cell lines.

3. MATERIALS AND METHODS

This section describes the materials and experimental procedures used for the development, characterisation, and biological evaluation of CBD-loaded nanotechnology-based delivery systems. Initially, solubility and miscibility studies were performed to select appropriate excipients for formulation development. Based on these results, SNEDDS and polymeric nanomicelles systems were prepared and optimised. The formulations were then characterised using DLS to determine particle size, PDI and zeta-potential, and selected formulations were further analysed using TEM to evaluate morphological features. Encapsulation efficiency was also determined for the optimised systems. Finally, the biological safety of the developed formulations was assessed through *in vitro* cell viability studies using the MTT assay in Caco-2 intestinal epithelial cells and SH-SY5Y neuroblastoma cell lines.

3.1. Sample

99% crystal isolate CBD was acquired from Joynt, Spain.

3.2. Standard and reagents

Labrafil® M 1944 CS, Labrafac™ Lipophile WL 1349 (medium-chain triglycerides (MCT)), Transcutol® HP, Labrasol® ASF and Capryol® 90 were kindly provided as free samples by Gattefossé (Saint-Priest, France). Massocare T80V Pharma (Tween 80®) was obtained from Commercial Química Massó (Barcelona, Spain). D-α-tocopheryl polyethylene glycol 1000 succinate (Vitamin E TPGS) was sourced from Vita Actives (Dublin, Ireland). Sodium deoxycholate was obtained from New Zealand Pharmaceutical (Palmerston North, New Zealand). Sodium alginate was sourced from Tokyo Chemical Industry Co., Ltd. (Tokyo, Japan).

3.3. Components of the nanoformulations

3.3.1. Oil phase

The oil used in the formulation is a critical component, responsible for drug solubilization and formulation loading capacity. In SNEDDS formulations, MCTs are widely used due to their better solubilizing ability and self-emulsification capacity, whereas long-chain triglycerides (LCTs) can enhance lymphatic transport, bypassing hepatic first-pass metabolism. In practice, a mixture of MCTs and LCTs can be employed to optimize

formulation properties (48). Beyond these roles, the lipidic core serves as a protective barrier, shielding the therapeutic compound from enzymatic and chemical breakdown within the gastrointestinal environment (64). Furthermore, the digestion of these lipids stimulates the secretion of endogenous biliary components, including bile salts and phospholipids, which interact with lipid digestion products to form mixed micellar systems that markedly improve drug bioaccessibility and absorption (48).

3.3.1.1. Labrafac™ Lipophile WL 1349

Labrafac™ Lipophile WL 1349 is a pharmaceutical-grade oily vehicle predominantly composed of MCTs, specifically caprylic (C8) and capric (C10) fatty acids (65) (Figure 5). Within the framework of the LFCS, this excipient is categorised as a primary lipid vehicle for Type I, Type II (SEDDS), and Type III (self-microemulsifying drug delivery system - SMEDDS) delivery systems (66). Its physicochemical properties as a liquid at room temperature allow it to function as a potent solubiliser for highly lipophilic active pharmaceutical ingredients (APIs), ensuring a high drug-loading capacity (48,66). In the specific context of cannabinoid delivery, Labrafac™ Lipophile WL 1349 has demonstrated a remarkable ability to dissolve CBD, with saturated solubility values reaching above 50% w/w (51). This MCT carrier is frequently selected for the development of SNEDDS because it promotes efficient spontaneous emulsification (48). Following oral administration, digestion of Labrafac™ triglycerides promotes biliary secretion of endogenous bile salts and phospholipids, which interact with lipid digestion products to form mixed micellar structures within the small intestine, thereby enhancing drug solubilisation and absorption (48).

The regulatory profile of Labrafac™ supports its extensive use in clinical applications, as it possesses a safe *status* (GRAS) and has a well-documented precedence of use in approved oral, topical, and parenteral pharmaceutical products (66).

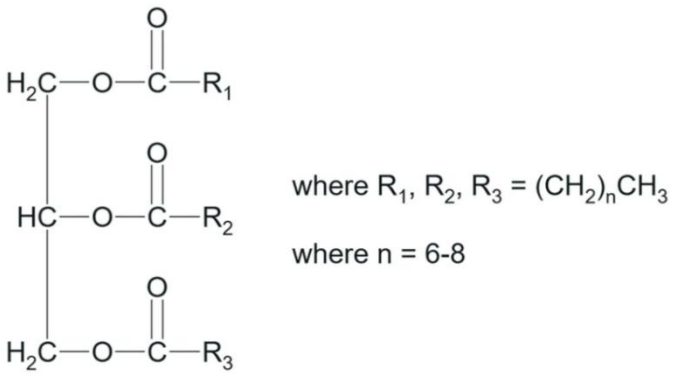

Figure 5. The molecular composition of Labrafac, including the different fatty acid combinations that can be found in the triglyceride mixture (65).

3.3.2. Surfactant

Surfactants (surface-active agents) are amphiphilic components essential in the design of nanoscale drug delivery systems, such as SNEDDS and polymeric micelles. These molecules consist of a hydrophilic (polar) head and a hydrophobic (non-polar) tail, allowing them to orient themselves at the interface between oil and water phases (67). Due to their amphiphilic nature, they localize at the oil-water interface and stabilize the colloidal system by reducing interfacial tension and lowering the free energy required for emulsification, thereby facilitating the spontaneous formation of fine colloidal droplets (64). Surfactants are broadly classified into ionic (anionic, cationic, and zwitterionic) and non-ionic categories based on the charge of their hydrophilic head group (67). In pharmaceutical development, non-ionic surfactants - such as polysorbates (Tween 20, Tween 80), ethoxylated castor oil derivatives (Cremophor EL, Cremophor RH 40), and polyglycolyzed glycerides (Labrasol, Labrafil) - are preferred due to their superior biocompatibility, low toxicity, and stability across a range of pH values (48,67). Additionally, polymeric surfactants and amphiphilic macromolecules, including poloxamers (Pluronic®), poloxamines (Tetronic®), and functional excipients like Vitamin E TPGS, have gained prominence for their ability to form robust micellar assemblies with high drug-loading capacities (42,44).

The selection of an appropriate surfactant is dictated by its Hydrophilic-Lipophilic Balance (HLB) and its CMC (44). Non-ionic surfactants with a HLB above 12 are generally preferred for the development of O/W nanoemulsions, as they promote efficient spontaneous emulsification and may facilitate the formation of droplets in the nanometric range. Beyond emulsification, several non-ionic surfactants, such as Tween 80 and Cremophor EL, can increase membrane fluidity and inhibit efflux transporters such as P-glycoprotein, further contributing to enhanced drug absorption (48).

3.3.2.1. Labrafil® M 1944 CS

Labrafil® M 1944 CS is a non-ionic, water-dispersible surfactant widely employed in lipid-based formulations to enhance the solubilisation and oral bioavailability of poorly water-soluble APIs. In aqueous environments, it undergoes spontaneous self-emulsification, forming coarse emulsions characteristic of SEDDS. Additionally, it may function as a co-emulsifier in topical formulations, contributing to improved emulsion stability (68). Chemically, it is defined as a complex mixture comprising mono-, di-, and triglycerides, alongside polyethylene glycol (PEG)-6 mono- and diesters of oleic acid (C18:1). Within global regulatory frameworks and pharmacopoeias, this excipient is identified as Oleoyl polyoxyl-6 glycerides (USP-NF), Oleoyl macrogol-6 glycerides (European Pharmacopoeia

(EP)), and is registered in the FDA Inactive Ingredient Database as Apricot Kernel Oil PEG-6 Esters (68). It possesses a viscosity ranging from 75 to 95 mPa·s at 20°C and a HLB value of approximately 9 ± 1. This intermediate HLB value contributes to its performance as a digestible lipid-based surfactant, making it particularly effective at maintaining lipophilic APIs in a solubilised state during the gastrointestinal transit (48,68).

3.3.2.2. Labrasol® ASF

Labrasol® ALF is a non-ionic, water-dispersible surfactant used in lipid-based formulations to improve the solubilisation and oral bioavailability of poorly water-soluble APIs (69,70). In aqueous media, it undergoes spontaneous self-emulsification, forming fine dispersions corresponding to microemulsion systems characteristic of SMEDDS, classified as LFCS Type III formulations. Chemically, this component consists of a small fraction of mono-, di-, and triglycerides, and mainly PEG-8 mono- and diesters of caprylic (C8) and capric (C10) acids (71) (Figure 6). In the USP-NF, it is identified as Caprylocaproyl Polyoxyl-8 Glycerides, while in the EP it is designated as Caprylocaproyl Macrogol-8 Glycerides. According to the FDA, the preferred substance name is PEG-8 Caprylic/Capric Glycerides (69). This surfactant, is supplied as a liquid excipient with a viscosity ranging from 80 to 110 mPa·s at 20 °C. It presents a CMC of 42 mg/L at 25 °C and a HLB value of 17 ± 1 (69,70). Furthermore, its high purity profile contributes to formulation stability and capsule compatibility. The safety of its use is supported by extensive toxicological data and its established use in approved pharmaceutical products (69).

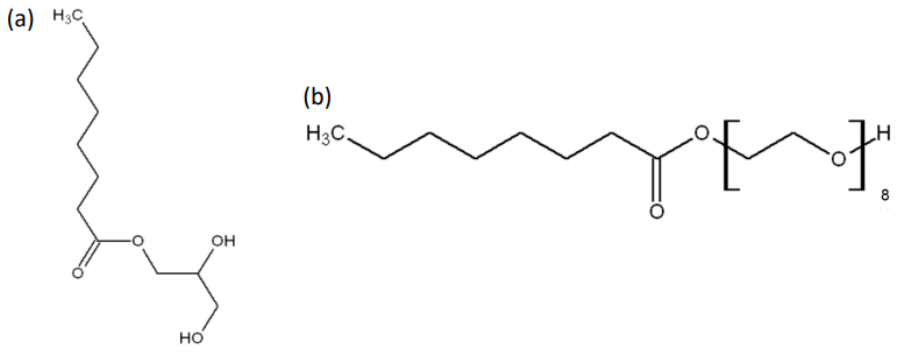

Figure 6. Main constituents of Labrasol® ALF: (a) glycerol esters derived from caprylic (C8) and capric (C10) acids, and (b) PEG-8 esters of caprylic (C8) and capric (C10) fatty acids (71).

3.3.2.3. Tween 80®

Tween 80®, also known as Polysorbate 80 (72), is a non-ionic hydrophilic surfactant extensively utilised in the development of advanced drug delivery systems, SNEDDS and polymeric micelles (48,73). Chemically, it is defined as polyoxyethylene sorbitan monooleate, consisting of a hydrophilic polyoxyethylene moiety and a hydrophobic fatty acid ester derived from oleic acid (Figure 7). Tween 80 is characterised by a HLB value of 15 (73,74), which classifies it as a highly hydrophilic agent ideal for the formation and stabilisation of O/W nanoemulsions. A defining technical parameter is its CMC, which is approximately 14 mg/L; this low value indicates that the surfactant molecules spontaneously self-assemble into micellar structures at very low concentrations (73).

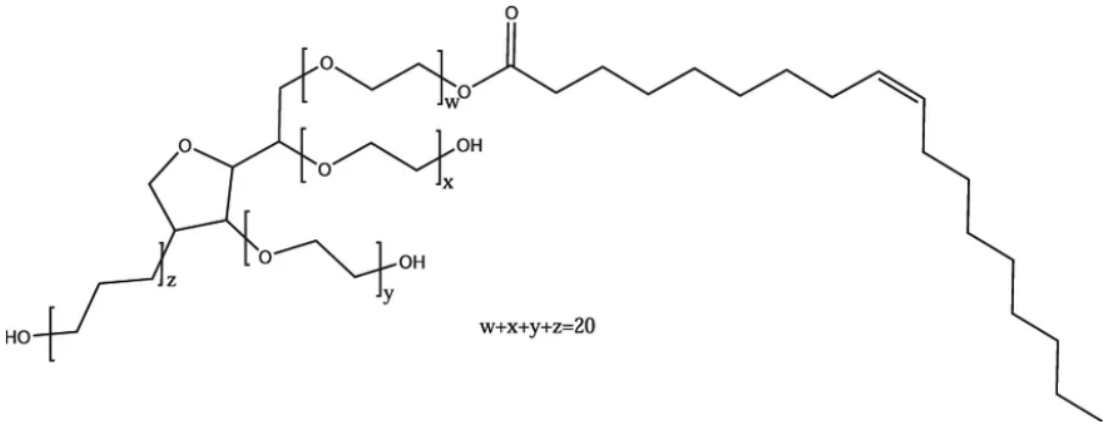

Figure 7. Molecular structure of Tween 80 (polysorbate 80) (72).

3.3.2.4. Capryol® 90

Capryol® 90 is a high-purity pharmaceutical excipient chemically defined as propylene glycol monocaprylate (Type II) according to the European Pharmacopoeia and Propylene Glycol Monocaprylate NF in the USP-NF. It is a non-ionic, water-insoluble surfactant that consists primarily of monoesters of caprylic acid (C8) with a small fraction of diesters (Figure 8) (48,75). It has a molecular weight of 202.29 g/mol (76), a HLB of 2 ± 1, and it is considered a bioavailability enhancer and a solubilizer for poor-water soluble APIs. It is widely utilised in the development of oral lipid-based systems, particularly as a cosurfactant or oil phase in SNEDDS and SMEDDS (75).

In oral SNEDDS, Capryol® 90 is often paired with high-HLB surfactants (such as Tween® 20 or Cremophor® RH 40) to reduce interfacial tension and improve the efficiency of spontaneous emulsification (48). Beyond oral applications, it is utilised in topical and transdermal dosage forms as a solubiliser and co-emulsifier to improve the structural stability of creams and emulgels (75).

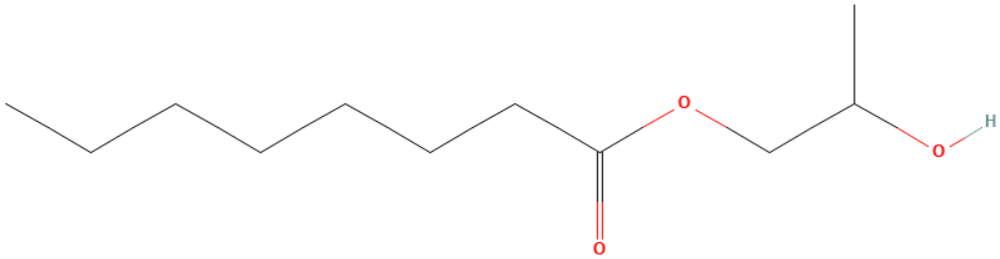

Figure 8. Molecular structure of Capryol® 90 (propylene glycol monocaprylate) (76).

3.3.3. Co-surfactant

Co-surfactants or cosolvents are frequently required, as a single surfactant alone may not be sufficient to achieve the necessary low interfacial tension. These agents synergistically cooperate with surfactants to enhance drug solubility and dispersibility in the oil phase, promoting nanoemulsion stability and homogeneity. Commonly used cosolvents include propylene glycol, PEG, ethanol, and Transcutol® HP. However, their concentration must be carefully controlled, as cosolvents can migrate to the aqueous phase upon dispersion, potentially leading to drug precipitation (48).

3.3.3.1. Transcutol® HP

Transcutol® HP is a purified form of diethylene glycol monoethyl ether (DEGEE) with a recognised safety profile (Figure 9) (77,78) and regulatory approval for topical and transdermal use by authorities such as the USP, EP and FDA (78,79). It is commonly utilised as a solvent and penetration enhancer, particularly for poorly water-soluble APIs, as it can improve drug solubility, formulation stability and bioavailability (78). In topical formulations, it also facilitates the permeation of compounds through the skin (79).

In nanoemulsion systems, DEGEE is frequently incorporated as a co-surfactant to support emulsion stability and enhance the transdermal transport of drugs such as diclofenac, celecoxib and minoxidil (80).

Physically, Transcutol® is described as a transparent and hygroscopic liquid with good miscibility in water and several organic solvents. It has a molecular weight of 134.17 g/mol and a molecular formula of $C_6H_{14}O_3$ (81,82). Compared with ethanol and propylene glycol, it demonstrates superior solubilising performance (77) and exhibits miscibility with excipients used in topical preparations (83). It is considered stable over a pH range of 4–9 and is usually added during the cooling phase of emulsion preparation to reduce the risk of API degradation (77,83). Additionally, it has an HLB of 4.2, which means that it can be used as both a solvent and surfactant (78).

Toxicological studies indicate that Transcutol® has low acute toxicity, however, the presence of impurities such as ethylene glycol or diethylene glycol may increase toxicity risks, emphasising the need for highly purified pharmaceutical grade (78).

Figure 9. Molecular structure of Transcutol® (diethylene glycol monoethyl ether (DEGEE)) (82).

3.3.3.2. Sodium deoxycholate (NaDC)

Sodium deoxycholate or NaDC is a natural anionic bile salt surfactant present in the bile of mammals and other vertebrates (84). Due to its distinctive steroidal structure and amphiphilic properties, it may be able to increase drug permeability across skin or mucosa. Several studies have investigated the ability of different classes of amphiphiles compounds to enhance drug permeability (84,85).

NaDC possesses a rigid steroid backbone with both hydrophobic and hydrophilic regions (Figure 10) (84,86), enabling it to function effectively as an emulsifying and solubilising agent (85). In biological systems, within the gastrointestinal tract, they also function as emulsifying and solubilising agents and represent key constituents of steroid-based detergents. This biosurfactant, is synthesised in the liver from cholesterol and subsequently stored in the gallbladder (84).

From a physicochemical perspective, NaDC appears as a white to off-white powder with a 357-365ºC melting point and water-soluble (87). It has a pH between 7.5 and 9.0 for a NaDC solution in water of 20 g/L at 20ºC (88). Furthermore, it has a molecular weight of 414.55 g/mol and an empirical formula of $C_{24}H_{39}NaO_4$ (87-89).

NaDC can form micellar aggregates and solubilise lipophilic substances such as fatty acids, cholesterol, lipids and fat-soluble compounds (90). It has also applications across multiple areas, such as food processing, cosmetics, drug development, molecular recognition systems and the fabrication of silica-based mesoporous materials (90). Moreover, NaDC is commonly incorporated into microemulsions, commercial products and industrial processes within the oil sector (86). In pharmaceutical technology, it can be combined with Tween 20 in aqueous systems to support the formation of lipid nanoparticles using the emulsification-solvent evaporation technique, where additional components are dissolved in the solvent phase (91,92).

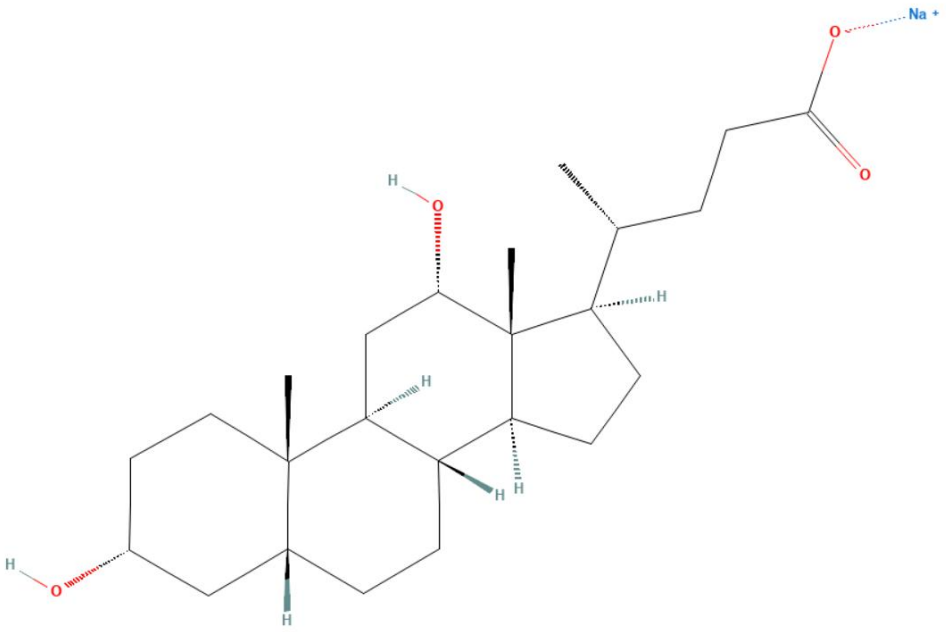

Figure 10. Molecular structure of sodium deoxycholate (89).

3.3.4. Other used components

3.3.4.1. Vitamin E TGPS

Vitamin E TPGS is a semi-synthetic derivative of natural vitamin E, that is formed through the esterification of vitamin E succinate with polyethylene glycol 1000 (Figure 11) (93). It is recognised by the FDA as a safe pharmaceutical excipient and is widely incorporated as an adjuvant in drug delivery systems. Its physicochemical and biological characteristics make it particularly valuable in this field, as it is highly biocompatible and can enhance the solubility and permeability of drugs. In addition, it has been associated with selective anticancer activity, further supporting its use in advanced therapeutic formulations (94,95).

TPGS is considered an amphiphilic molecule, having in its composition a hydrophilic polar head and a lipophilic alkyl tail, which gives it the ability to solubilise hydrophobic drugs and enhance their bioavailability (94).

It is presented as a waxy solid with a melting point between 37 and 41ºC (96), a molecular weight of 1513 g/mol and a HLB value of 13.2 (93,96). Its molecular formula is $C_{33}O_5H_{54}$ $(CH_2CH_2O)_n$, with the ´n` corresponding to the number of PEG molecules attached. TPGS´s was found to be nongenotoxic and safe, being found in array of fabricated nanoformulations for the treatment of tumours (96). Additionally, it has an CMC of 0.02 percent weight-wise (93,96). Furthermore, the formation of TPGS micelles in aqueous media can contribute to a reduction in particle size, while improving solubility and formulation stability (97,98).

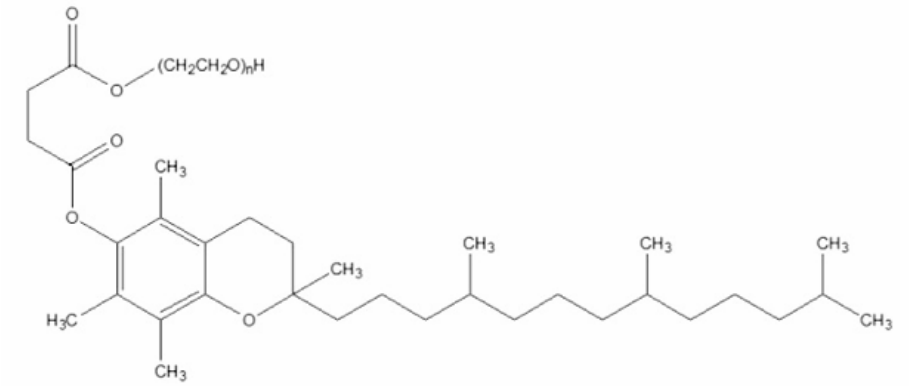

Figure 11. Molecular Structure of Vitamin E TPGS (42).

3.3.4.2. Sodium alginate

Sodium alginate is the sodium salt derivate of alginic acid, a polysaccharide obtained from the cell walls of brown algae, known for its chelating properties (99-101). It is a polyuronic acid composed of residues of β-D-manuronic and α-L-glucuronic acid (Figure 12) (100,102). This compound can absorb large quantities of water while maintain its structure, making it able to deliver hydrophilic drugs (99).

From a physicochemical perspective, sodium alginate is a hydrophilic solid powder, typically white to pale yellow in appearance, that dissolves easily in water. Its capacity to form gels in the presence of divalent ions makes it particularly suitable for drug delivery applications and cell immobilisation systems. It possesses an average molecular weight of 216.121 g/mol and a chemical formula of $(C_6H_7NaO_6)_n$ (102,103).

It is classified as an anionic polymer and it can be incorporated into controlled-release drug delivery systems in combination with other polymers, due to its low toxicity, low cost, biodegradability and biocompatibility (102). It was demonstrated that by using coacervation, particulate drug delivery systems produced from natural polymers were generally non-toxic and suitable for repeated administration. These systems can also protect active compounds from degradation, improve drug encapsulation efficiency and prolong drug release from the pharmaceutical formulation (99,102).

Sodium alginate can be used to prepare microcapsules for cosmetic applications (100) and, according to previous studies, their degradation within the body may affect the kinetics of drug release from the matrix (102).

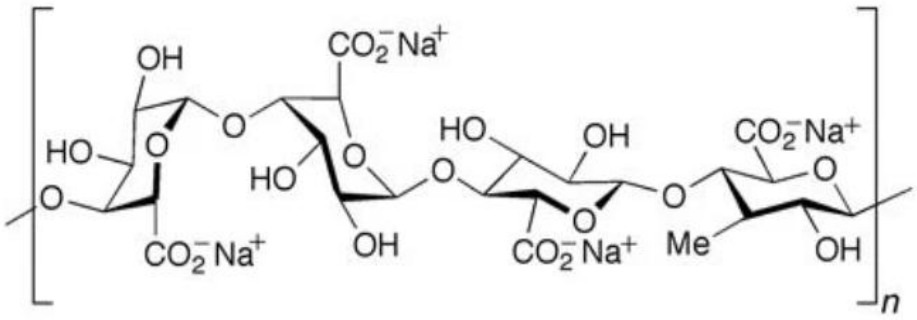

Figure 12. Molecular structure of sodium alginate (101).

3.4. Solubility and miscibility screening

The Solubility Screening was done to evaluate the solubility of CBD in selected excipients, namely Tween 80®, Labrafac™ Lipophile WL 1349, Labrafil® M 1944 CS, Labrasol® ASF and Capryol® 90. For each test, 0.075 g of CBD was added to 5 g of the respective excipient. The mixtures were stirred at room temperature until equilibrium was reached. Solubility was assessed visually by observing the presence or absence of undissolved particles, as well as the clarity and homogeneity of the resulting systems.

The miscibility of the selected excipients was investigated through systematic evaluation of binary and ternary mixtures. Binary mixtures were prepared by combining 2 g of each component in glass vials, including the following combinations: Tween 80® with Labrafac™ Lipophile WL 1349, Tween 80® with Labrafil® M 1944 CS, Labrafac™ Lipophile WL 1349 with Labrafil® M 1944 CS, Tween 80® with Capryol® 90, Tween 80® with Labrasol® ASF, and Capryol® 90 with Labrasol® ASF. Ternary mixtures were prepared by combining equal masses (2 g each) of selected excipients, namely Tween 80®, Labrafac™

Lipophile WL 1349, and Labrafil® M 1944 CS, as well as Tween 80®, Capryol® 90, and Labrasol® ASF. All samples were stirred at room temperature until equilibrium was reached. Miscibility was evaluated based on macroscopic observation, considering phase behaviour, transparency, and homogeneity.

3.5. Polymeric nanomicelles preparation

CBD-loaded polymeric nanomicelles were prepared using a lipid-surfactant system composed of CBD, Transcutol® HP, Labrafil® M 1944 CS/Labrasol® ASF and Vitamin E TPGS. The total final formulation mass was 25 g.

An amount of 0.075 g of CBD was selected for incorporation into all formulations (polymeric nanomicelles and SNEDDS) and maintained throughout the study to ensure consistency during formulation development and comparative characterisation. This amount was chosen as a representative loading for a potential oral or sublingual CBD dosage form rather than as an optimised therapeutic dose.

For the preparation of the formulations, we started by weighing the components using a balance with automatic internal calibration (circular draft shield; VWR International, Lisbon, Portugal). The required amount of CBD was accurately weighed into a suitable glass tube, followed by the addition of Transcutol® HP. The mixture was vortexed for 2 min to promote solubilisation of CBD. Labrafil® M 1944 CS or Labrasol® ASF were then incorporated, and the system was vortexed again for two more minutes. Subsequently, the established mass of Vitamin E TPGS was added, followed by vortex mixing for three minutes. To enhance homogenisation of the lipid phase, the formulation was subjected to a water bath at 55 °C for 4 min, followed by vortexing for 3 min, and again water bath for more 3 more minutes. All steps were performed at room temperature, except for the heating stages.

In parallel, the aqueous phase was prepared separately using purified water or phosphate buffer. Sodium alginate or NaDC were dissolved in the selected aqueous medium under vortex agitation until complete dispersion was achieved. After completion of the final heating cycle, the lipid phase was slowly added to the aqueous phase under gentle addition to promote nanostructure formation. The resulting mixture was vortexed for 8 min until a homogeneous dispersion was obtained.

The final formulations (25 g total mass) were then characterised in terms of transmittance (T) and pH. The pH was measured and adjusted in some formulations for the desired value using a pH Meter, PHS-3E (Nanbei, Zhengzhou, China). After 24 h of storage

at room temperature, DLS analysis was performed to evaluate particle size distribution, PDI, and zeta potential.

3.6. SNEDDS preparation

SNEDDS were prepared using combinations of CBD, Labrafil® M 1944 CS or Labrasol® ASF, MCT or Capryol® 90, and Tween 80®. To evaluate the influence of the incorporation sequence on formulation performance, the order of addition of the oil components MCT or Capryol® 90 and Labrafil® M 1944 CS or Labrasol® ASF was varied between formulations.

Initially, the required amount of CBD was accurately weighed using a balance (section 3.5.), followed by the addition of Labrafil® M 1944 CS or Labrasol® ASF. The mixture was vortexed for 3 min to promote CBD solubilisation. Subsequently, MCT or Capryol® 90 were incorporated and the system was vortexed for an additional 1 min. Tween 80® was then added, followed by vortex mixing for 2 min to obtain a homogeneous lipid formulation. Following preparation, the formulations were allowed to stand at room temperature for a sufficient period to enable the disappearance of air bubbles generated during vortex mixing. After preparation of the lipid phase, emulsification studies were performed to evaluate the self-emulsifying capacity of the formulations. Initially, 50 µL of formulation were dispersed in 5 mL of distilled water. The oily phase was slowly added to the emulsifying medium under continuous stirring at 37 °C, using a VMS-C7 Advanced magnetic hotplate stirrer (VWR, USA), as shown in figure 13. This was done to simulate physiological conditions and promote spontaneous emulsification (104). Formulations presenting a clear appearance and high transmittance values following dispersion were considered suitable for further emulsification studies (48). These selected formulations were subsequently evaluated in a 0.8 g/L NaDC aqueous solution to simulate bile salt conditions, using the same conditions used for distilled water.

Following emulsification, the formulations were characterised in terms of pH and transmittance. After 24 h of storage at room temperature, DLS analysis was performed to evaluate particle size distribution, PDI and zeta potential.

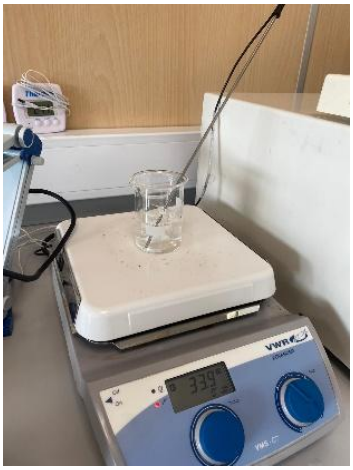

Figure 13. VMS-C7 Advanced magnetic hotplate stirrer (VWR, USA).

3.7. Coding system for formulation identification

For the identification of different formulations, a coding system was created. The abbreviation PN refers to polymeric nanomicelles, whereas S designates SNEDDS formulations. Formulations containing in their composition Labrafil® M 1944 CS are identified by the code LF, while those prepared with Labrasol® ASF have LS. The code MCT indicated the presence of Labrafac™ Lipophile WL 1349, and C corresponds to formulations containing Capryol® 90. Sodium alginate and sodium deoxycholate are represented by SA and NaDC, respectively. Formulations prepared with a reduced concentration of Transcutol® compared to the standard composition are identified by the suffix t.

The aqueous medium used in the formulation is identified as P for purified water, PB for phosphate buffer, NaDC for sodium deoxycholate and HCl for hydrochloric acid. When a component is used at a different concentration from the starting formulation, its concentration is indicated immediately after the corresponding code. For example, the code PN_LF_P_SA refers to a polymeric nanomicelles formulation, prepared with Labrafil® M 1944 CS, purified water and sodium alginate, at a standard concentration, whereas PN_LF_P_SA 0.14% indicates the same formulation, but containing sodium alginate at a modified concentration of 0.14%. For the SNEDDS formulations, the final part of the code indicates the emulsification medium used. For instance, in the formulation S_LS_MCT_NaDC, the suffix “NaDC” specifies that sodium deoxycholate was used as the emulsifying medium.

3.8. Formulation characterization

The developed formulations were evaluated using several complementary characterisation techniques to ensure an adequate understanding of their physicochemical and biological properties.

3.8.1. Dynamic light scattering (DLS)

DLS is a widely used analytical technique for determining particle size and size distribution of colloidal systems, particularly within the nano- and micro- ranges (105). Due to its rapid analysis, non-destructive nature, and minimal sample preparation requirements, it is extensively used for the physicochemical characterization of nanotechnology-based drug delivery systems (106). The technique is based on the analysis of fluctuations in the intensity of the light scattered by the particles undergoing Brownian motion in a liquid medium. These fluctuations are processed using an autocorrelation function to determine the translational diffusion coefficient, which is subsequently related to the particle size through the Stokes-Einstein equation, allowing the calculation of the hydrodynamic diameter (105).

$$D_H = \frac{k_B T}{3\pi\eta D}$$

Equation 1. Stokes-Einstein equation for the calculation of the hydrodynamic diameter (105).

In the equation, d_H represents the hydrodynamic diameter, k_B the Boltzmann constant, T the absolute temperature, η the viscosity of the medium, and D the translational diffusion coefficient (105). This hydrodynamic diameter reflects the effective size of the particle in solution, including the solvation layer and any surface-associated molecules.

In addition to particle size, DLS provides the PDI, which describes the width of the size distribution. Lower PDI values indicate a more homogeneous nanoparticle population, whereas higher values indicate a more heterogeneous population or aggregation. In practice, PDI values below 0.2 are generally considered indicative of a narrow and uniform size distribution, while values above 0.5 reflect a broad or polydisperse system that may compromise formulation stability (107).

In parallel with size characterisation, the surface charge of nanoparticles is commonly evaluated through zeta potential measurements. Zeta potential represents the electrical potential at the slipping plane of the electrical double layer surrounding a particle

in solution and provides an indirect measure of its surface charge. Zeta potential is a key indicator of colloidal stability, as it reflects the balance between attractive and repulsive forces between particles. High absolute values indicate strong electrostatic repulsion, which prevents particle aggregation and promotes dispersion stability. In general, values greater than ±30 mV are considered indicative of good stability, whereas values between ±20 mV and ±30 mV suggest moderate stability, and values close to neutrality (±10 mV or lower) are associated with a higher tendency for aggregation (108). Furthermore, zeta potential plays an important role in biological interactions, as particle surface charge influences cellular uptake and interaction with biological membranes. Positively charged nanoparticles may exhibit enhanced interaction with negatively charged cell membranes, although thus may also be associated with increased cytotoxicity (109).

Despite their advantages, all these measurements present limitations. DLS results are highly sensitive to experimental conditions and may be biased towards larger particles due to the intensity-weighted nature of light scattering (106). Similarly, zeta potential values are influenced by factors such as pH, ionic strength, and medium composition, requiring careful control and reporting of experimental conditions to ensure reliable interpretation (108).

Overall, the combined use of DLS and zeta potential measurements provides essential information on particle size, distribution, and surface charge, which are critical parameters for the design, optimisation, and evaluation of nanotechnology-based drug delivery systems.

3.8.1.1. Characterization of nanoformulations size distribution and surface charge

The formulations were evaluated using DLS equipment Brookhaven Instruments (Holtsville, NY, USA) (Figure 14). Particle size, size distribution, and surface charge were evaluated through the determination of the Z-average, PDI, and zeta potential, respectively. The equipment performed DLS measurements for particle size and distribution analysis, while zeta potential was determined by electrophoretic light scattering (ELS) based on Doppler velocimetry principles. For each formulation, measurements of Z-average diameter and PDI were performed using six runs, whereas zeta potential measurements were obtained using ten runs. The reported values correspond to the mean of the obtained measurements.

Unless otherwise stated, all formulations were prepared independently in duplicate (n = 2), and the reported values correspond to the mean of these independent

measurements. When a different number of replicates were used, this is indicated in the corresponding section.

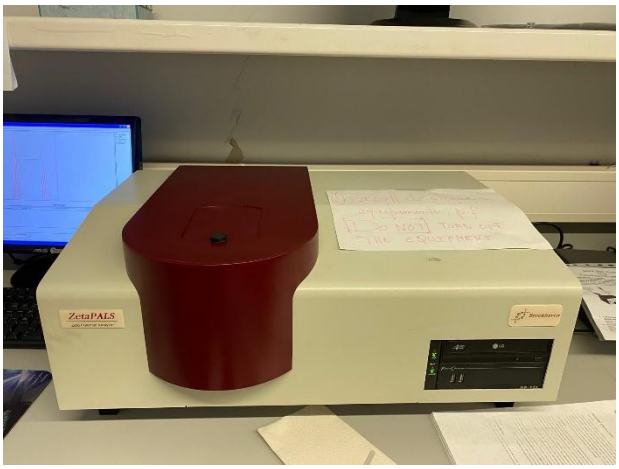

Figure 14. NanoBrook ZetaPALS by Brookhaven Instruments (Holtsville, NY, USA).

3.8.2. Transmission electron microscopy (TEM)

TEM is a high-resolution imaging technique widely used for the structural and morphological characterisation of materials at the nanoscale. It is considered one of the most powerful microscopy methods for investigating nanomaterials due to its ability to provide detailed information on size, shape, internal structure, and crystallographic properties at near-atomic resolution (110,111). The principle of TEM is based on the transmission of a high-energy electron beam through an ultrathin specimen. As electrons interact with the sample, they are either transmitted, scattered, or diffracted depending on the material's density and internal structure. These interactions generate contrast that allows the formation of highly detailed images, analogous in concept to optical microscopy but with significantly higher resolving power due to the much shorter wavelength of electrons (112). Because of this principle, TEM enables the direct observation of nanoscale features that cannot be resolved using conventional light microscopy. It provides information not only on external morphology but also on internal structural organisation (111). This makes it particularly relevant for the characterisation of drug delivery systems, where particle structure and uniformity are critical quality attributes. In addition to morphological analysis, TEM can be used to investigate particle size distribution and aggregation state, as well as interactions between nanomaterials and biological systems. In nanomedicine, this capability is particularly valuable for understanding nanoparticle localisation, cellular uptake, and intracellular distribution at the ultrastructural level (112,113). Despite its high resolution and extensive applicability, TEM has certain limitations. Sample preparation is

complex and often requires fixation, dehydration, and sectioning into ultrathin slices, which may introduce structural artefacts or alternative sample morphology. In addition, the technique provides two-dimensional projections of inherently three-dimensional structures, which may limit full spatial interpretation of complex nanomaterials (112).

Nevertheless, TEM remains an indispensable technique in nanoscience and nanomedicine due to its unmatched ability to provide direct visual evidence of nanoscale structure and organisation. When used in combination with complementary techniques such as DLS and biological assays, TEM contributes to a comprehensive understanding of nanomaterial properties and performance.

3.8.2.1. TEM analysis of nanoformulations morphology

The morphology and size of the selected formulations were visualized using a Transmission Electron Microscope, more specifically the model JEM-1400 (JEOL, Tokyo, Japan), as shown in Figure 15. The formulations were selected based on their particle size and PDI obtained by DLS and by the different components in their composition. The selected formulations were PN_LF_P_SA0.14%, PN_LS_P_SA0.14% and S_LS_MCT_NaDC.

A 1 µL sample was dissolved in 199 µL of distilled water and mixed entirely. One spot of diluted sample was subjected to a formvar/carbon grid (200 mesh - Cu 25) and subsequently coated with 2% w/v uranyl acetate and rested for 15 s to dry with air. The process operated at an accelerating voltage of 80 kV for grid analysis (114).

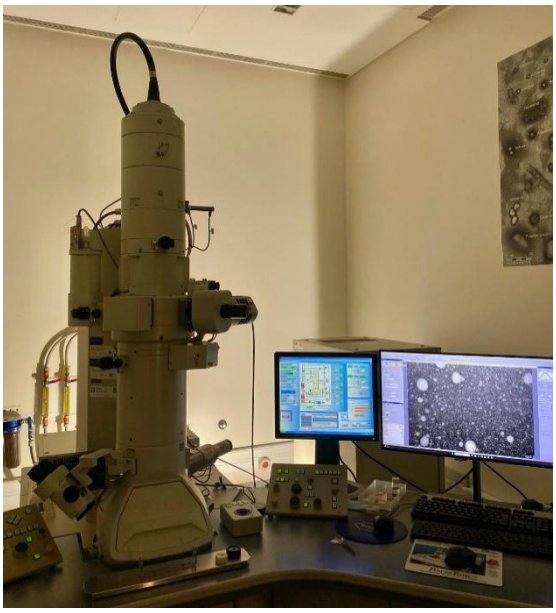

Figure 15. JEM-1400 TEM by JEOL (Tokyo, Japan).

3.8.3. Transmittance evaluation (T)

Transmittance evaluation is a fundamental method for verifying the transparency of a nanoformulation. This technique was done using a UV-6300PC Double Beam Spectrophotometer (VWR International, Lisbon, Portugal), as shown in Figure 16, operating at a wavelength of 700 nm, with purified water serving as the reference standard to quantify the degree of light penetration through the mixture. Furthermore, observing changes in these values provides a means to monitor the progression of the self-emulsification process. This specific methodology was employed as a screening tool to determine the feasibility of continuing with a formulation's analysis. A low transmittance value is typically associated with more substantial particle dimensions, allowing to identify unsuitable candidates early in the process. In contrast, elevated transmission levels signify the successful generation of minute nanoparticles, indicating that the formulation is suitable for advanced study (48).

Figure 16. UV-6300PC Double Beam Spectrophotometer by VWR International (Lisbon, Portugal).

3.8.4. Determination of CBD encapsulation efficiency

The encapsulation efficiency of CBD within the polymeric nanomicelles and SNEDDS was determined using an indirect quantification method based on chromatographic separation followed by UV spectrophotometric analysis. Four formulations were evaluated: S_LS_MCT_NaDC, S_LF_MCT_NaDC, PN_LF_P_SA 0.14%, and PN_LS_P_SA 0.14%.

3.8.4.1. Preparation of the CBD calibration curve

A calibration curve was initially prepared for CBD quantification. Standard CBD solutions were prepared in 70% ethanol through serial dilution to obtain concentrations of 1.6875, 3.375, 6.75, 12.5, 25, 50, 100, and 500 µg/mL. Absorbance measurements were

performed at 276 nm, selected based on a prior wavelength scan of CBD to identify its maximum absorption wavelength and to ensure minimal interference from formulation excipients, using a microplate reader (115). Linear regression analysis of absorbance versus concentration generated the following equation:

$$y = 0.0019x + 0.0003$$

where y corresponds to the absorbance value after blank subtraction and x represents the CBD concentration (µg/mL). The method demonstrated a coefficient of determination (R^2) of 0.9998.

3.8.4.2. Chromatographic separation

The separation of encapsulated and non-encapsulated CBD was performed using a 25 mL chromatographic column at room temperature under reduced light exposure conditions. Prior to sample application, the column was washed using 25 mL of the corresponding mobile phase. For SNEDDS formulations, NaDC solution was used as the mobile phase, while purified water was used for polymeric nanomicelles formulations. Initially, 4 mL of the corresponding blank formulation (without CBD) was loaded onto the column and allowed to elute completely. Subsequently, an additional 25 mL of the respective mobile phase was passed through the column, and the eluted fraction was collected as the blank control fraction in order to evaluate possible interference from the formulation excipients during UV analysis. After washing the column with 10 mL of the corresponding mobile phase, 4 mL of the CBD-loaded formulation was applied to the column. Once the sample had completely entered the column, an additional 25 mL of mobile phase was added and the eluted fraction containing the purified nanoformulations with encapsulated CBD was collected for analysis.

3.8.4.3. UV quantification and encapsulation efficiency calculation

After the separation, 200 µL of the collected samples were transferred to a 96-well microplate and analysed in triplicate ($n = 3$). Absorbance measurements were performed at 276 nm using a microplate reader. The concentration of encapsulated CBD was determined using the calibration curve equation shown in equation 2. The encapsulation efficiency (EE%) was subsequently calculated according to the following equation:

$$EE(\%) = \frac{\boldsymbol{Mass\ of\ encapsulated\ CBD}}{\boldsymbol{Total\ mass\ of\ CBD\ initially\ added}}\ \boldsymbol{x\ 100}$$

Equation 2. Encapsulation Efficiency equation.

3.8.5. MTT assay

The MTT assay is a widely used colorimetric method for the evaluation of cellular metabolic activity and is commonly applied as an indirect indicator of cell viability and cytotoxicity. The assay is based on the reduction of the tetrazolium salt 3-(4,5-dimethylthiazol-2-yl)-2,5-diphenyl-2H-tetrazolium bromide (MTT) into an insoluble coloured product known as formazan. This process occurs in metabolically active cells through intracellular redox reactions mediated by oxidoreductase and dehydrogenase enzymes, with electron donors such as NAD(P)H contributing to the reduction process (116). The amount of formazan formed is proportional to the metabolic activity of the cells and can be quantified spectrophotometrically after solubilisation, allowing the comparison of different experimental conditions. Due to its simplicity and reproducibility, the MTT assay is widely applied in studies assessing the biological effects of drugs and nanomaterials (117).

However, as the assay reflects metabolic activity rather than direct cell number, its results must be interpreted with caution, particularly in conditions where cellular metabolism may be affected independently of viability (116).

3.8.5.1. *In vitro* biological evaluation

MTT was conducted in both Caco-2 intestinal epithelial cells and SH-SY5Y neuroblastoma cell lines. Two different formulations were evaluated: polymeric nanomicelles (PN_P_LS_SA0.14%) and SNEDDS (S_LS_MCT_NaDC). For each formulation, both CBD-loaded and non-loaded (blank) formulations were previously prepared to serve as experimental controls.

The same protocol was applied to both cell lines, and all procedures were carried out under a laminar flow hood, except for the final step. A primary CBD stock solution was obtained by accurately weighing 3 mg of CBD and dissolving it in 1 mL of 70% ethanol. From this stock, three serial dilutions were prepared to obtain a total of four CBD concentrations for control purposes, as seen in Figure 17. Additional controls included 70% ethanol - as it was the medium used for dissolving the CBD controls - and water - as it was the medium used for the dilutions done for the formulations.

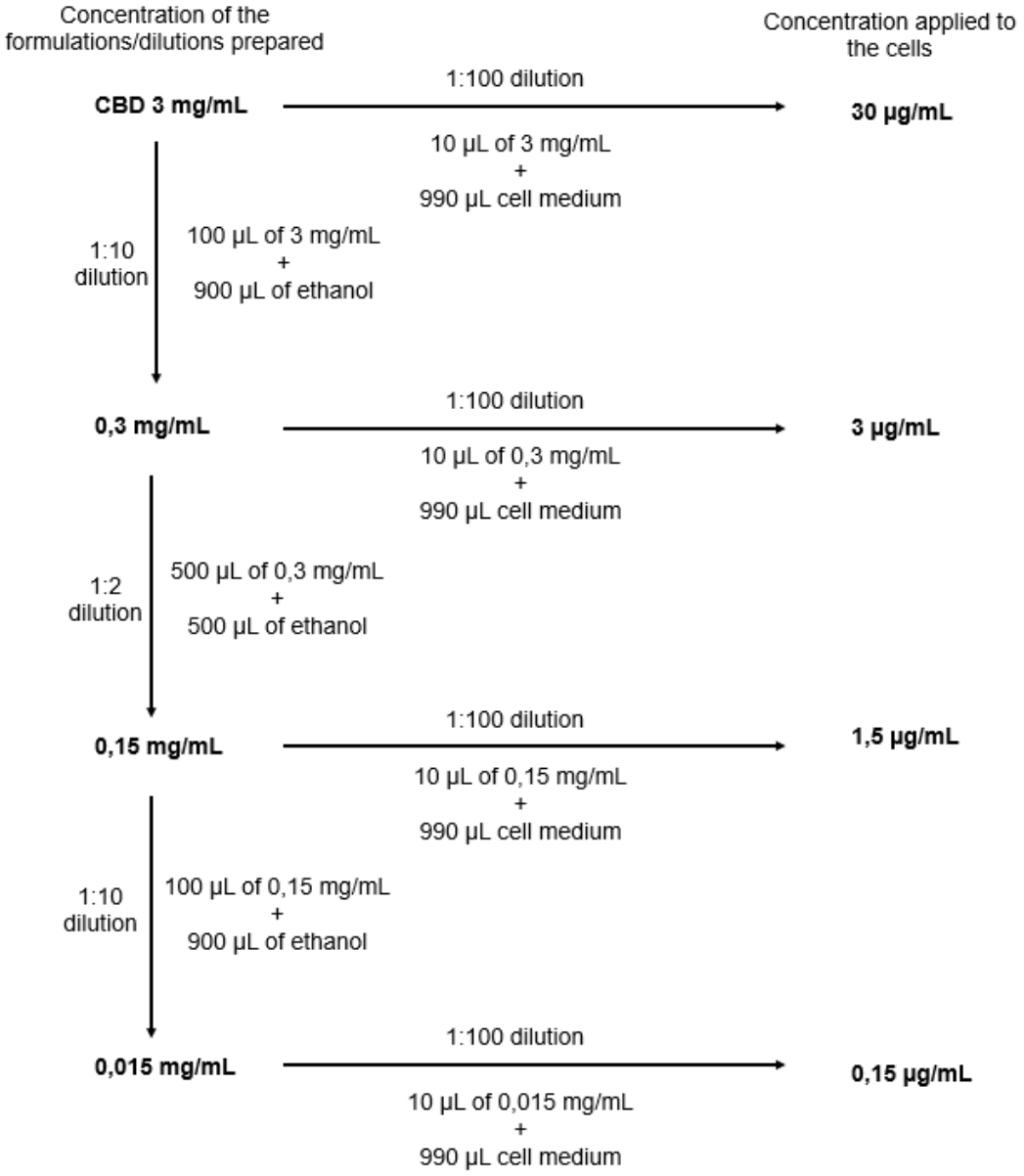

Figure 17. Schematic representation of the concentrations and dilutions used for the CBD control.

Subsequently, the formulations were diluted. Three serial dilutions were prepared for polymeric nanomicelles (both CBD-loaded and blank), whereas two dilutions were prepared for SNEDDS formulations (both CBD-loaded and blank), as illustrated in Figure 18 and 19, respectively. All formulation dilutions were prepared using purified water.

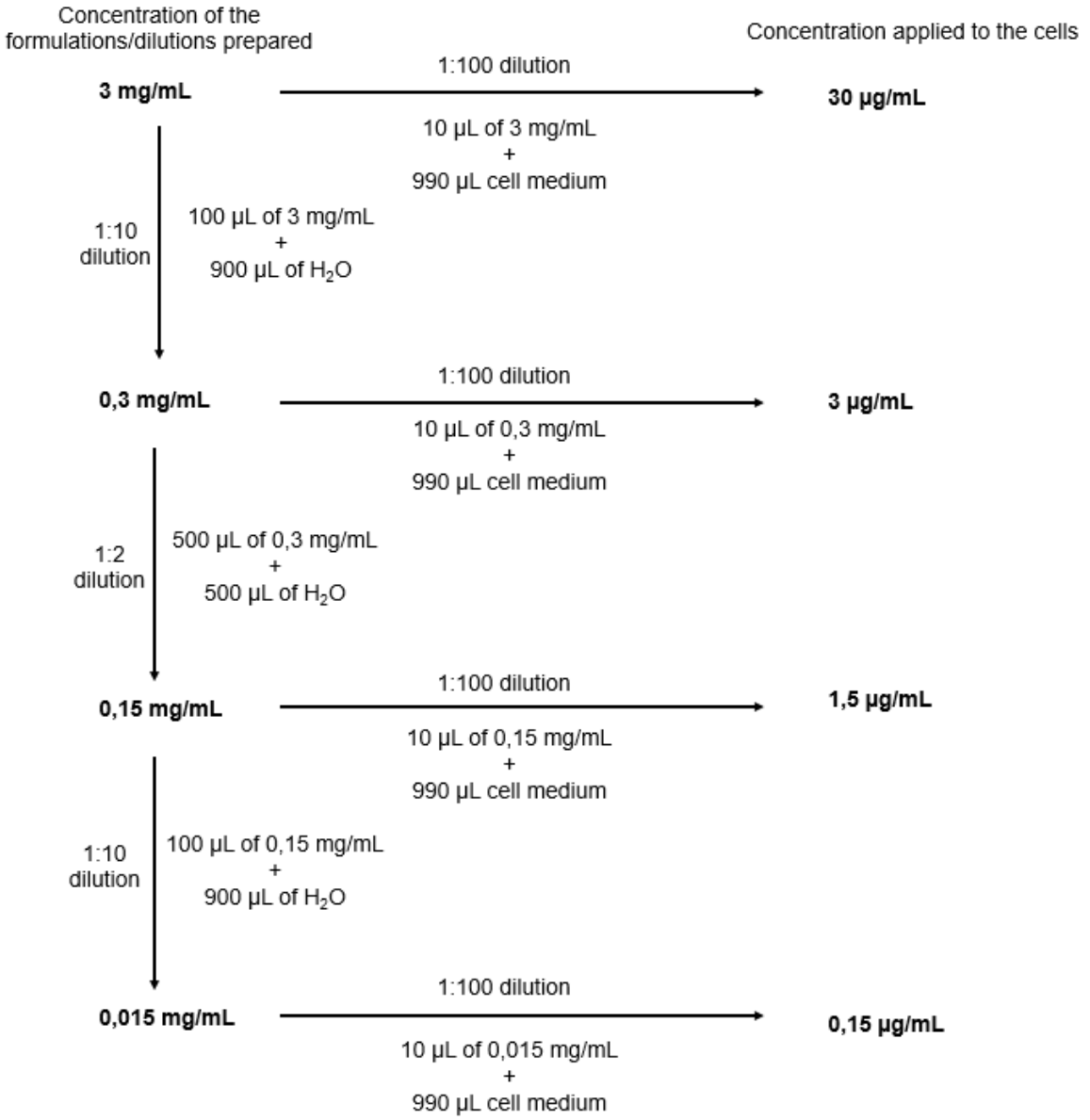

Figure 18. Schematic representation of the concentrations and dilutions used for the polymeric nanomicelles formulations with and without CBD.

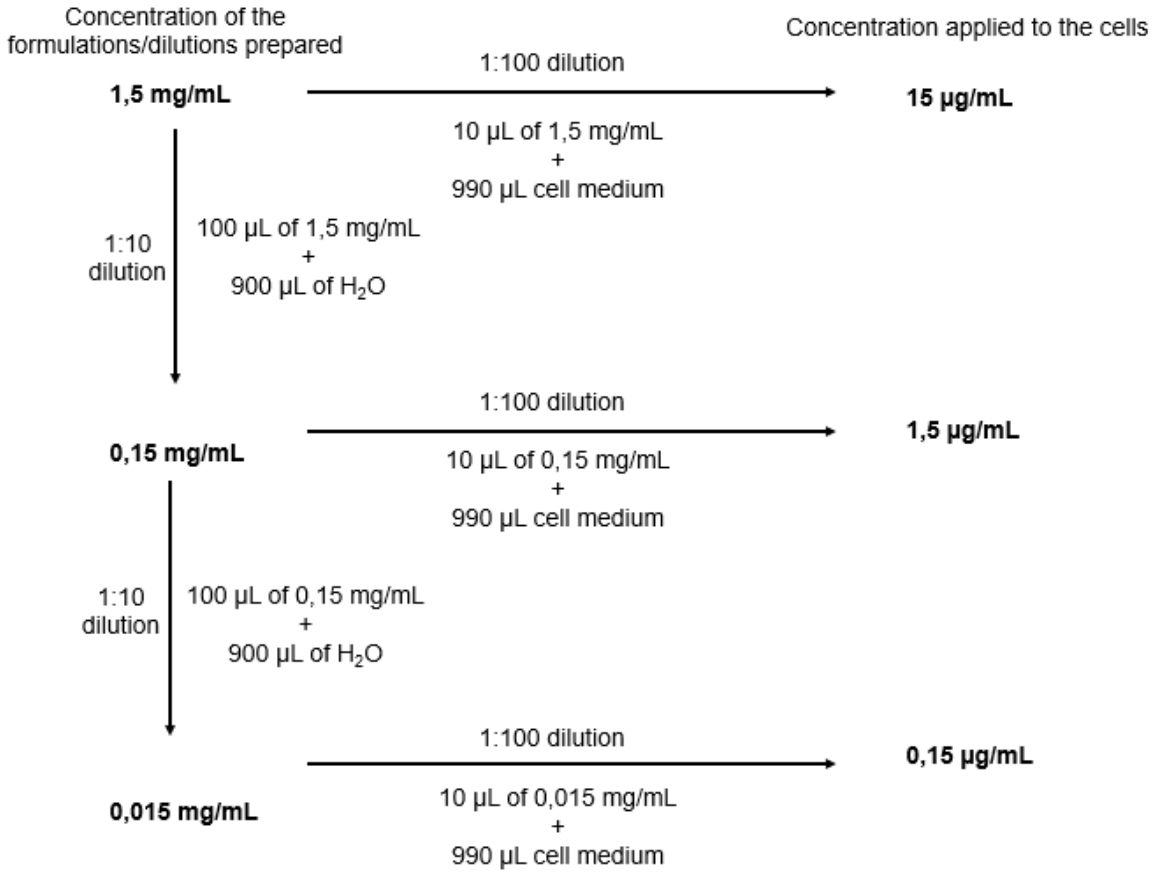

Figure 19. Schematic representation of the concentrations and dilutions used for the SNEDDS formulations with and without CBD.

For cell treatment, 10 µL of each test solution was mixed with 990 µL of serum-free cell culture medium (DMEM), as referred in figures 17, 18 and 19. The culture medium was then removed from 96-well plates containing adherent cells, and 200 µL of the prepared treatment solutions were added to each well. Each condition was performed in quadruplicate. The plates were subsequently incubated for 24 hours at 37ºC.

After 24 hours, the treatment medium was removed and 10 µL of MTT solution (5 mg/mL) together with 100 µL of fresh serum-free cell culture medium was added to each well. The plates were then incubated at 37°C for 3 hours in a cell incubator.

Following incubation, the work was no longer performed under the laminar flow hood. The MTT-containing medium was carefully removed and 200 µL of DMSO was added to each well. The 96-well plate was then shaken on a plate shaker for 10 minutes to ensure complete solubilisation. Finally, absorbance was measured at 550 nm and 650 nm; the

readings at 650 nm were used to correct for background noise by subtracting them from the values obtained at 550 nm, to obtain more accurate measurements. All calculations were then performed using these corrected absorbance values.

3.8.5.2. Statistical analysis

Statistical analysis was performed using GraphPad Prism 8 Software.

3.9. Stability study

A stability study was conducted to evaluate the physical stability of selected formulations under accelerated storage conditions. One polymeric nanomicelles formulation (PN_LF_P_SA) and one SNEDDS formulation (S_MCT_LF), emulsified in purified water and in sodium deoxycholate solution, were stored at 40 °C for four and five months, respectively. The pH of the formulations was monitored monthly throughout the storage period. In addition, visual inspection was performed to assess possible changes in appearance, including phase separation, precipitation, turbidity, or colour changes. Representative photographs were recorded during the study.

4. RESULTS/ DISCUSSION

4.1. Solubility and miscibility screening

Solubility and miscibility studies were carried out to support the selection of appropriate excipients for the development of both polymeric nanomicelles and SNEDDS formulations.

4.1.1. Solubility screening

For the solubility screening, 0.075 g of CBD was added to 5 g of each selected excipient, as previously described. Among the tested components, Tween 80® exhibited the slowest CBD solubilisation time, requiring approximately 13 min of continuous vortex to obtain a homogeneous system. In contrast, Labrafac™ Lipophile WL 1349, Labrafil® M 1944 CS and Capryol® 90 promoted a significantly faster apparent solubilisation of CBD, with homogeneous systems being obtained within less than 1 min. Compared to the remaining excipients, Labrasol® ASF demonstrated a moderately longer CBD solubilisation time, reaching complete visual homogenisation after approximately 1 min and 30 s. The specific solubilisation times observed as well as the visual appearance for each excipient are presented in Table 4. Representative images of the obtained systems immediately after vortex mixing are presented in Figure 20.

Table 4. Solubilisation time of CBD in selected excipients and corresponding visual appearance of the resulting systems.

Excipient	Solubilisation Time	Visual Appearance
Tween 80®	12 min 30 s	Clear homogeneous system.
Labrafac™ Lipophile WL 1349	45 s	Clear homogeneous system.
Labrafil® M 1944 CS	30 s	Homogeneous system with bubble formation, which dissipated upon standing.
Capryol® 90	56 s	Clear homogeneous system.
Labrasol® ASF	1 min 30 s	Homogeneous system with bubble formation, which dissipated upon standing.

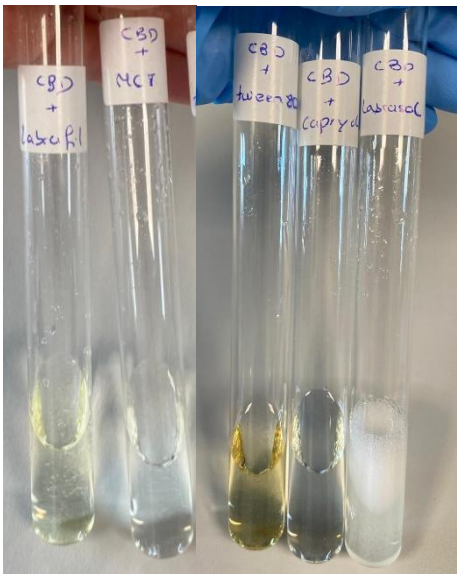

Figure 20. Representative visual appearance of the CBD-containing excipient systems immediately after vortex mixing. From left to right: Labrafil®, MCT, Tween 80®, Capryol® 90, and Labrasol® ASF formulations.

The observed differences in the solubilisation time may be related to the physicochemical properties of the excipients, particularly their viscosity and affinity for CBD. As CBD is a highly lipophilic compound (log P ~ 6.3) (53), it may exhibit greater affinity for lipid-based excipients with pronounced lipophilic characteristics, such as Labrafac™ Lipophile WL 1349 and Labrafil® M 1944 CS (118). In contrast, Tween 80® is a non-ionic surfactant with a high hydrophilic-lipophilic balance (HLB = 15) (53) and a comparatively higher viscosity than other surfactants, which may influence mass transfer and reduce the diffusion rate of CBD, potentially contributing to slower solubilisation.

However, a study evaluating the saturated solubility of CBD after 24 hours of equilibration, rather than the solubilisation kinetics, reported that CBD exhibited higher solubility in Tween 80® than in Labrasol® and Labrafil® M 1944 CS, which does not directly align with the slower solubilisation behaviour observed in the present work (53). These discrepancies may reflect the fact that equilibrium solubility and solubilisation rate are distinct parameters. While the literature supports the lipophilic nature of CBD and the surfactant characteristics of Tween 80®, the proposed influence of viscosity on CBD diffusion and solubilisation kinetics remains speculative and would require further investigation.

4.1.2. Miscibility screening

Miscibility studies were performed between the excipients to evaluate their ability to form homogeneous systems. For each mixture, 2 g of each excipient were combined and vortex mixed until a visually homogeneous system was obtained, as previously described.

Among the evaluated binary systems, Tween 80® combined with MCT, Labrafil® M 1944 CS, Capryol® 90, and Labrasol® ASF exhibited rapid miscibility, resulting in homogeneous systems within approximately 30 s of vortex mixing. Similarly, the ternary mixture with Tween 80®, MCT, and Labrafil® M 1944 CS also demonstrated rapid homogenisation, requiring approximately 30 s to obtain a visually uniform system. In contrast, the MCT and Labrafil® M 1944 CS binary mixture exhibited the slowest miscibility behaviour among the tested systems, requiring approximately 1 min and 30 s of vortex mixing to achieve visual homogenisation. The ternary mixture containing Tween 80®, Capryol® 90, and Labrasol® ASF also required a slightly longer mixing time, reaching a homogeneous appearance after approximately 1 min. The specific miscibility times and corresponding visual appearance of the evaluated systems are presented in Table 5. Representative images of the obtained mixtures immediately after vortex mixing are shown in Figure 21.

Table 5. Experimental miscibility times and corresponding visual appearance of the evaluated binary and ternary systems.

Excipient	Miscibility Time	Visual Appearance
Tween 80®+ MCT	30 s	Clear homogeneous system.
Tween 80®+ Labrafil®	30 s	Clear homogeneous system.
MCT+ Labrafil®	1 min 30 s	Clear homogeneous system.
MCT+ Labrafil®+ Tween 80®	30 s	Clear homogeneous system.
Tween 80®+ Capryol® 90	30 s	Clear homogeneous system.
Tween 80®+ Labrasol®	30 s	Homogeneous system with bubble formation, which dissipated upon standing.
Capryol® 90+ Labrasol®	20 s	Clear homogeneous system.
Tween 80®+ Capryol® 90+ Labrasol®	1 min	Homogeneous system with bubble formation, which dissipated upon standing.

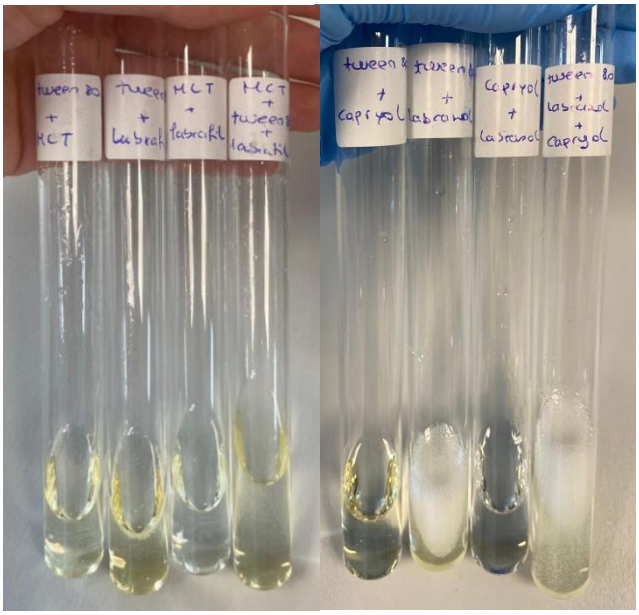

Figure 21. Representative visual appearance of the evaluated binary and ternary excipient mixtures immediately after vortex mixing. From left to right: Tween 80® + MCT, Tween 80® + Labrafil®, MCT + Labrafil®, MCT + Labrafil® + Tween 80®, Tween 80® + Capryol® 90, Tween 80® + Labrasol® ASF, Capryol® 90 + Labrasol® ASF, and Tween 80® + Capryol® 90 + Labrasol® ASF.

The rapid homogenisation observed in most binary and ternary systems containing Tween 80® (approximately 30 s) suggests that its amphiphilic nature may facilitate interactions between lipid and surfactant phases, thereby promoting the formation of homogeneous mixtures (53). In contrast, the slower miscibility observed for the binary mixture of MCT and Labrafil® M 1944 CS (approximately 1 min 30 s) may be related to differences in their fatty acid composition. MCT is mainly composed of saturated medium-chain fatty acids (C8-C10) (119), whereas Labrafil® consists predominantly of long-chain monounsaturated oleoyl glycerides (C18:1) (118). These differences in chain length, degree of saturation, and related physicochemical properties may influence the mixing behaviour, requiring longer vortex mixing to achieve a uniform system (119).

4.2. Physicochemical evaluation and optimisation of the formulations

4.2.1. DLS characterisation of polymeric nanomicelles

In the process of optimization of the CBD formulations, several parameters were adjusted to determine the most suitable system in terms of particle size, PDI, and surface charge. In some formulations, the pH was modified while the concentrations of the remaining components were kept constant. In others, the composition of the formulation

was changed while maintaining the same pH. It also happened that some components were modified or their concentration adjusted.

4.2.1.1. Effect of NaDC concentration variation in formulations prepared with different aqueous phases

The effect of NaDC concentration on the physicochemical properties of the formulations was initially evaluated using two different aqueous media: phosphate buffer and purified water.

To assess this effect, all excipients were maintained at constant concentrations, while the NaDC concentration in the aqueous phase was varied between 0.1%, 0.2%, 0.3%, and 0.4% (w/w), considering a final formulation weight of 25 g, as shown in table 6.

In the formulation codes, the suffix “PB” refers to formulations prepared with phosphate buffer, whereas “P” corresponds to formulations prepared with purified water. The NaDC concentration used in each formulation is indicated immediately after the “NaDC” designation.

At this stage of the study, the pH of the formulations was not adjusted, as the objective was solely to evaluate the influence of NaDC concentration and the effect of the different aqueous media on the formulation characteristics.

Table 6. Concentrations of the excipients used for each formulation prepared with PB as the aqueous medium.

Formulation	CBD (g)	Transcutol HP (g)	Labrafil® (g)	TPGS (g)	NaDC (g)	PB (g)
PN_LF_PB_NaDC 0.1%	0.075	0.389	0.380	2.476	0.025	21.655
PN_LF_PB_NaDC 0.2%	0.075	0.389	0.380	2.476	0.050	21.630
PN_LF_PB_NaDC 0.3%	0.075	0.389	0.380	2.476	0.075	21.605
PN_LF_PB_NaDC 0.4%	0.075	0.389	0.380	2.476	0.100	21.580

The results obtained for formulations prepared with phosphate buffer are presented in Table 7. A correlation between NaDC concentration and the measured physicochemical parameters was suggested, as shown in Figures 22 to 24.

Analysis of Figure 22 and Table 7, shows that all formulations presented relatively small particle sizes, with z-average values below 15 nm. Additionally, an increase in particle size was observed with increasing NaDC concentration. This behaviour may be attributed to the progressive incorporation or adsorption of NaDC molecules within the polymeric nanomicellar system, leading to an increase in the hydrodynamic diameter of the particles. However, no significant increase in particle size was observed between the formulations containing 0.3% and 0.4% NaDC. This behaviour may indicate that the system reached a saturation point, beyond which additional NaDC molecules could no longer be efficiently incorporated into the structures. Such a plateau may suggest that the nanomicellar system approached a structural saturation threshold, where the available sites for surfactant incorporation became limited (120).

A similar pattern was observed for the PDI, as shown in Figure 23. Increasing NaDC concentration resulted in higher PDI values, indicating a gradual increase in system heterogeneity. This increase may be associated with the progressive formation of mixed nanomicellar assemblies as NaDC is incorporated into the system. Nevertheless, the formulations containing 0.3% and 0.4% NaDC exhibited very similar PDI values (0.258 and 0.261, respectively), further supporting the hypothesis of saturation of the nanomicellar system at higher surfactant concentrations (120).

Regarding zeta potential, Figure 24 shows that increasing NaDC concentration resulted in progressively more negative surface charge values. This behaviour can be explained by the anionic nature of NaDC, which promotes the adsorption of deoxycholate ions onto the surface of the particles, thereby increasing the negative surface charge and consequently the magnitude of the zeta potential (121,122). However, the presence of phosphate ions and counterions in the buffer may also influence the measured zeta potential by compressing the electrical double layer surrounding the particles, leading to partial charge screening (41,73). Consequently, the zeta potential values obtained for formulations prepared with phosphate buffer likely reflect the combined effects of NaDC adsorption and electrostatic screening associated with the ionic composition of the medium (123).

Morever, interactions between other excipients and NaDC, such as oils or solubilisers, can further complicate the relationship between surfactant concentration and

zeta potential. These interactions can affect the adsorption of surfactant molecules onto the nanoparticle surface and alter the overall characteristics of the system (73,122).

Table 7. DLS values for formulations containing different NaDC concentrations in PB aqueous medium.

Formulation	Z-Average (nm)	PDI	Zeta-Potential (mV)	pH	T
PN_LF_PB_NaDC 0.1%	12.8	0.175	0.01	7.20	99.50%
PN_ LF_PB_NaDC 0.2%	13.7	0.223	-0.13	7.31	99.50%
PN_ LF _PB_NaDC 0.3%	14.6	0.261	-1.50	7.30	99.20%
PN_ LF_PB_NaDC 0.4%	14.6	0.258	-2.84	7.41	99.20%

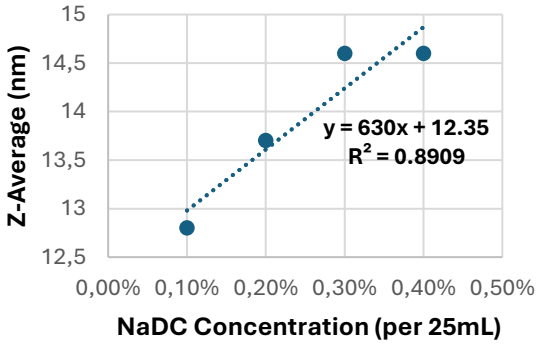

Figure 22. Effect of NaDC concentration on the z-average of formulations prepared with PB medium.

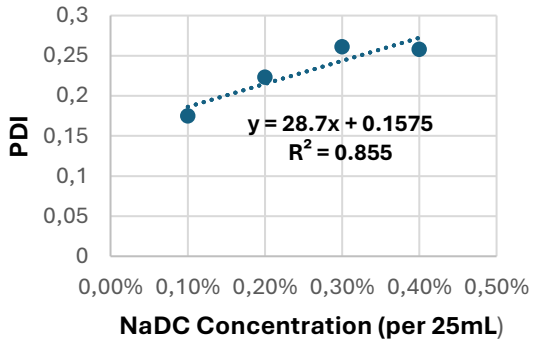

Figure 23. Effect of NaDC concentration on the PDI of formulations prepared with PB medium.

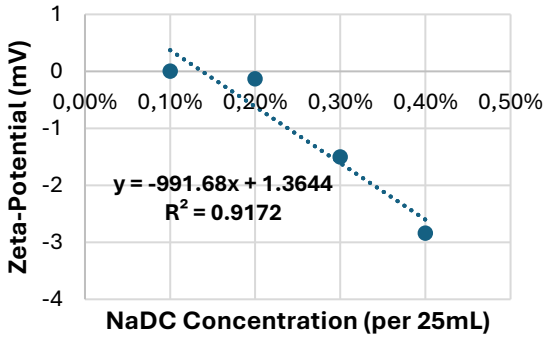

Figure 24. Effect of NaDC concentration on the Zeta Potential of formulations prepared with PB medium.

For the formulations prepared with purified water, the concentration used for each excipient was the same as the for the formulations where PB was the aqueous medium. The only change was the medium used in the formulations, as shown in Table 8.

Table 8. Concentrations of the excipients used for each formulation prepared with purified water as the aqueous medium.

Formulation	CBD (g)	Transcutol HP (g)	Labrafil® (g)	TPGS (g)	NaDC (g)	Purified water (g)
PN_LF_P_NaDC 0.1%	0.075	0.389	0.380	2.476	0.025	21.655
PN_LF_P_NaDC 0.2%	0.075	0.389	0.380	2.476	0.050	21.630
PN_LF_P_NaDC 0.3%	0.075	0.389	0.380	2.476	0.075	21.605
PN_LF_P_NaDC 0.4%	0.075	0.389	0.380	2.476	0.100	21.580

For the formulations prepared using purified water as the aqueous medium, the results shown in Table 9 suggest a correlation between NaDC concentration and both z-average particle size and PDI, as shown in Figures 25 and 26. An approximately linear relationship was observed for both parameters, with R^2 values of 0.8867 and 0.887 for particle size and PDI, respectively. In contrast to the formulations prepared with phosphate buffer, where a clear tendency between NaDC concentration and zeta potential was also observed, this behaviour was not evident for the purified water systems. This difference may be associated with the absence of background electrolytes in purified water, which reduces ionic strength and consequently decreases electrostatic screening effects (121,123). Under low ionic strength conditions, the electrical double layer surrounding colloidal particles is more extended, which can enhance the sensitivity of the measured zeta potential to changes in formulation composition (73). In contrast, phosphate buffer provides a higher ionic strength environment that promotes partial charge screening, resulting in more attenuated variations in surface potential across the formulations (73,124).

Particle size generally increased with increasing NaDC concentration. However, formulation PN_P_NaDC 0.3% presented a smaller particle size compared to formulation PN_P_NaDC 0.2%. This behaviour may indicate differences in the organisation of the

nanomicellar structures or variations in the incorporation and distribution of NaDC molecules within the system.

A similar pattern was observed for the PDI values, which increased with increasing NaDC concentration. This suggests that higher surfactant concentrations may promote greater system heterogeneity, resulting in broader particle size distributions. At the highest NaDC concentrations, PDI values reached 0.305 and 0.324, which are considered relatively high for colloidal systems. Such values suggest a loss of homogeneity within the formulation. In colloidal systems, PDI values above 0.3 have been associated with the presence of polydisperse populations and reduced structural uniformity, often reflecting dynamic aggregation or the coexistence of multiple particle populations within the system (122,123,125).

Regarding zeta potential, an increase in negative surface charge was initially observed between formulations PN_P_NaDC 0.1% and PN_P_NaDC 0.2%, with zeta potential values changing from -2.62 mV to -7.53 mV, respectively. However, at higher NaDC concentrations, the magnitude of the negative charge decreased, reaching -6.51 mV for formulation PN_P_NaDC 0.3% and -3.24 mV for formulation PN_P_NaDC 0.4%. This behaviour may be associated with saturation occurring at the nanoparticle interface. Since NaDC acts as an anionic surfactant, increasing its concentration initially promotes greater adsorption of deoxycholate ions onto the particle surface, resulting in more negative zeta potential values. However, beyond a certain concentration, saturation of the available adsorption sites may occur, as previously mentioned (85).

Considering that the CMC of NaDC ranges from approximately 2 to 6 mM (equivalent to 0.8291 - 2.4873 g/L), saturation may have been reached between formulations PN_P_NaDC 0.3% and PN_P_NaDC 0.4%, where NaDC concentrations corresponded to approximately 3 g/L and 4 g/L, respectively. Above the CMC, additional NaDC molecules are more likely to form micelles in the aqueous phase rather than adsorb onto the nanoparticle surface (85). Consequently, further increases in surfactant concentration may no longer enhance the negative surface charge. Furthermore, the increase in PDI observed at higher NaDC concentrations may suggest the coexistence of different particle populations within the system. Since DLS measurements are intensity-weighted, the presence of structures with different sizes may influence the reported average particle size and contribute to the non-linear behaviour observed for formulation PN_P_NaDC 0.3% (122). However, additional characterisation techniques would be required to confirm this hypothesis.

Additionally, reorganisation of surfactant molecules at the particle interface or partial desorption of deoxycholate ions into the aqueous medium may contribute to the reduction in surface charge density observed at higher NaDC concentrations (85). These may explain the reduced magnitude of the zeta potential values obtained for the formulations containing 0.3% and 0.4% NaDC.

Table 9. DLS values for formulations containing different NaDC concentrations in purified water.

Formulation	Z-Average (nm)	PDI	Zeta-Potential (mV)	pH	T
PN_LF_P_NaDC 0.1%	10.8	0.244	-2.62	6.84	99.20%
PN_ LF_P_NaDC 0.2%	15.6	0.296	-7.53	7.56	98.40%
PN_ LF_P_NaDC 0.3%	14.3	0.305	-6.51	7.56	99.20%
PN_LF_P_NaDC 0.4%	18.1	0.324	-3.24	7.69	99.90%

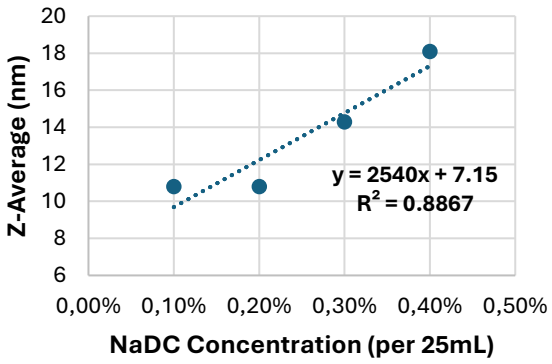

Figure 25. Effect of NaDC concentration on the z-average of formulations prepared with purified water.

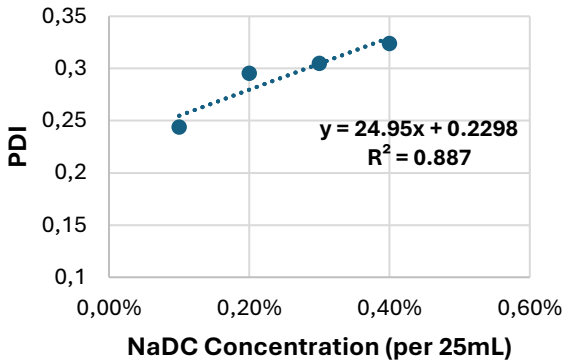

Figure 26. Effect of NaDC concentration on the PDI of formulations prepared with purified water.

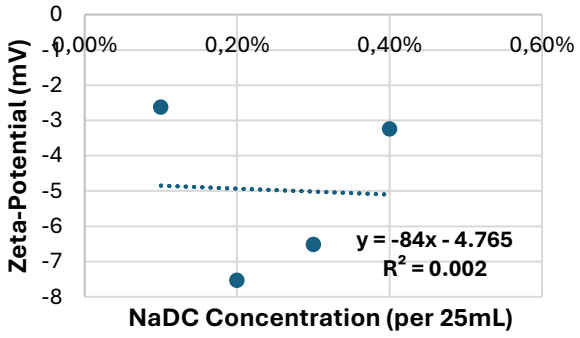

Figure 27. Effect of NaDC concentration on the Zeta Potential of formulations prepared with purified water.

Based on these results, purified water was selected as the aqueous medium for further studies due to the overall physicochemical behaviour of the formulations. In addition to being a simpler system with reduced ionic strength, formulations prepared with purified water consistently exhibited higher zeta potential values compared to those prepared with phosphate buffer. This may suggest improved electrostatic stabilisation of the particles in purified water, which is typically associated with enhanced colloidal stability.

Within the purified water formulations, the 0.2% NaDC system was selected for further development. This formulation showed the most negative zeta potential among the tested formulations, indicating stronger electrostatic repulsion between particles and potentially improved colloidal stability. For this reason, the 0.2% NaDC formulation was considered the most suitable for continuation of the study.

4.2.1.2. Effect of pH variation on formulations with NaDC

After selecting formulation PN_LF_P_NaDC 0.2%, the effect of pH on the physicochemical properties of the system was further investigated. A pH range between 6.5 and 8.0 was evaluated, and the average of the values obtained are presented in Table 10. The composition of the formulation was the same as described in Table 8 for the PN_LF_P_NaDC 0.2% formulation.

Table 10. DLS parameters of formulations containing 0.2% NaDC prepared at different pH values.

Formulation	Z-Average (nm)	PDI	Zeta-Potential (mV)	pH	T
PN_LF_P_NaDC 0.2%_6.5	13.4	0.256	-6.01	6.51	97.80%
PN_LF_P_NaDC 0.2%_7	11.8	0.271	-3.16	7.03	99.30%
PN_LF_P_NaDC 0.2%_7.5	15.6	0.283	-6.61	7.49	98.95%
PN_LF_P_NaDC 0.2%_8	32.9	0.322	-4.83	7.98	98.30%

As shown in Figures 28 and 30, no clear linear relationship was observed between pH and either z-average or zeta potential. However, the formulations prepared at higher pH values exhibited a tendency towards increased PDI values, as shown in Figure 29.

While formulations prepared at pH 6.5, 7.0, and 7.5 presented relatively small particle sizes (from 13.4 to 15.6 nm), a substantial increase in particle size was observed at pH 8.0, reaching 32.9 nm. Similarly, PDI values increased progressively with increasing pH, from 0.256 at pH 6.5 to 0.322 at pH 8.0. Previous studies have demonstrated that sodium deoxycholate aggregates are highly sensitive to pH and ionic conditions, with changes in these parameters affecting the size and organisation of the assemblies (123,124). Although the specific trends reported in the literature may differ from those observed in the present study, these findings collectively highlight the strong influence of pH on the physicochemical behaviour of bile salt-based systems (123). Such differences may arise from variations in formulation composition, the presence of additional excipients, and the complex intermolecular interactions governing nanomicellar systems (42,122). In the present work, this pH sensitivity is particularly evident at pH 8.0, where a marked increase in particle size and PDI was observed, suggesting a deviation from the behaviour seen at lower pH values.

The increase in PDI suggests greater heterogeneity within the system at higher pH values, leading to broader particle size distributions. In particular, the PDI value obtained at pH 8.0 exceeded 0.3, which is generally associated with reduced formulation homogeneity and lower colloidal stability (126). These changes may be related to alterations in the ionisation state of the excipients as pH increases, which can affect intermolecular interactions and the structural organisation of the nanomicellar system. Such changes may promote particle aggregation or reduced uniformity at higher pH values (127).

Regarding zeta potential, the formulation prepared at pH 7.5 presented the most negative zeta potential value (-6.61 mV) among the tested formulations. Although the zeta potential values obtained were relatively low overall, the formulation with a pH of 7.5 combined the most negative surface charge with a relatively small particle size (15.6 nm) and an moderate PDI value (0.283). Therefore, pH 7.5 was selected for the preparation of the subsequent formulations, as it presented the most favourable balance between particle size, dispersity, and surface charge.

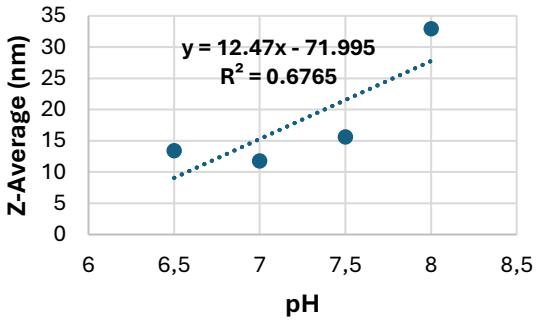

Figure 28. Effect of the variation of pH in the z-average parameter.

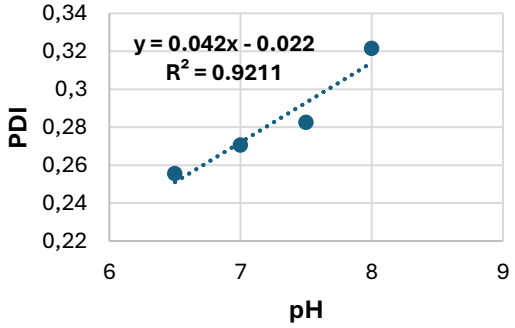

Figure 29. Effect of the variation of pH in the PDI parameter.

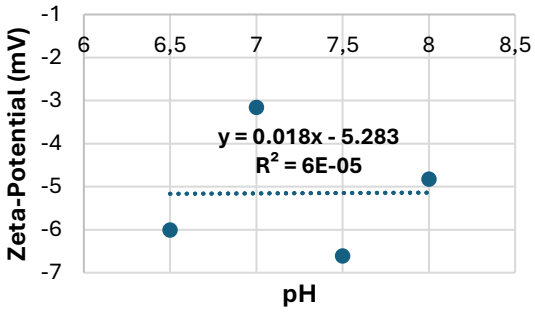

Figure 30. Effect of the variation of pH in the zeta potential parameter.

4.2.1.3. Effect of change of Transcutol® HP concentration on the formulation parameters

To evaluate the effect of Transcutol® HP on the physicochemical properties of the formulation, its concentration was reduced from 0.389 g to 0.200 g, as shown in Table 11. This adjustment was performed to investigate whether lowering the concentration of Transcutol could improve the characteristics of the formulation. The corresponding DLS results, presented in Table 12, correspond to the average values obtained from two independent measurements. The effect of reducing the Transcutol concentration on the physicochemical properties of the formulation was evaluated by comparing the modified formulation with the previously selected PN_LF_P_NaDC 0.2%_7.5 system.

Table 11. Concentration of the excipients used in the formulation with reduced Transcutol® concentration.

Formulation	CBD (g)	Transcutol HP (g)	Labrafil® (g)	TPGS (g)	NaDC (g)	Purified water (g)
PN_LF_P_NaDC 0.2%_t	0.075	0.200	0.380	2.476	0.050	21.819

Table 12. DLS parameters of the formulation with reduced Transcutol® concentration.

Formulation	Z-Average (nm)	PDI	Zeta-Potential (mV)	pH	T
PN_LF_P_NaDC 0.2%_t	11.9	0.282	- 4.40	7.50	98.65%

A decrease in particle size was observed, with the z-average decreasing from 15.6 nm to 11.9 nm. This behaviour may suggest that lower concentrations of Transcutol favour the formation of a more compact system. Transcutol® HP acts as a co-solvent and penetration enhancer and has been reported to influence the internal organisation and interfacial properties of lipid-based nanosystems. Variations in its concentration may affect the packing of the nanostructures and consequently influence particle size and surface characteristics (48,64). However, no significant improvement was observed for the remaining physicochemical parameters, as the PDI values remained essentially unchanged, indicating that the reduction in Transcutol concentration did not substantially improve formulation homogeneity.

Additionally, the magnitude of the zeta potential decreased from -6.61 mV to -4.40 mV, indicating a reduction in the negative surface charge of the particles. This reduction in zeta potential may indicate that decreasing the amount of Transcutol® altered the interfacial organisation of the formulation, affecting the exposure and distribution of charged species at the particle surface (64,128). Similar effects have been reported for co-solvent-containing lipid-based systems, where changes in co-solvent concentration can influence the arrangement of interfacial components and consequently modify electrokinetic properties (48). These findings are in line with previous reports describing the sensitivity of lipid-based nanostructures to variations in co-solvent content (48,128), although the magnitude of the zeta potential reduction observed here appears more pronounced than that typically reported in simpler systems (122,128).

Since the optimisation strategy aimed to obtain formulations with more negative zeta potential values, in order to favour electrostatic stabilisation, this result was not considered advantageous. Therefore, although the reduction in Transcutol® concentration resulted in smaller particle size, the absence of significant improvements in dispersity and the reduction in zeta potential magnitude indicated that this modification was not beneficial for the overall optimisation of the formulation. For this reason, formulations containing such a low concentration of Transcutol® were not further pursued.

4.2.1.4. Replacement of NaDC with sodium alginate in the formulation

In an attempt to increase the negative surface charge of the formulation, NaDC was replaced with sodium alginate, an anionic polymer containing ionisable carboxyl groups. For the initial formulation design, a molar ratio of 1:15 (sodium alginate: Vitamin E TPGS) was selected, considering a molecular weight of 198 g/mol for the sodium alginate repeating unit. Based on the amount of Vitamin E TPGS used in the formulation (2.476 g), this corresponded to an initial sodium alginate concentration of 0.022 g, as shown in Table 13.

At this stage of the study, the influence of different surfactants on the physicochemical properties of the formulations was also investigated by comparing Labrafil® and Labrasol® based systems.

Table 13. Concentration of the excipients used in the PN_LF_P_SA formulation.

Formulation	CBD (g)	Transcutol HP (g)	Labrafil® (g)	TPGS (g)	SA (g)	Purified water (g)
PN_LF_P_SA	0.075	0.389	0.380	2.476	0.022	21.658

Following the replacement of NaDC with sodium alginate, the effect of pH on the physicochemical properties of the formulation containing Labrafil® as surfactant was evaluated. As performed for the previous formulations, a pH range between 6.5 and 8.0 was tested in order to determine the most suitable pH conditions for the sodium alginate-based system. The corresponding DLS results are presented in Table 14.

Table 14. DLS values for formulations with the sodium alginate, prepared at different pH values.

Formulation	Z-Average (nm)	PDI	Zeta-Potential (mV)	pH	T
PN_LF_P_SA_6.5	17.5	0.230	-8.32	6.47	98.35%
PN_LF_P_SA_7	18.3	0.233	-9.14	6.97	97.60%
PN_LF_P_SA_7.5	19.3	0.247	-8.68	7.49	97.70%
PN_LF_P_SA_8	19.7	0.247	-5.49	7.97	97.60%

Overall, the formulations exhibited relatively small particle sizes, PDI values below 0.3, and high transmittance percentages across the pH tested, indicating the formation of homogeneous systems.

A slight increase in particle size can be observed with increasing pH, with values ranging from 17.5 nm at pH 6.5 to 19.7 nm at pH 8.0, as shown in Figure 31. A similar tendency was observed for the PDI values, which increased from 0.230 to 0.247 as pH increased, as observed in Figure 32. The increase in particle size and PDI at higher pH values may be related to changes in the ionisation state of sodium alginate. As pH increases, a greater proportion of the carboxylic acid groups present in sodium alginate becomes ionised (99).

Regarding zeta potential, the sodium alginate-based formulations exhibited slightly more negative values compared to the NaDC formulations. The most negative value was obtained for the formulation prepared at pH 7.0 (-9.14 mV). However, the overall improvement was relatively limited, as all zeta potential values remained below -10 mV, indicating limited electrostatic stabilisation of the formulations. The limited increase in zeta potential magnitude, despite the introduction of an anionic polymer such as sodium alginate, may be partially explained by the presence of the PEGylated TPGS corona (93). The PEG chains may contribute to a shielding effect, increasing the distance between the charged groups and the shear plane, thereby reducing the measured electrophoretic mobility (128). Similar masking effects of surface charge by PEG-containing surfactants have been previously reported in colloidal systems (48). At pH values above 7.0, the magnitude of the zeta potential progressively decreased, reaching - 5.49 mV at pH 8.0, as shown in Figure 33. This behaviour may indicate that increased ionisation of sodium alginate at higher pH leads to conformational rearrangements that reduce the effective exposure of charged groups at the particle interface (124,128).

Although the formulation prepared at pH 7.0 exhibited the most negative zeta potential value, the differences observed between pH 7.0 and pH 7.5 were relatively small. Additionally, the formulation prepared at pH 7.5 maintained acceptable particle size, PDI, and surface charge values. Therefore, pH 7.5 was selected for subsequent studies in order to maintain consistency with the previously optimised formulations and facilitate comparison between the different formulation systems.

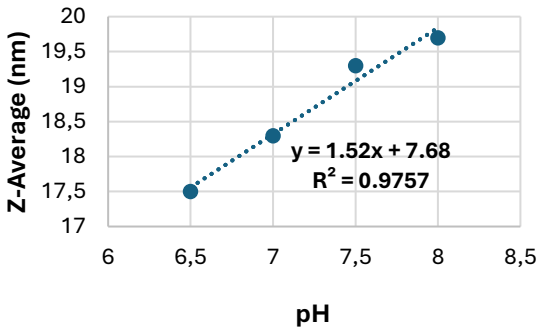

Figure 31. Effect of the variation of pH in the z-average parameter.

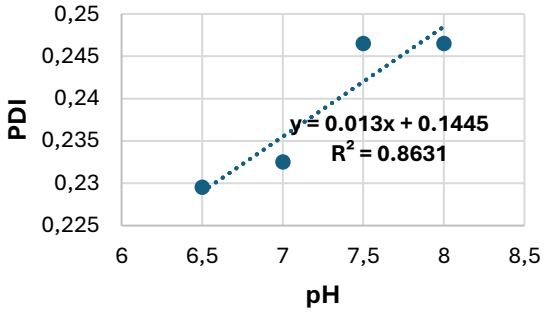

Figure 32. Effect of the variation of pH in the PDI parameter.

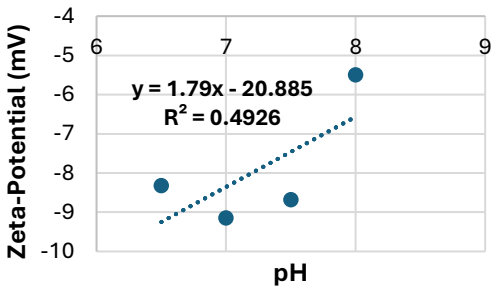

Figure 33. Effect of the variation of pH in the zeta potential parameter.

4.2.1.5. Effect of different concentrations of sodium alginate and different surfactants in the formulation

To further assess whether more negative zeta potential values could be achieved, the concentration of sodium alginate was increased to 0.12%, 0.14%, and 0.16% (w/w), as shown in Table 15. Two groups of formulations were prepared using the same sodium alginate concentrations and overall composition, differing only in the surfactant used. One set of formulations was prepared with Labrafil®, while the other was prepared with Labrasol®. This approach allowed the evaluation of the effect of sodium alginate concentration as well as the influence of surfactant type on the physicochemical properties of the formulations.

Table 15. Composition of the formulations containing different sodium alginate concentrations, prepared with either Labrafil® or Labrasol®.

Formulation	CBD (g)	Transcutol HP (g)	Labrafil®/ Labrasol® (g)	TPGS (g)	SA (g)	Purified water (g)
PN_P_SA	0.075	0.389	0.380	2.476	0.022	21.658
PN_P_SA 0.12%	0.075	0.389	0.380	2.476	0.030	21.650
PN_P_SA 0.14%	0.075	0.389	0.380	2.476	0.035	21.645
PN_P_SA 0.16%	0.075	0.389	0.380	2.476	0.040	21.640

The DLS results obtained for the formulations prepared with Labrafil® are presented in Table 16. Analysis of Figures 34 to 36 indicates that no clear correlation was observed between sodium alginate increased concentration and the DLS parameters. All formulations exhibited relatively small particle sizes, ranging from 17.7 to 20.7 nm, as well as low PDI values (<0.250), indicating the formation of homogeneous systems with small particle size distributions.

Although no consistent relationship between the concentration of sodium alginate and particle size or PDI was observed, changes in zeta potential values were detected with increasing polymer concentration. The formulation containing 0.14% sodium alginate exhibited the most negative zeta potential value (-13.58 mV), followed by the 0.16% formulation (-10.91 mV). These values were more negative than those previously obtained for the formulations containing lower sodium alginate concentrations, suggesting that increasing the concentration of sodium alginate may contribute to enhanced surface charge density due to the presence of additional ionised carboxyl groups (129,130). However, this effect was not linear, as the formulation containing 0.12% sodium alginate presented a less negative zeta potential value (-7.31 mV) than the initial formulation. Similar non-linear behaviours have been reported in polymer-containing colloidal systems, where increasing polymer concentration initially enhances the density of ionisable groups at the particle surface, resulting in more negative zeta potential values (122). However, beyond a certain concentration, conformational rearrangements of the polymer chains, interfacial saturation (128), or shielding effects caused by counter-ions may limit further increases in surface charge and even reduce the measured zeta potential magnitude (73,123). These mechanisms may contribute to the behaviour observed for the 0.16% sodium alginate formulation.

Overall, the lack of a clear trend across the evaluated concentrations suggests that further experiments are required to better elucidate the observed behaviour. In particular, performing additional measurements in triplicate would provide improved statistical reliability and a more robust understanding of the influence of sodium alginate concentration on the system.

Among the evaluated formulations, the system containing 0.14% sodium alginate presented the most favourable balance between particle size, dispersity, and zeta potential, particularly due to its more negative surface charge, which may contribute to improved electrostatic stabilisation when compared to the remaining formulations

Table 16. DLS values for formulations containing different sodium alginate concentrations, with Labrafil® as the surfactant.

Formulation	Z-Average (nm)	PDI	Zeta-Potential (mV)	pH	T
PN_LF_P_SA	19.3	0.247	-8.68	7.49	97.70%
PN_LF_P_SA 0.12%	17.7	0.228	-7.31	7.42	97.20%
PN_LF_P_SA 0.14%	20.7	0.238	-13.58	7.53	96.14%
PN_LF_P_SA 0.16%	18.8	0.233	-10.91	7.44	97.55%

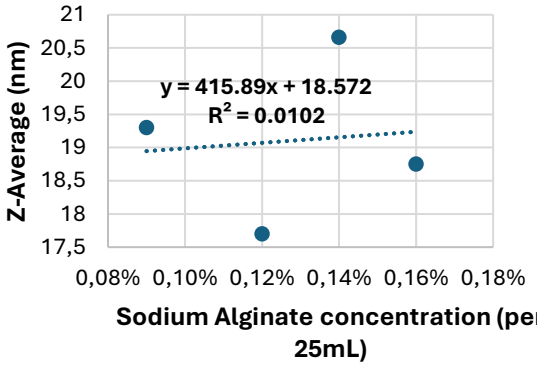

Figure 34. Effect of SA concentration on the particle size of Labrafil® - based formulations.

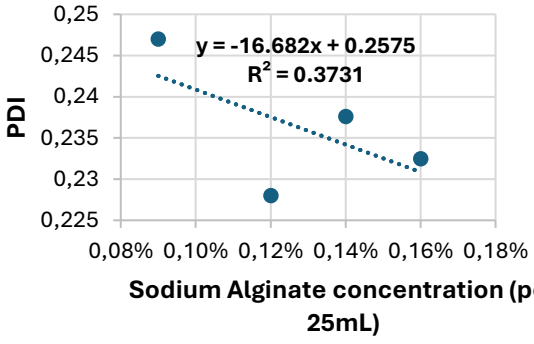

Figure 35. Effect of SA concentrations on the PDI of Labrafil® - based formulations.

.

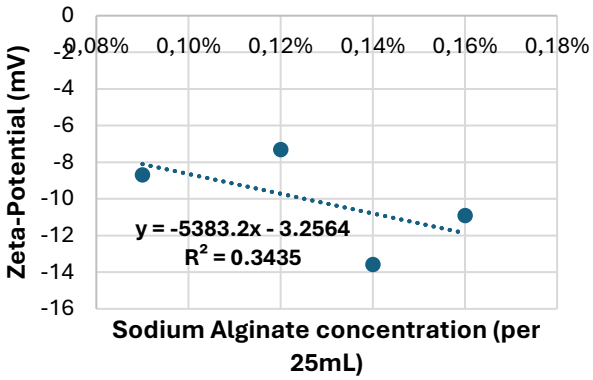

Figure 36. Effect of SA concentrations on the zeta potential of Labrafil® - based formulation.

The formulations prepared with Labrasol® had the same excipient concentrations as the corresponding Labrafil® formulations, with the only difference being the surfactant employed, as shown in Table 15. Similar to the previous formulations, no clear relationship was observed between sodium alginate concentration and the DLS parameters evaluated, as shown in Figures 37 to 39.

Overall, the formulations exhibited small particle sizes (from 16.0 to 17.3 nm) and low PDI values (<0.270), as shown in Table 17. In contrast, a effect was observed on zeta potential values. At the lowest concentration, formulation PN_LS_P_SA, exhibited a near-neutral surface charge (-0.06 mV), indicating a contribution of SA to surface charge. Upon increasing the concentration to 0.12%, a marked shift towards more negative values was observed (-9.94 mV), reaching a maximum at 0.14% (-13.10 mV), in formulation PN_LS_P_SA 0.14%. However, a further increase to 0.16% resulted in a reduction in the magnitude of the zeta potential (-7.46 mV), indicating a non-linear behaviour that could be associated with surface saturation or rearrangement at the particle interface.

Table 17. DLS values for formulations containing different sodium alginate concentrations, with Labrasol® as the surfactant.

Formulation	Z-Average (nm)	PDI	Zeta-Potential (mV)	pH	T
PN_LS_P_SA	17.3	0.265	-0.06	7.40	98.30%
PN_LS_P_SA 0.12%	16.0	0.245	-9.94	7.51	98.50%
PN_LS_P_SA 0.14%	17.2	0.251	-13.10	7.46	97.53%
PN_LS_P_SA 0.16%	16.5	0.246	-7.46	7.49	98.00%

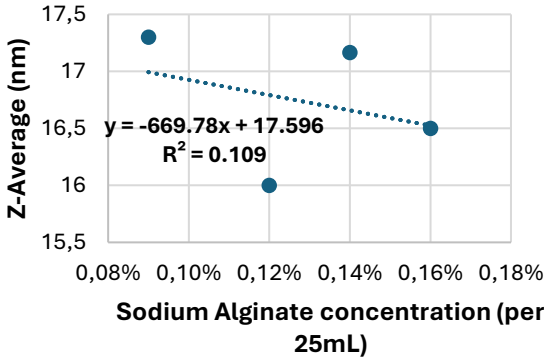

Figure 37. Effect of different SA concentrations on the particle size of Labrasol®- based formulations.

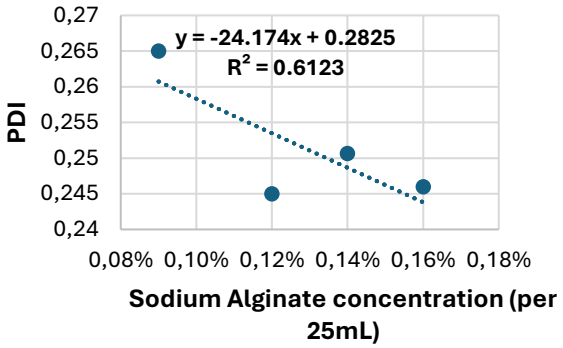

Figure 38. Effect of different SA concentrations on the PDI of Labrasol®- based formulations.

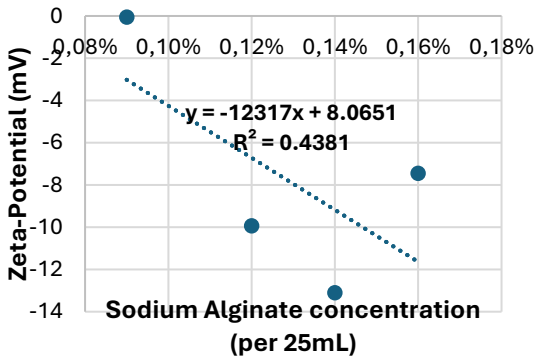

Figure 39. Effect of different SA concentrations on the zeta potential of Labrasol®- based formulations.

Comparing Labrafil® and Labrasol® formulations, both systems produced nanometric particles with moderate PDI values (<0.300). Labrasol® - based formulations exhibited smaller particle sizes, whereas both surfactant systems generally presented similar zeta potential values, with the most negative surface charge being observed around 0.14% sodium alginate. The smaller particle sizes observed for the Labrasol® formulations may be related to the physicochemical characteristics of this surfactant. Labrasol® contains mainly medium-chain glycerides and possesses a higher HLB value than Labrafil® (73,131), which has been reported to favour the formation of smaller colloidal structures and improve interfacial curvature in lipid-based delivery systems (132). In contrast, the longer-chain fatty acid derivatives present in Labrafil® may promote the formation of slightly larger nanostructures (48,131). Similar differences between medium- and long-chain lipid excipients have been previously described in self-emulsifying and nanomicellar systems (131).

However, the Labrasol® formulation PN_LS_P_SA, exhibited a substantially more neutral zeta potential value (-0.06 mV) compared to the corresponding Labrafil® formulation

(-8.68 mV). As this discrepancy is not consistent with the behaviour observed for the remaining formulations and parameters, it may be related to experimental variability rather than a true surfactant effect. Therefore, additional studies with a higher number of replicates, would be necessary to obtain more robust conclusions regarding the influence of the surfactant on the formulation.

4.2.1.6. Effect of reduced Transcutol® concentration on formulation properties

To evaluate the effect of Transcutol® concentration on the physicochemical properties of the formulations, its quantity was reduced from 0.389 g to 0.200 g, as shown in Table 18. This modification was performed to assess whether decreasing the concentration of Transcutol® could influence the surface charge of the particles, similarly to what had previously been investigated for the NaDC-containing formulations.

Table 18. Composition of the formulations containing different sodium alginate concentrations, prepared with either Labrafil® or Labrasol® and a reduced Transcutol® concentration.

Formulation	CBD (g)	Transcutol HP (g)	Labrafil®/ Labrasol® (g)	TPGS (g)	SA (g)	Purified water (g)
PN_P_SA	0.075	0.200	0.380	2.476	0.022	21.847
PN_P_SA 0.12%	0.075	0.200	0.380	2.476	0.030	21.839
PN_P_SA 0.14%	0.075	0.200	0.380	2.476	0.035	21.834
PN_P_SA 0.16%	0.075	0.200	0.380	2.476	0.040	21.829

The DLS results obtained for the formulations prepared with Labrafil® as surfactant are presented in Table 19, whereas the corresponding results for the Labrasol® formulations are shown in Table 20. For the Labrafil® - based formulations, the standard sodium alginate concentration formulation (PN_LF_P_SA) was also included for comparison purposes. In the case of the Labrasol® formulations, only the systems containing 0.14% and 0.16% sodium alginate were evaluated.

Analysis of Figures 40 to 42 indicates that no clear correlation was observed between sodium alginate concentration and the evaluated DLS parameters in the Labrafil®

formulations. Although the z-average values shown in Figure 40 presented a relatively high coefficient of determination (R^2 = 0.9231), the particle sizes obtained for the 0.14% and 0.16% formulations were identical. Therefore, this apparent correlation should be interpreted cautiously, as it may not represent a true concentration-dependent effect.

It is also possible to observe, from the results presented in Table 20, that the Labrasol® - based formulations generally exhibited smaller particle sizes compared to the corresponding Labrafil® systems. In contrast, the Labrafil® formulations tended to present lower PDI values, indicating slightly narrower particle size distributions and greater formulation homogeneity. These differences are consistent with the trends previously observed for the corresponding systems and further highlight the influence of surfactant type on the physicochemical characteristics of the formulations (131,132), particularly in terms of interfacial packing and nanostructure organisation.

Regarding zeta potential, the standard Labrafil® formulation exhibited the most negative surface charge among the Labrafil® systems. However, both Labrasol® formulations presented even more negative zeta potential values, reaching -15.09 mV and -15.81 mV for PN_LS_P_SA_0.14%_t and PN_LS_P_SA_0.16%_t, respectively. The higher negative zeta potential observed in the Labrasol® - based formulations after reduction of Transcutol® may be associated with changes in the interfacial organisation of the system (128). A decrease in co-solvent content can reduce interfacial fluidisation, potentially affecting the spatial arrangement and exposure of charged species at the particle surface (48,128). Differences in surfactant architecture may further influence the extent of electrostatic shielding within the nanomicellar corona, thereby modulating the measured surface charge (73,128).

However, to accurately assess the influence of surfactant type on formulation behaviour, additional studies including a higher number of concentrations, would be necessary to obtain more robust and reliable conclusions.

Table 19. DLS values for Labrafil® formulation with different SA concentrations and reduced Transcutol® concentration.

Formulation	Z-Average (nm)	PDI	Zeta-Potential (mV)	pH	T
PN_LF_P_SA_t	18.5	0.234	-11.32	7.49	97.93%
PN_LF_P_SA_0.14%_t	18.2	0.223	-10.35	7.47	97.10%
PN_LF_P_SA_0.16%_t	18.2	0.230	-6.30	7.47	96.90%

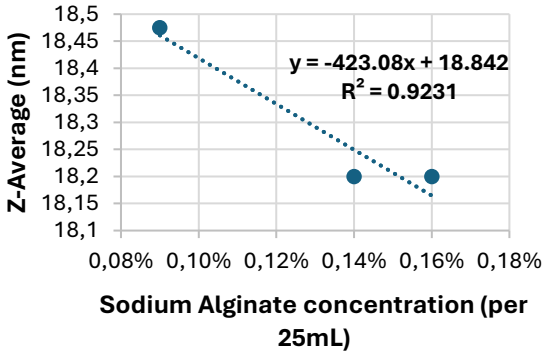

Figure 40. Effect of SA concentration in the z-average of Labrafill® formulations with reduced Transcutol®.

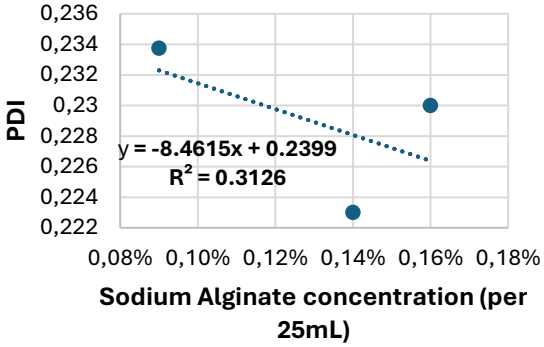

Figure 41. Effect of SA concentration in the PDI of Labrafil® formulations with reduced Transcutol®.

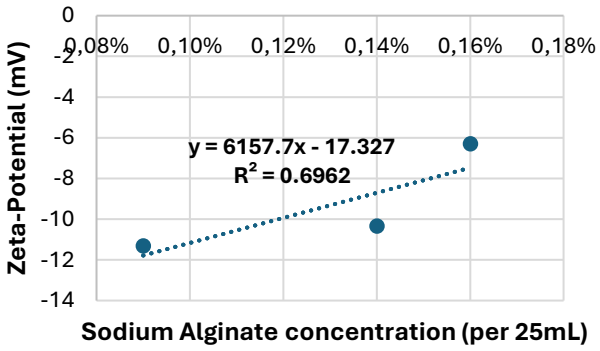

Figure 42. Effect of SA concentration on zeta potential of Labrafill® formulations with reduced Transcutol®.

Table 20. DLS values for Labrasol® formulations with different SA concentrations and reduced Transcutol®.

Formulation	Z-Average (nm)	PDI	Zeta-Potential (mV)	pH	T
PN_LS_P_SA_0.14%_t	17.3	0.253	-15.09	7.5	97.20%
PN_LS_P_SA_0.16%_t	17.2	0.255	-15.81	7.5	97.10%

Figures 43 to 48 present the physicochemical properties of formulations prepared with standard and reduced Transcutol® concentrations for both Labrafil® and Labrasol® systems.

In the Labrafil® - based systems (Figure 43 to 45), the formulation containing 0.14% sodium alginate (PN_LF_P_SA 0.14%_t) showed slightly lower particle size and PDI values compared to its corresponding formulation prepared with the standard Transcutol® concentration, indicating a minor improvement in size distribution. This may be attributed to the function of Transcutol® as a co-solvent, which can modify interfacial fluidity and affect the packing of surfactant molecules at the oil–water interface (64). Additionally, this formulation exhibited a decrease in zeta potential when compared to the PN_LF_P_SA 0.14% formulation. Changes in surface charge magnitude are often associated with modifications in the interfacial layer, which can influence the degree to which ionisable groups are exposed at the particle surface (128). However, this behaviour was not consistently observed for the remaining formulations, suggesting that the effect of reducing Transcutol® concentration may not follow a clear trend within the studied systems. A further decrease in zeta potential was observed for PN_LF_P_SA 0.16%_t (−6.30 mV), compared to the corresponding standard formulation (−10.91 mV).

For the Labrasol® - based systems (Figure 46 to 48), the effect of reducing Transcutol® concentration on particle size and PDI was not pronounced, with only minor variations observed and no clear trend across formulations. However, the formulations PN_LS_P_SA 0.14%_t and PN_LS_P_SA 0.16%_t exhibited more negative zeta potential values (-15.09 mV and -15.81 mV, respectively), compared to the corresponding standard formulation, suggesting a slight increase in surface charge magnitude under reduced Transcutol® conditions in these specific systems. This increase may indicate a reorganisation of the nanomicellar corona, where anionic species become more exposed at the particle surface due to reduced co-solvent fluidisation, as previously mentioned.

Overall, these results suggest that the effect of Transcutol® concentration on the physicochemical properties of the nanomicellar systems is subtle and dependent on formulation composition. While some isolated differences were observed, particularly in zeta potential for specific Labrasol® - based formulations, no consistent trend was identified across all systems. Further studies with additional replicates would be necessary to confirm these observations and better elucidate the role of Transcutol® in these formulations.

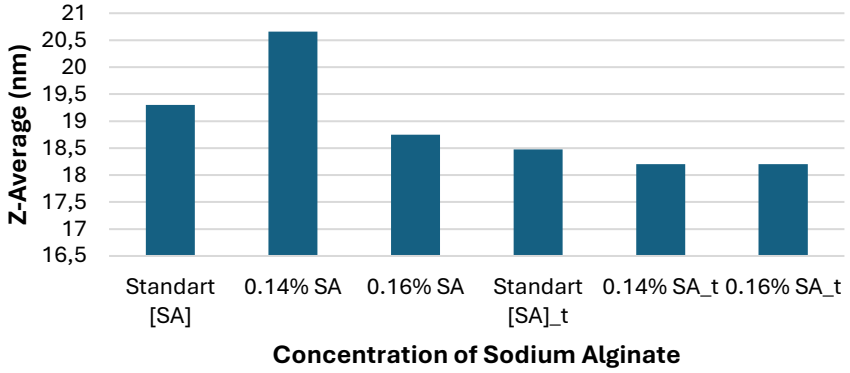

Figure 43. Effect of SA concentration on z-average in Labrafill® formulations without and with reduced Transcutol®.

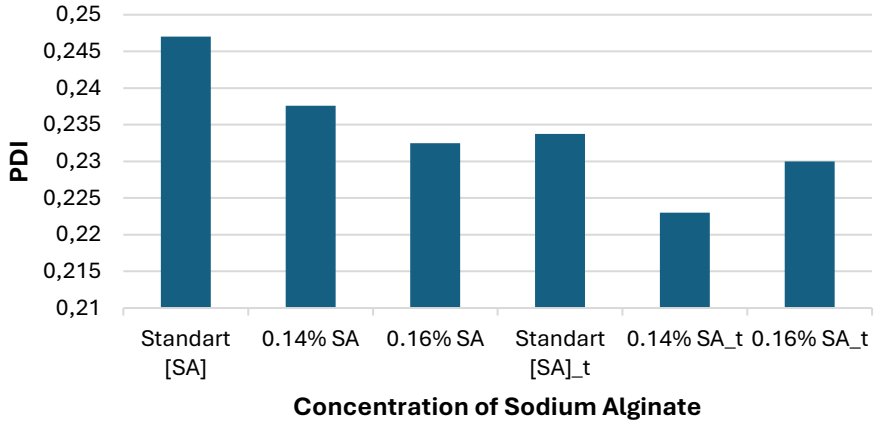

Figure 44. Effect of SA concentration on PDI in Labrafill® formulations without and with reduced Transcutol®.

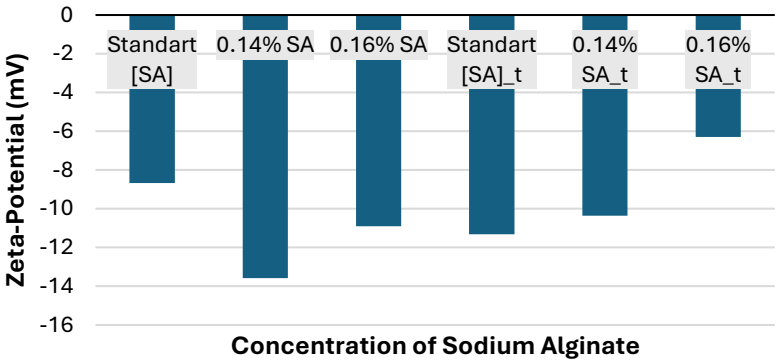

Figure 45. Effect of SA concentration on zeta potential in Labrafill® formulations without and with reduced Transcutol®.

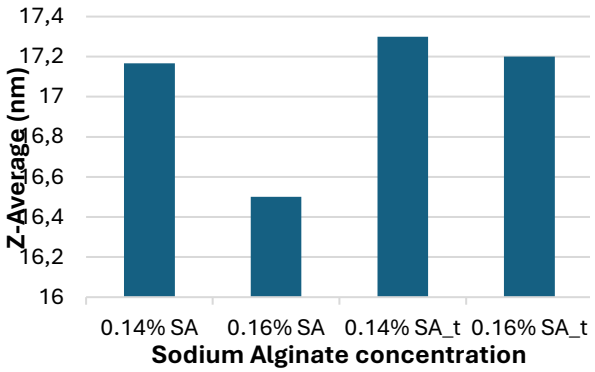

Figure 46. Effect of SA concentration on z-average in Labrasol® formulations without and with reduced Transcutol®.

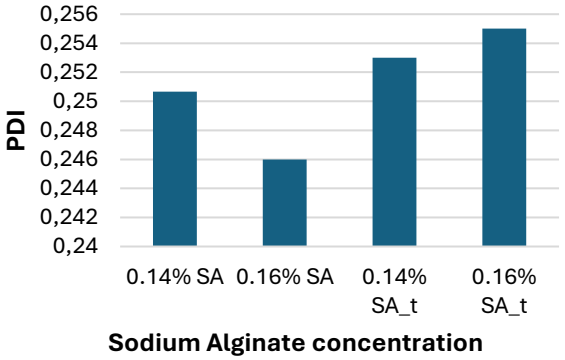

Figure 47. Effect of SA concentration on PDI in Labrasol® formulations without and with reduced Transcutol®.

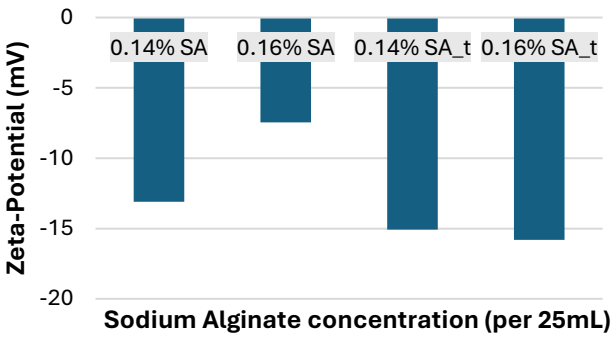

Figure 48. Effect of SA concentration on zeta potential in Labrasol® formulations without and with reduced Transcutol®.

4.2.2. SNEDDS development

In the process of development of the SNEDDS formulations, different surfactants and oils were evaluated in order to obtain the most optimised system. For it, the order of the components added during formulation preparation was also tested to assess its influence on the physicochemical parameters. The concentrations used for each component was also tested throughout the optimisation process.

Transmittance evaluation was used as an initial screening method to assess whether the formulations were within the nanoscale range. Since nano-sized systems generally exhibit transparent or translucent appearances and high transmittance values, this parameter was used as a preliminary indicator of successful nanoemulsion formation and to determine whether the formulations should proceed to further characterisation studies (48,128).

The CBD concentration used in the SNEDDS formulations was the same as that previously used for the polymeric nanomicelles (0.075 g). However, CBD was not initially incorporated into the first developed formulations, as these preliminary studies were focused on evaluating the ability of the systems to form nano-sized formulations. CBD was only added after formulations exhibiting high transmittance values, indicative that nanoscale systems had been successfully obtained.

4.2.2.1. Optimisation of the excipients concentrations

For the initial formulations, MCT, Tween 80®, and Labrafil® were selected as excipients. Table 21 presents the concentrations used for each component, as well as the modifications performed throughout the formulation optimisation process. The order of addition of the excipients followed the same sequence in which they are presented in the table, with all formulations prepared to a final mass of approximately 5 g.

The first set of concentrations tested for formulation 1, identified as condition 1 in Table 21, presented an opaque, whitish appearance, as shown in Figure 49. Due to this result, the concentrations of Labrafil® and Tween 80® were inverted, as indicated in condition 2 in Table 21. This modification resulted in a substantially more transparent system, as shown in Figure 50. Tween 80® is a highly hydrophilic surfactant with a high HLB value (73), whereas Labrafil® is more lipophilic and viscous (68). Increasing the relative proportion of Tween 80® may enhance the reduction of interfacial tension and favour the spontaneous formation of smaller droplets (48), which is commonly associated with increased transparency in SNEDDS systems (64,128).

Subsequently, the concentration of MCT was reduced from 1.242 g to 1.000 g, and the removed amount was redistributed either to Tween 80® (condition 3) or to Labrafil® (condition 4). The resulting transmittance values were 98.70% and 95.90% for conditions 3 and 4, respectively, with the corresponding formulations shown in Figures 51 and 52. Although the difference between both systems was relatively small, condition 3 was selected for further studies due to its higher transmittance value, suggesting the formation of a more transparent nano-sized system. The lower transmittance observed for condition 4 may be associated with its higher Labrafil® concentration, which, as previously discussed, could favour the formation of larger droplets due to the more lipophilic and viscous nature of this component. In addition, increasing the oil-to-surfactant ratio generally requires a larger interfacial area to be stabilised during emulsification, which may favour the formation of larger droplets and consequently lower transmittance values (64,67,128).

Table 21. Composition of formulation 1 and the concentration modifications performed throughout the optimisation process, identified by the corresponding numbers shown above.

Components	1	2	3	4
MCT	1.242 g	1.242 g	1.000 g	1.000 g
Labrafil®	2.980 g	0.746 g	0.746 g	0.987 g
Tween 80®	0.746 g	2.980 g	3.202 g	2.980 g

Figure 49. Condition 1 for formulation 1.

Figure 50. Condition 2 for formulation 1.

Figure 51. Condition 3 for formulation 1.

Figure 52. Condition 4 for formulation 1.

Next, CBD was incorporated into condition 3 of formulation 1, with the corresponding 0.075 g being deducted from the Tween 80® concentration. This study was performed in triplicate, resulting in an average transmittance value of 96.83%. These results suggest that the incorporation of CBD did not significantly affect the transparency or overall characteristics of the formulation. This behaviour may indicate that the amount of CBD incorporated remained within the solubilisation capacity of the system and did not promote

droplet growth or phase separation (51,64). The resulting formulation was identified as S_MCT_LF_P, with the suffix “P” indicating that the emulsification process was performed using purified water as the aqueous phase. Due to the high transmittance obtained, indicating the maintenance of a nano-sized system, the formulation S_MCT_LF was subsequently characterised by DLS in order to determine the z-average, PDI, and zeta potential values.

For formulation 2, MCT was replaced with Capryol®, while the remaining components, concentrations, and order of addition were maintained identical to those used in condition 3 of formulation 1 (S_MCT_LF_P). In this case, Capryol® was the first component added during the process. The obtained transmittance values were 12.90%, when the emulsification process was performed using purified water, and 15.00% when NaDC 0.8 g/L was used as the aqueous phase. These low transmittance values, together with the opaque appearance of the systems shown in Figure 53, indicate that the formed particles were not within the nanoscale range. The poor transmittance obtained with Capryol® may be related to differences in polarity and compatibility between the oil phase and the selected surfactants (132). Efficient spontaneous emulsification depends on favourable interactions between the excipients, and inadequate compatibility may result in larger droplets and reduced transparency (48,128). Therefore, this formulation was not further characterised or developed.

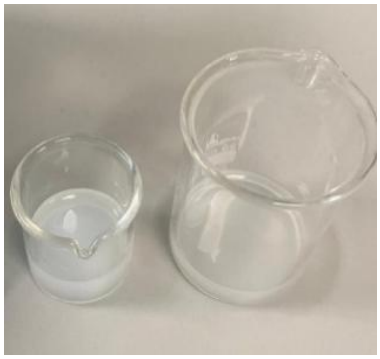

Figure 53. Formulation 2 emulsified in purified water (left) and NaDC 0.8 g/L (right).

For formulation 3, Capryol® was maintained as the oil phase, as in formulation 2, while Labrafil® was replaced with Labrasol® in order to evaluate the effect of the surfactant on the formulation properties. This modification resulted in a more transparent system compared to formulation 2, with a transmittance value of 73.70% when emulsified in purified water, as shown in Figure 54. Labrasol® possesses a higher HLB value and greater

hydrophilic character than Labrafil® (68,69), which may facilitate interfacial tension reduction and favour the formation of smaller droplets during emulsification (48,64). This formulation was identified as S_C_LS_P and, due to its favourable preliminary characterisation results, was further analysed by DLS.

Figure 54. Appearance of formulation 3 emulsified in purified water.

4.2.2.2. Characterisation of formulations using DLS

At this stage, the studies focused on the formulations previously developed, maintaining the same component concentrations while evaluating the effect of the order of the excipients added on the physicochemical properties of the systems. During this phase, all formulations contained incorporated CBD, and no pH adjustment was performed, as pH is not expected to significantly influence SNEDDS performance and delivery. All presented results correspond to the average values obtained from the performed duplicates/triplicates.

For formulation S_MCT_LF, the z-average, PDI, and zeta potential were determined after emulsification in purified water and NaDC 0.8 g/L (used to simulate bile salt conditions), with the obtained results presented in Table 22.

Analysing the results obtained for formulations S_MCT_LF_P and S_MCT_LF_NaDC, both systems presented high transmittance values (98.30% and 98.60%, respectively), indicating the successful formation of transparent nanoscale dispersions. This is further supported by the Z-average values, with particle sizes of 31.4 nm for S_MCT_LF_P and 43.1 nm for S_MCT_LF_NaDC, confirming that the self-emulsifying capability of the formulation was maintained under both aqueous conditions. However, the formulation emulsified in NaDC 0.8 g/L exhibited a larger particle size and higher PDI value (0.285) compared to the formulation emulsified in purified water (0.176).

This behaviour may suggest that the presence of NaDC, affects the interfacial organisation of the nanoemulsion droplets. Bile salts are known to interact with surfactant layers and may alter droplet structure and size distribution (122,124). Nevertheless, both PDI values remain below 0.30, indicating moderate homogeneity and the absence of significant aggregation (125).

Regarding zeta potential, the formulation emulsified in purified water presented an almost neutral value (0.61 mV), whereas the system emulsified in NaDC exhibited a slightly more negative surface charge (−1.26 mV). Although both values remain close to neutrality, the more negative zeta potential observed in the presence of NaDC is likely associated with the adsorption of deoxycholate ions by the nanoemulsion (122). Despite this effect, the surface charge values remain low, suggesting that the stability of both systems is predominantly governed by steric stabilisation mechanisms provided by the non-ionic surfactants rather than electrostatic repulsion (48,67).

Overall, both formulations demonstrated good structural integrity and maintained nanoscale characteristics under the tested conditions, although the presence of NaDC appeared to slightly increase particle size and dispersity.

Table 22. DLS values for formulation S_MCT_LF emulsification in purified water and NaDC 0.8 g/L.

Formulation	Z-Average (nm)	PDI	Zeta-Potential (mV)	pH	T
S_MCT_LF_P	31.4	0.176	0.61	5.8	98.30%
S_MCT_LF_NaDC	43.1	0.285	-1.26	7.45	98.60%

In an attempt to improve the physicochemical properties of the formulation and evaluate the influence of the order of excipient addition on formulation behaviour, the order of incorporation of MCT and Labrafil® was modified, with Labrafil® being added first and MCT second. Tween 80® was consistently added as the final excipient, while the concentrations of all other excipients were maintained unchanged. The resulting formulation was subsequently emulsified in purified water, NaDC 0.8 g/L, and HCl solution at pH 1.2 (133). The acidic medium was included to simulate gastric conditions and evaluate the influence of a highly acidic environment on the physicochemical parameters of the system, since gastrointestinal fluids may reach very low pH values (133). The obtained z-average, PDI, and zeta potential results are presented in Table 23.

The results obtained for the S_LF_MCT formulation indicate that changing the order of the excipients addition may have influenced the physicochemical properties of the system. Although all formulations maintained high transmittance values (>96%), confirming the formation of transparent nanoscale dispersions, an increase in particle size was observed when compared to the previous S_MCT_LF systems. The Z-average values ranged from approximately 52.7 to 55.1 nm (Figure 55). This observation suggests that changing the order of component addition may affect the self-assembly process and consequently influence droplet size.

The PDI values remained below 0.300 for all formulations, as shown in figure 56, indicating acceptable homogeneity and the absence of major aggregation.

Regarding zeta potential, observing figure 57, its possible to conclued that the emulsification medium had an effect on the surface charge. The formulation emulsified in purified water presented a slightly negative zeta potential (−2.17 mV), while the formulation emulsified in HCl exhibited an almost neutral value (0.73 mV). In contrast, the system emulsified in NaDC 0.8 g/L showed a substantially more negative zeta potential (−15.84 mV). This behaviour may be attributed to the interaction of deoxycholate ions with the droplet interface, leading to increased exposure of negatively charged species and consequently more negative zeta potential values. Similar effects have been reported for bile salt-containing colloidal systems (122,124).

Overall, the results suggest that the order of component addition may influence droplet formation and interfacial organisation within the SNEDDS system. Furthermore, the emulsification medium appears to play a significant role in determining the surface charge of the formulations, particularly in the presence of bile salt, such as NaDC.

Table 23. Effect of the emulsification medium on the DLS parameters of the S_LF_MCT formulation.

Formulation	Z-Average (nm)	PDI	Zeta-Potential (mV)	pH	T
S_LF_MCT_P	54.0	0.257	-2.17	5.87	96.70%
S_LF_MCT_NaDC	55.1	0.282	-15.84	7.57	97.90%
S_LF_MCT_HCl	52.7	0.257	0.73	1.15	97.15%

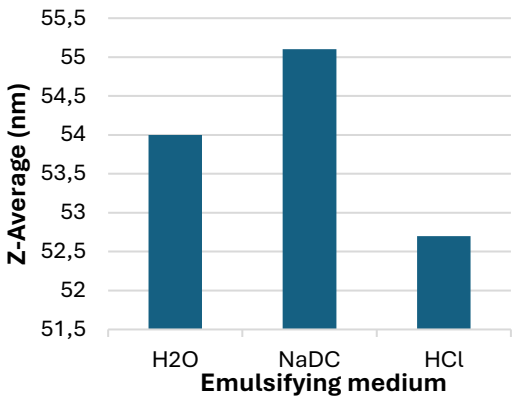

Figure 55. Z-average values of the S_LF_MCT formulation after emulsification in different media.

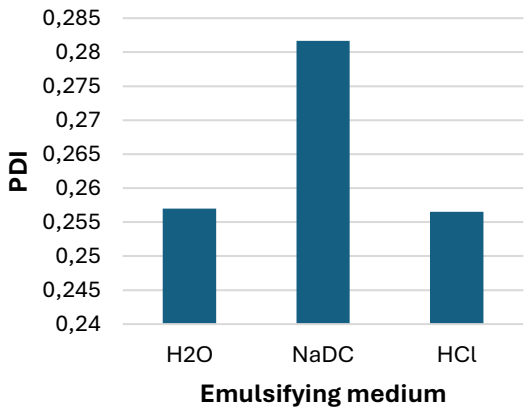

Figure 56. PDI values of the S_LF_MCT formulation after emulsification in different media.

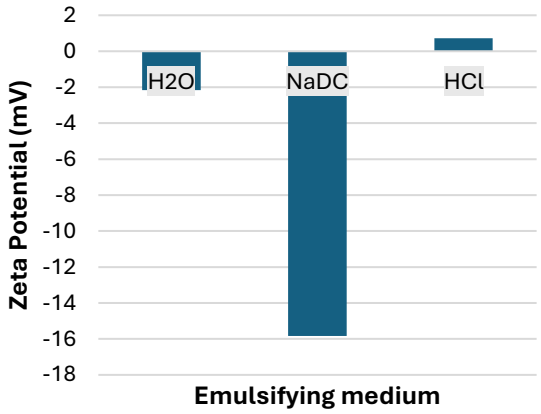

Figure 57. Zeta potential values of the S_LF_MCT formulation after emulsification in different media.

Next, Labrafil® was replaced with Labrasol® in order to evaluate the influence of surfactant type on the physicochemical properties of the formulation. The resulting formulation was identified as S_LS_MCT. The DLS results obtained for this formulation after emulsification in different media are presented in Table 24.

The results obtained demonstrate that replacing Labrafil® with Labrasol® had a significant impact on the physicochemical properties of the formulation. All formulations presented very high transmittance values (>99%), indicating the formation of highly transparent nanoscale dispersions, independently of the emulsification medium used.

Compared to the corresponding Labrafil® - based formulations (S_LF_MCT), the Labrasol® systems exhibited considerably smaller particle sizes, with Z-average values ranging between 18.7 and 21.0 nm, as shown in Figure 58, whereas the Labrafil® formulations presented values above 50 nm. These results suggest that Labrasol® promotes more efficient self-emulsification and the formation of smaller droplets, likely due to its higher hydrophilic character and HLB value (48).

Regarding PDI, the Labrasol® formulations emulsified in purified water and HCl presented lower values (0.149 and 0.152, respectively) compared to the corresponding Labrafil® systems, indicating improved homogeneity and narrower size distributions. However, the formulation emulsified in NaDC exhibited a higher PDI value (0.248), suggesting that the presence of bile salts may influence the interfacial organisation of the droplets and slightly increase size distribution heterogeneity (122). Nevertheless, all PDI values remained below 0.300, indicating acceptable formulation uniformity (125), as shown in Figure 59.

The zeta potential values, shown in Figure 60, also showed a strong dependence on the emulsification medium. The formulation emulsified in purified water presented the most negative surface charge (-10.54 mV), indicating improved electrostatic stabilisation compared to the corresponding Labrafil® formulation (-2.17 mV). In contrast, the NaDC-emulsified formulation exhibited a less negative zeta potential (-3.70 mV). This behaviour differs from that observed for the corresponding Labrafil® formulation, where NaDC promoted a substantial increase in negative surface charge. These results suggest that the effect of bile salts on the interfacial properties of the system may depend on the surfactant composition and the arrangement of the interfacial layer (122,132). The formulation emulsified in HCl presented a zeta potential value of 2.22 mV, which may be related to changes in the physicochemical properties of the formulation under highly acidic conditions.

Overall, the results indicate that replacing Labrafil® with Labrasol® may improve the self-emulsifying properties of the system, resulting in smaller particle sizes and lower PDI values. Furthermore, the different emulsification media significantly influenced the surface charge of the formulations, particularly under NaDC and acidic conditions.

Table 24. Effect of the emulsification medium on the DLS parameters in the S_LS_MCT formulation.

Formulation	Z-Average (nm)	PDI	Zeta-Potential (mV)	pH	T
S_LS_MCT_P	18.7	0.149	-10.54	6.14	99.50%
S_LS_MCT_NaDC	18.9	0.248	-3.70	7.59	99.57%
S_LS_MCT_HCl	21.0	0.152	2.22	1.06	99.30%

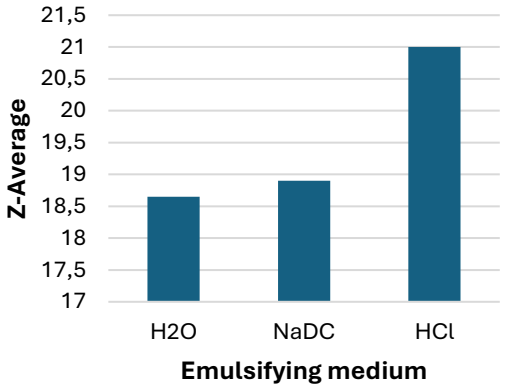

Figure 58. Z-average values of the S_LS_MCT formulation after emulsification in different media.

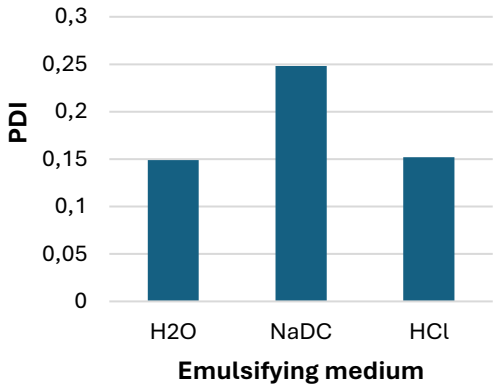

Figure 59. PDI values of the S_LS_MCT formulation after emulsification in different media.

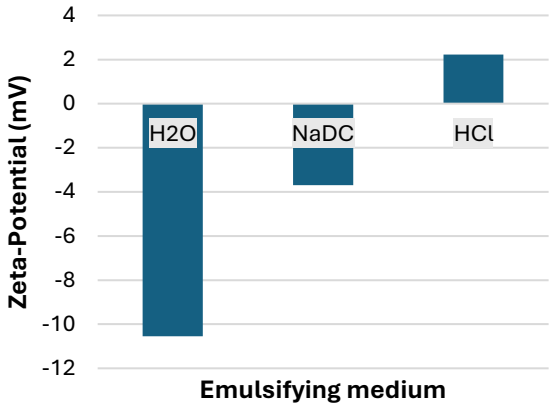

Figure 60. Zeta potential values of the S_LS_MCT formulation after emulsification in different media.

Subsequently, formulation 3 (S_C_LS), previously developed during the initial optimisation studies, was characterised by DLS. The obtained results are presented in Table 25.

The results obtained show a different behaviour compared to the previous MCT systems. Although the formulations maintained relatively high transmittance values, particularly when emulsified in NaDC (98.40%), the DLS results revealed substantially larger particle sizes, with Z-average values of 247.0 nm when emulsified in purified water, and 238.6 nm when emulsified in NaDC. These values indicate that the systems are no longer within the lower nanometric range observed for the formulations with MCT.

The PDI values obtained were also higher than those previously observed, particularly for the formulation emulsified in NaDC (0.387). This indicates increased dispersity and lower homogeneity of the system, suggesting the presence of populations with different droplet sizes.

Regarding zeta potential, both systems exhibited values close to neutrality, with -0.16 mV for S_C_LS_P and -3.86 mV for S_C_LS_NaDC. These low surface charge values suggest weak electrostatic stabilisation and indicate that the systems may be more susceptible to aggregation over time. The slightly more negative zeta potential observed under NaDC conditions is likely related to the adsorption of deoxycholate ions at the droplet interface, similarly to what was observed previously.

When compared with the MCT Labrasol® formulations, the Capryol® systems exhibited significantly larger particle sizes and higher PDI values, indicating poorer self-emulsification efficiency and reduced formulation homogeneity. Replacing MCT with Capryol® resulted in an increase in particle size from approximately 19 nm to about 240 nm, highlighting the strong influence of the oil phase on the self-emulsification behaviour of the system (132). These differences may be related to the physicochemical characteristics of Capryol®, which can influence interfacial organisation and droplet formation during emulsification (132,134) Variations in the interactions between the oil phase and the surfactant layer have been reported to influence droplet size and size distribution in self-emulsifying systems (67).

Overall, the results suggest that replacing MCT with Capryol® negatively affected the self-emulsification efficiency of the system, leading to the formation of larger and less homogeneous dispersions. Therefore, the use of Capryol® was not considered advantageous for further optimisation of the formulation.

Table 25. DLS characterisation parameters of formulation S_C_LS after emulsification in different media.

Formulation	Z-Average (nm)	PDI	Zeta-Potential (mV)	pH	T
S_C_LS_P	247.0	0.317	-0.16	5.51	89.20%
S_C_LS_NaDC	238.6	0.387	-3.86	7.36	98.40%

As performed previously, the order of addition in formulation S_C_LS was modified, with Labrasol® added first followed by Capryol®. This was carried out to evaluate whether the order of component incorporation influences the physicochemical properties of the system, as observed for the S_LS_MCT formulation. The DLS results for the new formulation S_LS_C are presented in Table 26.

The results obtained indicate that changing the order of addition (Labrasol® followed by Capryol®) did not markedly improve the overall physicochemical performance of the system, although some differences were observed between the emulsification media.

In terms of particle size, both formulations exhibited relatively large Z-average values (253.8 nm for S_LS_C_P and 187.6 nm for S_LS_C_NaDC), confirming that the system remained considerably larger than the MCT formulations. Nevertheless, a reduction in particle size was observed in the presence of NaDC, suggesting that bile salt components may influence the interfacial organisation of the system and affect droplet formation (122,124).

The PDI values indicate moderate dispersity, particularly for the system emulsified with NaDC (0.338), suggesting a broader particle size distribution and reduced homogeneity. Although the formulation emulsified in purified water showed a slightly lower PDI value (0.299), both systems remained less homogeneous when compared to previously SNEDDS formulations.

A notable effect was observed in the zeta potential values. While the formulation emulsified in purified water presented a moderately negative surface charge (−9.08 mV), the NaDC system exhibited a highly negative value (−33.0 mV). This contrasts with the values observed in purified water and indicates a marked influence of bile salt components on the interfacial properties of the formulation. This behaviour may be associated with increased adsorption of deoxycholate ions at the droplet surface, resulting in greater exposure of negatively charged species (122,124) .

Overall, these results suggest that the order of component addition influenced the interfacial properties of the system, particularly under bile salt conditions. However, despite the pronounced effect observed on zeta potential, the Capryol® formulations remained less efficient in producing small and homogeneous dispersions when compared with the MCT formulations. Therefore, replacing MCT with Capryol® was not considered advantageous for further optimisation.

Table 26. DLS characterisation parameters of formulation S_LS_C after emulsification in different media.

Formulation	Z-Average (nm)	PDI	Zeta-Potential (mV)	pH	T
S_LS_C_P	253.8	0.299	-9.08	5.50	84.90%
S_LS_C_NaDC	187.6	0.338	-33.0	7.34	97.95%

4.3. Visualisation of the formulations developed using TEM

Three formulations were selected for morphological evaluation: two polymeric nanomicelles formulations and one SNEDDS formulation. For the polymeric nanomicelles, one formulation containing Labrafil® (PN_LF_P_SA 0.14%) and another containing Labrasol® (PN_LS_P_SA 0.14%) were chosen in order to evaluate whether the surfactant type influenced micelle morphology. The selected SNEDDS formulation was prepared using Labrasol® as the surfactant (S_LS_MCT), with emulsification performed in NaDC. The formulations chosen for analysis were also among those presenting the smallest particle sizes, allowing comparison between the morphological observations and the particle size values previously obtained by DLS.

The three formulations were analysed at four magnifications: 25,000x, 50,000x, 100,000x and 200,000x, except for formulation PN_LF_P_SA_ 0.14% which was only analysed at the last three magnifications. For all images, it was used an acceleration voltage of 80 kV. Particle size measurements presented in the some of the images were obtained using the ImageJ software.

4.3.1. PN formulation with Labrafil® (PN_LF_P_SA_ 0.14%)

According to the DLS results presented in Table 27, the formulation exhibited an average particle size of 20.7 nm and a PDI of 0.238. Observing the TEM images shown in Figure 61, particularly at the 200,000x magnification, particles with sizes ranging from 7.14 nm to 10.22 nm can be observed. The smaller particle sizes observed by TEM compared to DLS are expected, as DLS measures the hydrodynamic diameter of the particles in suspension, which includes the solvation layer and possible particle-particle interactions, whereas TEM analysis is performed on dried samples and therefore reflects the actual core dimensions of the particles. In addition, DLS measurements are highly sensitive to the presence of small aggregates or larger particles within the dispersion, which may contribute to increased average size and PDI values (135). The TEM images also suggest the absence of significant aggregation, supporting the relatively moderate PDI values obtained by DLS and indicating good homogeneity of the formulation. Overall, the results obtained from both techniques are consistent, confirming the formation of small and well-dispersed nanostructures.

Morphological analysis of the TEM images suggests the presence of predominantly spherical nanostructures with slightly irregular and non-uniform contours (121,129). Such morphology is commonly observed in polymeric micellar systems and is considered favourable for colloidal stability (41).

Table 27. DLS values of the PN_LF_P_SA 0.14% formulation selected for TEM characterization.

Formulation	Z-Average (nm)	PDI	Zeta-Potential (mV)	pH	T
PN_LF_P_SA 0.14%	20.7	0.238	-13.58	7.53	96.14%

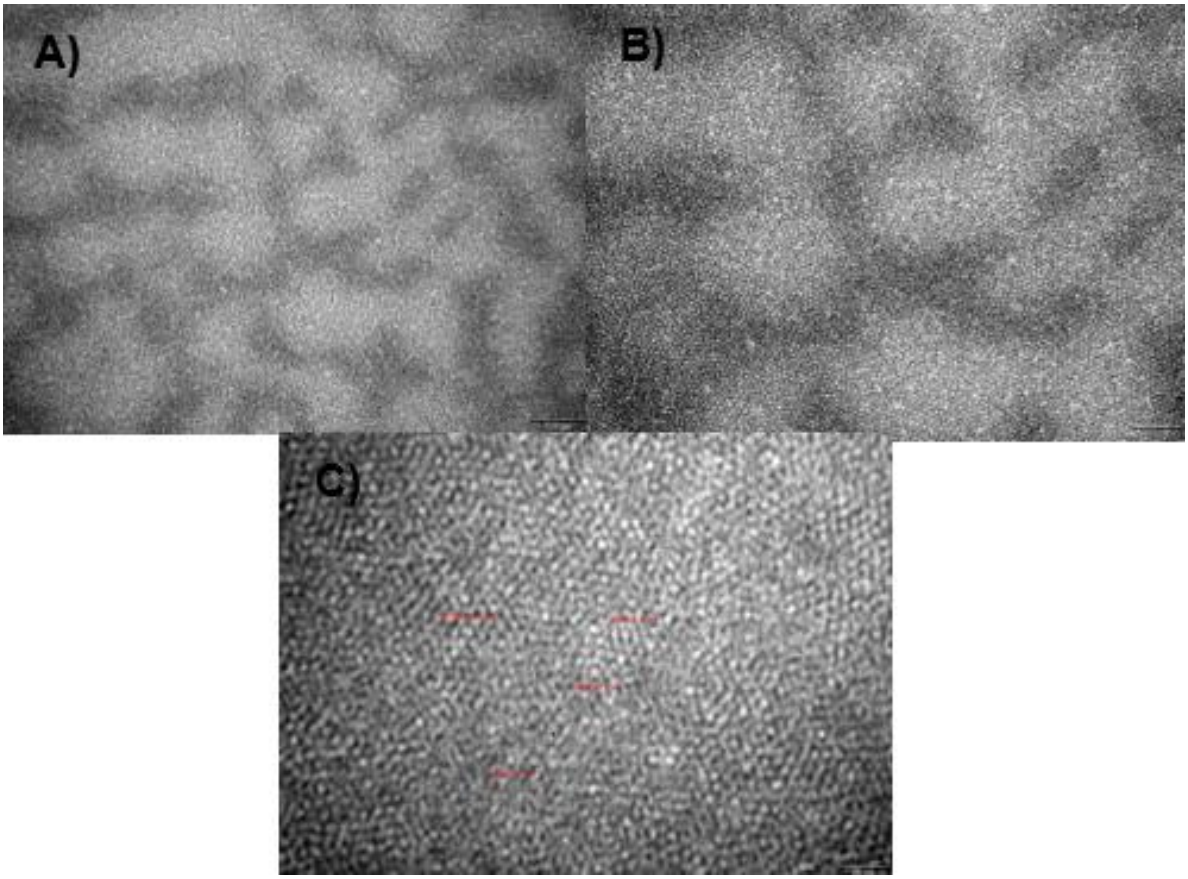

Figure 61. TEM images of formulation PN_LF_P_SA 0.14% at different magnifications: A) 50,000x, B) 100,000x and C) 200,000x.

4.3.2. PN formulation with Labrasol® (PN_LS_P_SA_0.14%)

According to the DLS results presented in Table 28, the formulation PN_LS_P_SA_0.14% exhibited an average particle size of 17.2 nm and PDI of 0.251. Observation of the TEM images shown in Figure 62, particularly at 100,000x and 200,000x magnifications, revealed particles with sizes ranging from 14.99 to 38.58 nm. These observations are in good agreement with the DLS measurements and confirm the formation of nanometric structures (135). The TEM images may also suggest, particularly at the higher magnifications, the presence of slight particle aggregation, although this was not evident at lower magnifications. Overall, the results obtained from both techniques remain complementary and confirm the formation of nanometric structures.

Morphological analysis suggested the presence of predominantly spherical and relatively well-defined particles, with clearer individual boundaries and a more homogeneous distribution throughout the sample than those observed for PN_LF_P_SA_0.14%, present in Figure 61. Although, in the formulation

PN_LS_P_SA_0.14%, some variability in particle size and slight particle association can still be identified, the overall morphology appears more organised and structurally homogeneous compared to the PN_LF_P_SA_0.14% formulation.

Table 28. DLS values of the PN_LS_P_SA 0.14% formulation selected for TEM characterization.

Formulation	Z-Average (nm)	PDI	Zeta-Potential (mV)	pH	T
PN_LS_P_SA_0.14%	17.2	0.251	-13.10	7.46	97.53%

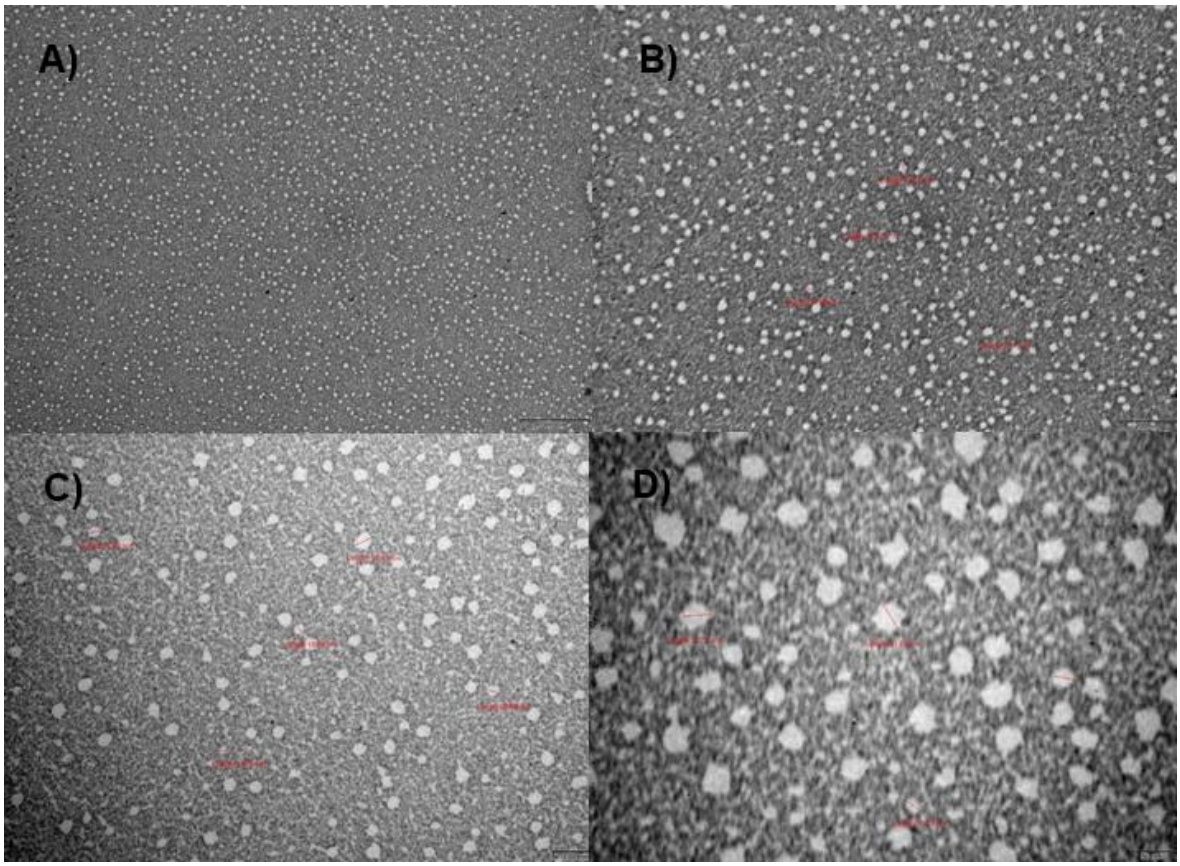

Figure 62. TEM images of formulation PN_LS_P_SA 0.14% at different magnifications: A) 25,000X, B) 50,000x, C) 100,000x and D) 200,000x.

4.3.3. SNEDDS formulation with Labrasol® (S_LS_MCT)

According to the DLS results presented in Table 29, formulation S_LS_MCT emulsified in NaDC exhibited an average particle size of 18.9 nm and a PDI of 0.248. Observation of the TEM images shown in Figure 63, particularly at the 100,000x and 200,000x magnifications, revealed particles with sizes ranging from 13.03 nm to 25.23 nm.

The particle sizes observed by TEM are consistent with the DLS measurements, confirming the formation of nanometric structures within the formulation. The slightly broader size range visualised by TEM is also in agreement with the PDI value obtained by DLS, which suggests moderate size heterogeneity within the system while still indicating acceptable homogeneity (135).

Morphological analysis indicated the presence of predominantly spherical and relatively well-defined particles with a generally homogeneous distribution throughout the sample. Although some variability in particle size could be observed, no evidence of significant aggregation was detected in the TEM images, supporting the good dispersion of the nanoemulsion droplets.

Table 29. DLS values of the SNEDDS formulation selected for TEM characterization.

Formulation	Z-Average (nm)	PDI	Zeta-Potential (mV)	pH	T
S_LS_MCT_NaDC	18.9	0.248	-3.70	7.59	99.57%

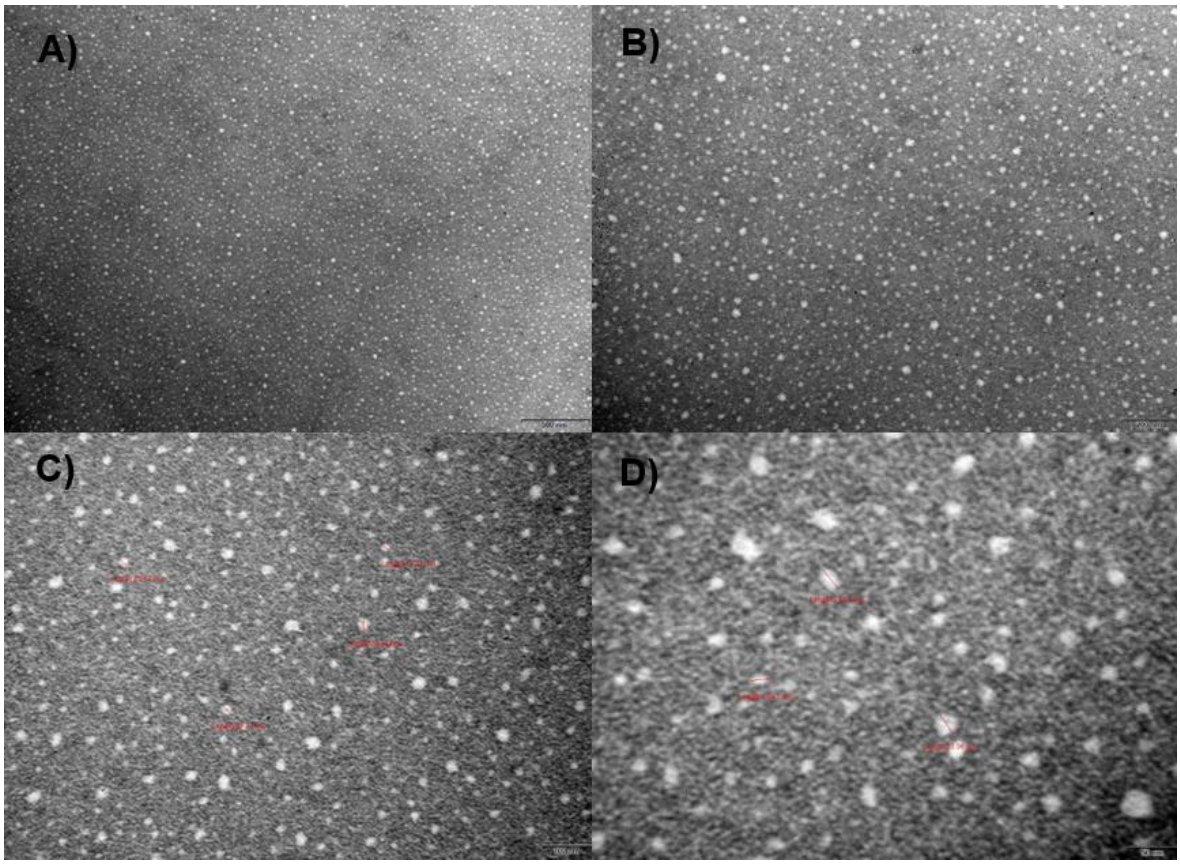

Figure 63. TEM images of formulation S_LS_MCT_NaDC at different magnifications: A) 25,000X, B) 50,000x, C) 100,000x and D) 200,000x.

4.4. Encapsulation efficiency

4.4.1. Calibration curve of CBD

The quantification of CBD was done using a UV spectrophotometric calibration curve at 276 nm. The method showed high linearity over the investigated concentration range (1.69-500 µg/mL), described by the equation:

$$y = 0.0019x + 0.0003$$

The high coefficient of determination (R^2 = 0.9998), shown in Figure 64, indicates a strong linear relationship and supports the suitability of the method for interpolation of experimental absorbance data.

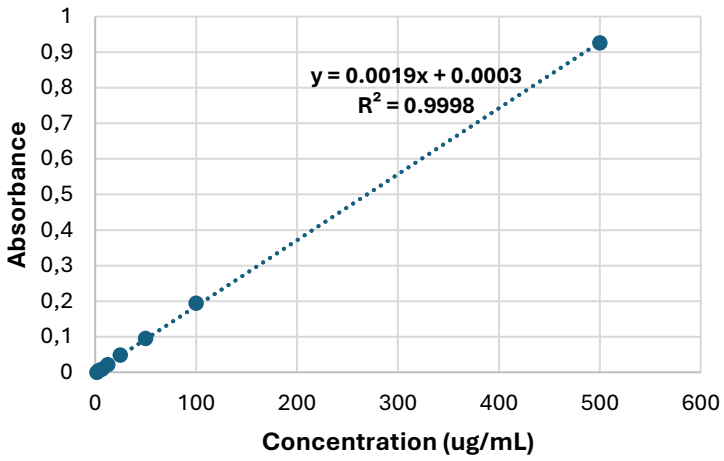

Figure 64. Calibration curve of CBD obtained by UV spectrophotometry at 276 nm.

4.4.2. Encapsulation efficiency of the nanoformulations

Encapsulation efficiency varied depending on the nanocarrier system and formulation composition. Based on an initial CBD loading of 75 mg per formulation, both the encapsulation percentage and the absolute drug content were determined, for four formulations: S_LF_MCT_NaDC, S_LS_MCT_NaDC, PN_LS_P_SA 0.14% and PN_LF_P_SA 0.14%. The values shown in Table 30 correspond to mean results obtained from technical triplicates (n = 3), providing an initial indication of formulation performance.

The SNEDDS formulations (S_LF_MCT_NaDC and S_LS_MCT_NaDC) exhibited consistently high encapsulation efficiencies of 99.87% and 98.94%, respectively, corresponding to approximately 74 mg of retained CBD. This behaviour may be attributed to the strong solubilisation capacity of the lipidic core, where the highly lipophilic nature of CBD (approximately 6.3) favours partitioning into medium-chain triglycerides (136,137).

Stabilisation by NaDC may further contribute to maintaining droplet integrity and limiting drug leakage during processing. The minimal differences between both formulations suggest that substitution of the Labrafil component with Labrasol does not significantly influence the encapsulation performance under the conditions tested.

In contrast, the polymeric nanomicelles formulations showed a strong dependence on formulation composition. While PN_LS_P_SA 0.14% achieved an encapsulation efficiency of 99.87%, comparable to the SNEDDS formulations, PN_LF_P_SA 0.14% exhibited a markedly lower encapsulation efficiency of 57.71%, corresponding to 43.28 mg of retained CBD. This reduction may be associated with differences in drug - core affinity and micellar stability. Polymeric micelles are dynamic systems governed by the CMC, and formulation variations in stability may lead to partial dissociation under dilution conditions during processing. Such instability could result in premature drug release, with free CBD potentially being lost during processing, thereby affecting the apparent encapsulation efficiency (138,139).

Table 30. Encapsulation efficiency and mass of encapsulated CBD in SNEDDS and polymeric nanomicelles (initial CBD load: 75 mg).

Formulation	Nanocarrier Type	Encapsulation Efficiency *	Mass of Encapsulated CBD (mg)
S_LF_MCT_NaDC	SNEDDS	99.87%	74.90 mg
S_LS_MCT_NaDC	SNEDDS	98.94%	74.20 mg
PN_LS_P_SA 0.14%	Polymeric Nanomicelles	99.87%	74.90 mg
PN_LF_P_SA 0.14%	Polymeric Nanomicelles	57.71%	43.28 mg

* Note: Values were calculated from the mean absorbance of technical triplicates (n = 3) using microplate reader analysis.

However, these results are based on a limited number of technical replicates (n = 3). Although they provide an initial comparison between formulations, additional independent replicates would be necessary to improve statistical robustness and strengthen the reliability of the conclusions, particularly for the polymeric nanomicelles systems where higher variability was observed.

4.5. *In vitro* cell viability assessment (MTT Assay)

The cytotoxicity of the developed nanocarrier systems was evaluated using the MTT assay to assess the cellular viability of the formulations. For these studies, two formulations were selected: one polymeric nanomicelles formulation (PN_LS_P_SA 0.14%) and one SNEDDS formulation (S_LS_MCT emulsified in NaDC). These formulations were selected based on their physicochemical characterisation, including nanometric particle size, acceptable homogeneity (DLS), favourable morphological features (TEM), and high encapsulation efficiency. Additionally, both formulations contained Labrasol® as the surfactant, which was intentionally maintained to minimise formulation-related variability.

Different formulation concentrations prepared through serial dilutions of the stock formulations, were tested in order to evaluate possible concentration-dependent effects on cellular viability. Additionally, formulations containing CBD and the corresponding formulations without CBD were evaluated for both polymeric nanomicelles and SNEDDS systems. This approach aimed to determine whether any observed cytotoxic effects were associated with the formulation excipients themselves or with the presence and concentration of CBD incorporated within the systems. The cytotoxicity studies were conducted using Caco-2 and SH-SY5Y cell lines, allowing evaluation of the biological behaviour of the formulations in intestinal and neuronal cellular models, respectively.

4.5.1. CACO-2 intestinal cells

4.5.1.1. *In vitro* cytotoxicity of free CBD

To establish the baseline cytotoxicity profile of free CBD and evaluate its potential effects on the intestinal epithelium, an MTT assay was performed using the Caco-2 cell line. Cells were exposed to increasing concentrations of free CBD (0.15, 1.5, 3, and 30 µg/mL), together with an ethanol vehicle control. The tested concentrations were prepared through serial dilutions, followed by dilution in serum-free culture medium, ensuring that the final ethanol concentration remained constant and non-toxic across all experimental groups.

The vehicle control did not affect cell viability, which was considered as 100%, confirming that the ethanol concentration used as carrier had no cytotoxic effect, as shown in Figure 65. Exposure to the lower CBD concentrations (0.15 and 1.5 µg/mL) did not significantly reduce cell viability, with values remaining above 90%. However, a concentration-dependent decrease in cell viability was observed at higher concentrations. At 3 µg/mL, a moderate but statistically significant reduction in viability was detected (at 86.94%; $p = 0.00286$). This effect became substantially more pronounced at the highest

concentration tested (30 µg/mL), where cell viability decreased to 17.89% ($p = 1.33 \times 10^{-12}$), indicating marked cytotoxicity of free CBD at elevated concentrations.

The results obtained demonstrate that free CBD induces a concentration- dependent cytotoxic effect on these cells. The pronounced reduction in viability between 3 and 30 µg/mL (~9.5 and 95 µM) suggests a median lethal concentration (LC_{50}) within this concentration range. This is consistent with previously reported findings in CaCo-2 epithelial cells, where a marked decrease in viability was observed after 24 h exposure, with a LC_{50} of 4.34 µM. Notably, significant cytotoxic effects were already evident at 5 µM, with progressive loss of cell viability, cell shrinkage, and reduced adhesion observed at 10 and 20 µM, indicating a strong dose-dependent impairment of epithelial integrity. Accordingly, the pronounced cytotoxicity observed at 30 µg/mL (~95 µM) in the present study further supports the notion that high concentrations of non-encapsulated CBD may compromise epithelial cell viability and structural integrity (140).

Although free CBD showed acceptable minimal cytotoxicity at lower concentrations (≤1.5 µg/mL), the marked decrease in viability at higher concentrations highlights the potential limitations associated with the administration of free CBD at elevated doses.

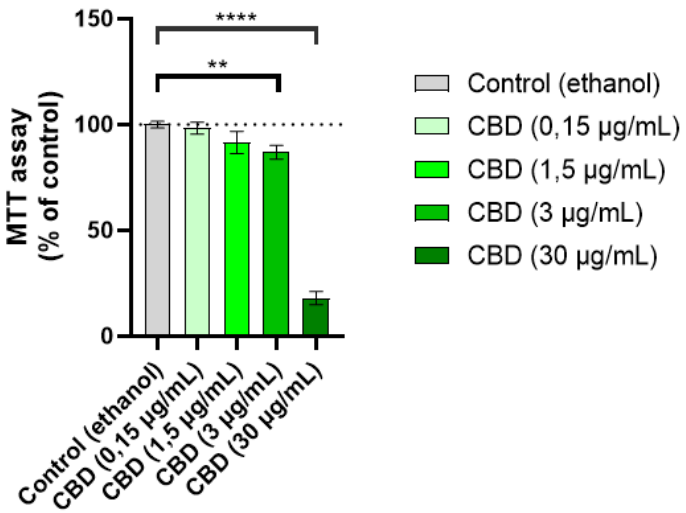

Figure 65. Effect of free CBD on Caco-2 cell viability assessed by MTT assay. Cells were treated with free CBD (0.15–30 µg/mL) in serum-free medium. The vehicle control (ethanol) was considered as 100% viability. Results are presented as mean ± SEM from two independent experiments performed in quadruplicate. Statistical significance: **p < 0.01 and ****p < 0.0001 versus the vehicle control.

4.5.1.2. *In vitro* cytotoxicity of CBD nanoformulations

To evaluate the developed nanocarriers and distinguish between the intrinsic cytotoxicity of the carrier systems and the effect of encapsulated CBD, Caco-2 cells were exposed to both blank and CBD-loaded nanoformulations. The formulations tested included polymeric nanomicelles, Figure 66 graphs (A) and (B), and SNEDDS, shown in Figure 66 graphs (C) and (D). Before cellular exposure, stock formulations were serially diluted in water and then diluted in serum-free culture medium. Cells exposed to the corresponding volume of purified water in serum-free medium were used as the vehicle control and considered as 100% viability.

The upper panels of Figure 66 show the cytotoxicity profiles of blank polymeric nanomicelles and CBD-loaded polymeric nanomicelles over a concentration range of 0.15 to 30 µg/mL. For the blank PN formulation, graph (A), a non-linear variation in cell viability was observed. At lower concentrations, viability decreased to 89.99% at 0.15 µg/mL ($p = 0.00393$) and to 66.85% at 1.5 µg/mL ($p = 9.8 \times 10^{-5}$). Interestingly, viability recovered to values close to the control at 3 µg/mL. This behaviour may be related to changes in the aggregation state of the excipients. At lower concentrations, individual molecular species or loosely associated structures may interact more directly with the cell membrane, potentially contributing to reduced viability. At higher concentrations, the formation of more organised nanostructures may reduce such direct interactions, leading to partial recovery in cell viability at intermediate concentrations (138,139). However, exposure to the highest concentration tested (30 µg/mL) resulted in complete loss of cell viability ($p = 2.122 \times 10^{-17}$), likely because the amount of surfactant/polymeric material exceeded the cellular tolerance threshold.

A similar trend was observed for the CBD-loaded polymeric nanomicelles, graph (B). At 0.15 µg/mL, a slight but significant reduction in viability was detected ($p = 0.01032$). In contrast, at 1.5 and 3 µg/mL, cell viability remained close to the control values. At 3 µg/mL, viability values were at 110.88%, which may indicate a mild increase in metabolic activity. Compared to the previously obtained results for free CBD, the encapsulated formulation maintained substantially higher viability values at intermediate concentrations, suggesting that nanoencapsulation may reduce the direct cytotoxic effects of CBD by limiting its interaction with intestinal epithelial cells (125). However, at the highest tested concentration (30 µg/mL), a marked reduction in cell viability was observed, decreasing to 1.46% for the blank formulation and 1.15% for the CBD-loaded system ($p = 2.004 \times 10^{-17}$). These results indicate that the formulation system alone already induces a very strong cytotoxic effect at this concentration, with both formulations showing similarly low viability values. The slight further reduction observed upon incorporation of CBD is consistent with the previously

reported decrease in cell viability for free CBD at 30 µg/mL, although the differences between blank and loaded systems remain minimal.

The lower panels of Figure 66 present the cytotoxicity profiles of blank and CBD-loaded SNEDDS formulations. These systems were only evaluated at the lower concentrations of 0.15 and 1.5 µg/mL. Both formulations showed a relatively stable viability profile, with cell viability remaining close to 90% at all tested concentrations. For the blank SNEDDS formulation, graph (C), a slight but statistically significant reduction in viability to 88.49% was observed only at the lowest concentration tested (0.15 µg/mL, $p = 0.00094$). Although a similar viability value was observed at 1.5 µg/mL, this reduction was not statistically significant when compared to the control. For the CBD-loaded SNEDDS formulation, both tested concentrations showed minor but statistically significant decreases in cell viability relative to the control group, while still maintaining viability values of 88.53% at 0.15 µg/mL ($p = 0.02454$) and of 90.35% at 1.5 µg/mL ($p = 0.00257$). The similar behaviour observed between blank and CBD-loaded SNEDDS suggests that CBD incorporation did not markedly alter the overall cytotoxicity profile within the tested concentration range. The observed reduction in cell viability may be associated with the concentration and type of surfactant required to stabilize the nanoparticles (141).

Overall, the *in vitro* cytotoxicity studies in Caco-2 cells allowed the establishment of a baseline safety profile for free CBD and the evaluation of the biocompatibility of the developed nanocarriers. However, a more complete assessment of these systems is still required, including the extension of the SNEDDS concentration range to determine its toxicity threshold. In addition, performing additional independent replicates will be important to improve statistical robustness and confirm the reproducibility of these preliminary results.

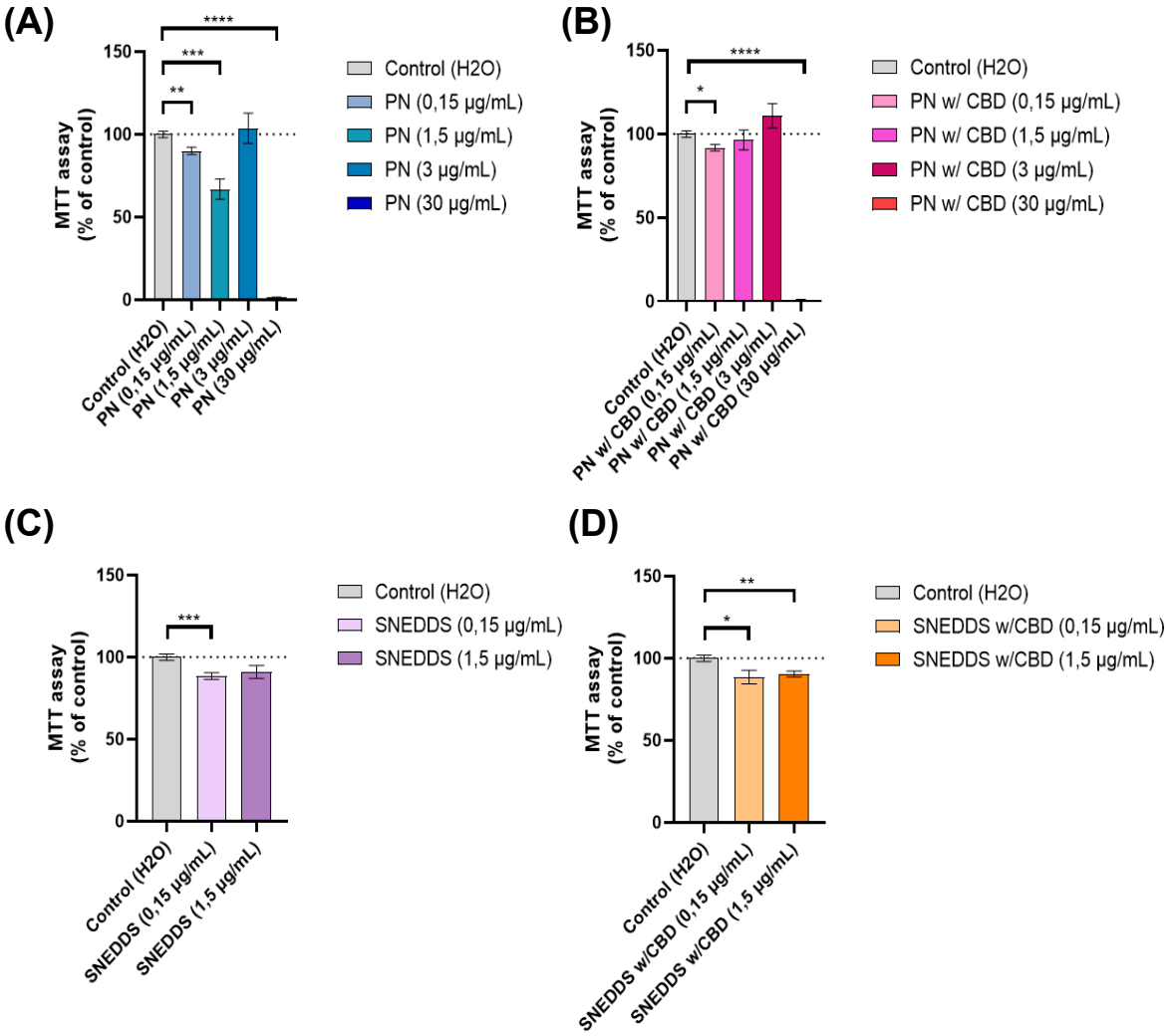

Figure 66. Viability of Caco-2 cells after exposure to blank and CBD-loaded nanoformulations: (A) blank polymeric nanomicelles (PN), (B) CBD-loaded polymeric nanomicelles (PN w/ CBD), (C) blank SNEDDS, and (D) CBD-loaded SNEDDS (SNEDDS w/ CBD). The vehicle control (H_2O) was considered as 100% viability. Results are presented as mean ± SEM from two independent experiments performed in quadruplicate. Statistical significance: *p < 0.05, **p <0.01, ***p < 0.001, and ****p < 0.0001 versus the vehicle control.

4.5.2. SH-SY5Y neuronal cellular models

4.5.2.1. *In vitro* cytotoxicity of free CBD

To evaluate the baseline neurotoxicity and metabolic effects of free CBD, an MTT assay was performed using the human neuroblastoma cell line SH-SY5Y over a concentration range of 0.15-30 µg/mL (Figure 67). Cells were treated in serum-free culture medium, and the vehicle control (ethanol) was considered as 100% cell viability. Although statistical annotations were not included in the graphical representation for clarity purposes, all tested concentrations showed statistically significant differences compared to the control.

Unlike the concentration-dependent cytotoxicity observed in Caco-2 cells, in the SH-SY5Y cells free CBD displayed a hormetic-like response (142). At lower concentrations, CBD promoted a significant increase in metabolic activity, with cell viability values reaching 128.56% at 0.15 µg/mL ($p = 0.00205$) and 119.72% at 1.5 µg/mL ($p = 0.01706$). This effect was most pronounced at 3 µg/mL, where metabolic activity increased to 139.27% ($p = 6.924 \times 10^{-5}$). At the highest tested concentration (30 µg/mL), a reduction in cell viability was observed (87.10%, $p = 0.0448$). These results may indicate that, at lower concentrations, CBD induces a mild increase in metabolic activity, potentially associated with enhanced mitochondrial enzyme activity rather than true proliferative effect (115). Comparison with the Caco-2 results further demonstrated a marked cell-type-dependent response to CBD exposure. At 3 µg/mL, free CBD already induced a reduction in Caco-2 viability to 86.94%, whereas SH-SY5Y cells exhibited their highest metabolic activity. Similarly, at 30 µg/mL, Caco-2 cells showed a pronounced loss of viability, whereas SH-SY5Y cells maintained substantially higher viability values, with only a moderate decrease to 87.10%. This differential response suggests that neuronal-like SH-SY5Y cells may be less susceptible to CBD-induced cytotoxicity under the tested conditions, compared to intestinal epithelial Caco-2 cells.

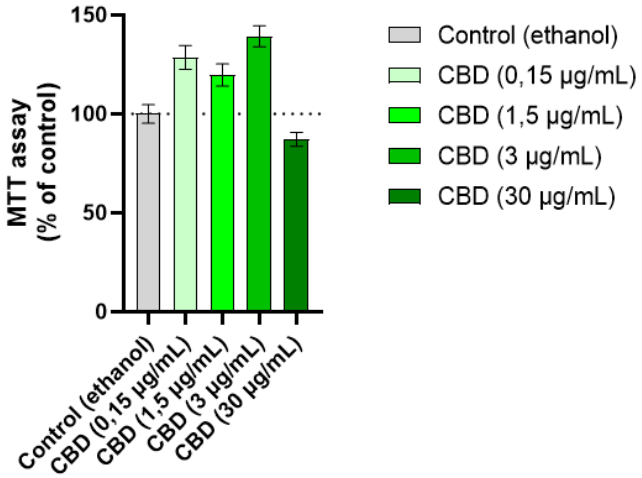

Figure 67. Effect of free CBD on SH-SY5Y cell viability. Cells were treated with free CBD (0.15-30 µg/mL) in serum-free medium. The vehicle control (ethanol) was considered as 100% viability. Statistical annotations were omitted from the graph for clarity; however, all concentrations showed statistically significant differences compared to the control (0.15 µg/mL, $p = 0.00205$; 1.5 µg/mL, $p = 0.01706$; 3 µg/mL, $p = 6.924 \times 10^{-5}$; 30 µg/mL, $p = 0.0448$).

4.5.2.2. *In vitro* cytotoxicity of CBD nanoformulations

To further evaluate the neuro-biocompatibility of the developed delivery systems, SH-SY5Y human neuroblastoma cells were exposed to both polymeric nanomicelles and SNEDDS (Figure 68). All formulations were prepared in serum-free culture medium, and the vehicle control (H_2O) was considered as 100% cell viability. Statistical markers were omitted from the graphs (A) and (B) to improve figure clarity; however, all significant differences were considered during data analysis.

The upper panels of Figure 68 show the cell viability profiles of blank polymeric nanomicelles (graph A) and CBD-loaded polymeric nanomicelles (graph B) over a concentration range of 0.15-30 µg/mL. In contrast to the results previously observed in Caco-2 cells, SH-SY5Y cells showed generally higher apparent resistance to both formulations, with metabolic activity values remaining above 100% across most tested concentrations.

For the blank PN formulation (graph A), cell viability increased significantly to 143.46% at 0.15 µg/mL ($p = 0.00194$). Although a slight decrease was observed at 1.5 µg/mL (123.43%), viability increased again at 3 µg/mL, reaching 193.45% ($p = 0.00713$). Even at the highest tested concentration (30 µg/mL), viability remained elevated at 144.98% ($p = 0.0013$). This behaviour may be associated with the self-assembly behaviour of amphiphilic polymers and the formation of stable micellar structures, which can reduce direct interaction between hydrophobic polymer segments and the cellular membrane (115,139). Consequently, the system may influence cellular metabolic activity without inducing cytotoxic effects (115,140).

Similarly, the CBD-loaded nanomicelles (graph B) demonstrated consistently elevated metabolic activity across all tested concentrations, with 154.32%, 149.77%, 169.03%, and 146.22% viability observed at 0.15, 1.5, 3, and 30 µg/mL, respectively. When compared with the results obtained for free CBD, particularly at 30 µg/mL where viability decreased to approximately 87%, nanoencapsulation appeared to prevent this reduction in cell viability. These findings suggest that polymeric nanomicelles may improve cellular tolerance towards CBD exposure at higher concentrations.

The lower panels of Figure 68 show the viability profiles of blank SNEDDS (C) and CBD-loaded SNEDDS (D) at concentrations of 0.15 and 1.5 µg/mL. Both formulations demonstrated a concentration-dependent increase in cell viability. For the blank SNEDDS (graph C), viability increased, reaching 137.21% at 1.5 µg/mL ($p = 0.00201$). A similar profile was observed for the CBD-loaded SNEDDS (graph D), which maintained viability values close to the control at 0.15 µg/mL and increased to 131.39% at 1.5 µg/mL ($p = 0.00265$).

The similar behaviour observed for both blank and loaded SNEDDS formulations suggests that the increase in the cell viability may be mainly associated with the carrier system rather than with CBD itself. However, additional studies using a wider concentration range would be necessary to better characterise the safety profile of the SNEDDS formulations and allow more robust conclusions regarding their concentration-dependent effects.

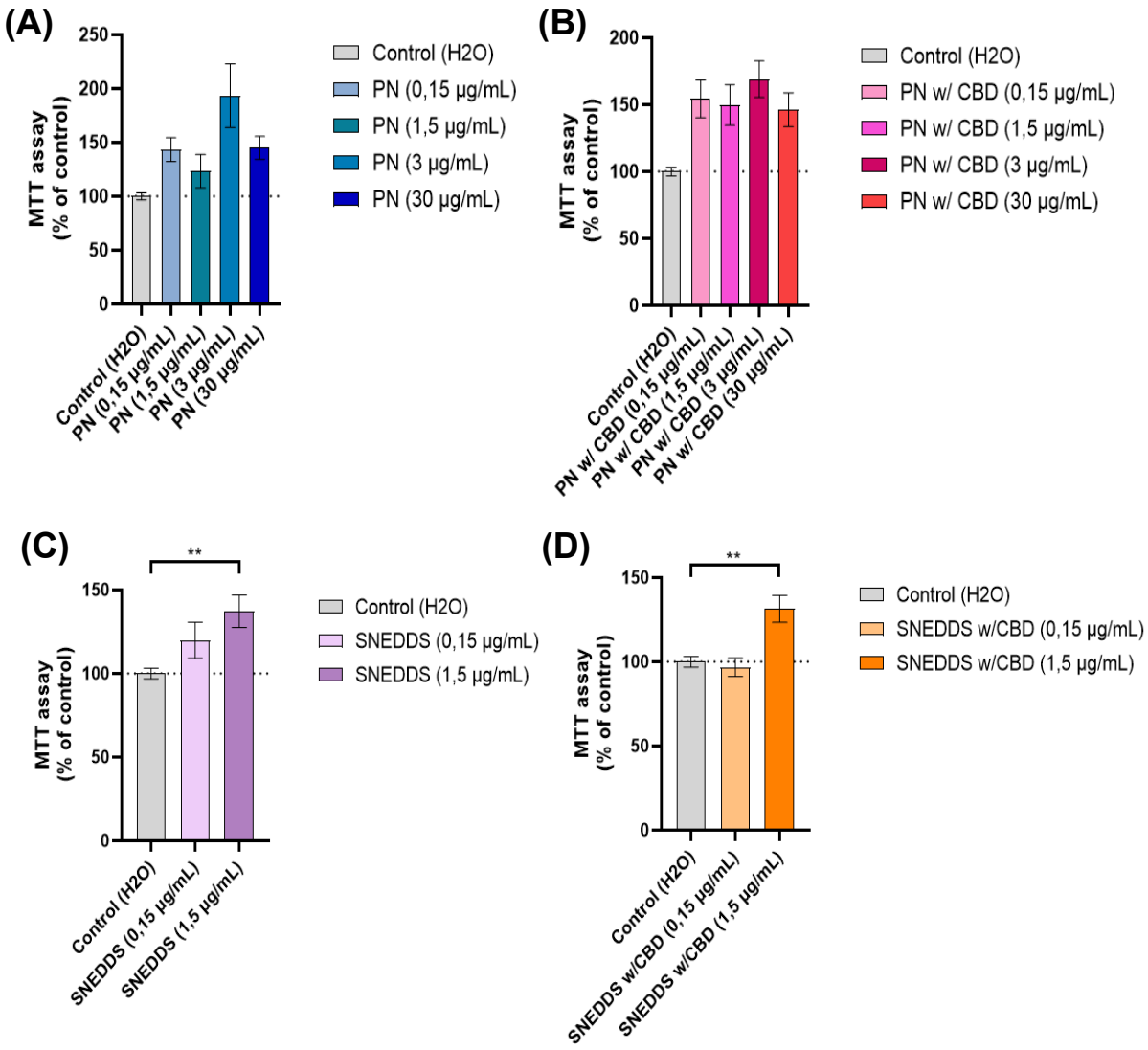

Figure 68. Cell viability of SH-SY5Y cells after exposure to blank and CBD-loaded nanoformulations: (A) Blank polymeric nanomicelles (PN), (B) CBD-loaded polymeric nanomicelles (PN w/ CBD), (C) Blank SNEDDS, and (D) CBD-loaded SNEDDS (SNEDDS w/ CBD). The vehicle control (H_2O) was considered as 100% cell viability. Data are presented as mean ± SEM from two independent experiments, performed in quadruplicate. In panel (A), statistically significant differences compared to the control were observed at 0.15 µg/mL ($p = 0.00194$), 3 µg/mL ($p = 0.00713$), and 30 µg/mL ($p = 0.0013$). In panel (B), all tested concentrations showed statistically significant differences compared to the control: 0.15 µg/mL ($p = 0.00208$), 1.5 µg/mL ($p = 0.00453$), 3 µg/mL ($p = 0.000224$), and 30 µg/mL ($p = 0.00336$). For panels (C) and (D), statistical significance is indicated in the graphs (**$p < 0.01$ vs vehicle control).

Overall, comparison with the Caco-2 results highlights a clear cell-type-dependent response to the developed nanoformulations. While Caco-2 cells showed higher sensitivity towards high concentrations of CBD and surfactant-containing systems, SH-SY5Y neuronal cells demonstrated substantially greater tolerance. Both delivery systems maintained high metabolic activity in neuronal cells, with polymeric nanomicelles showing particularly favourable consistent profiles across the tested concentration range.

4.6. Stability assessment at 40 °C

An accelerated stability study was conducted on formulations S_MCT_LF, emulsified in purified water and NaDC, and PN_LF_P_SA by storing them at 40 °C and monitoring their pH and visual changes over time.

4.6.1. pH stability assessment

As shown in Table 31, the SNEDDS formulation emulsified in purified water (S_MCT_LF_P) showed an initial pH of 5.80, which decreased to 4.51 after the first month of storage. Subsequently, only minor fluctuations were observed, with pH values remaining between 4.30 and 4.46 throughout the remainder of the study period.

A similar trend was observed for the SNEDDS formulation emulsified in NaDC solution (S_MCT_LF_NaDC). The initial pH decreased progressively from 7.36 to 5.41 after approximately five months of storage, indicating a gradual acidification of the system.

The polymeric nanomicelles formulation (PN_LF_P_SA) exhibited the greatest pH variation. The initial pH of 7.48 decreased continuously throughout the study, reaching a final value of 4.85 after four months of storage.

Table 31. Evolution of pH values during accelerated storage at 40 °C for the selected SNEDDS and polymeric nanomicelles formulations.

Storage time	S_MCT_LF_P	S_MCT_LF_NaDC	PN_LF_P_SA
Initial	5.80	7.36	7.48
1 month	4.51	6.71	6.11
2 months	4.46	6.42	5.50
3 months	4.32	5.92	5.10
4 months	4.36	5.69	4.85
5 months	4.30	5.41	Not measured

The progressive decrease in pH observed for all formulations may indicate chemical changes occurring during storage under accelerated conditions. Possible explanations include oxidation processes or structural rearrangements within the carrier systems. However, as no chemical stability studies were performed, the exact mechanisms responsible for the pH decrease cannot be confirmed.

Overall, all formulations showed a reduction in pH during storage at 40 °C, although no abrupt pH changes were observed after the initial decrease. The SNEDDS formulations demonstrated a more gradual pH decline, whereas the polymeric nanomicelles exhibited a more pronounced reduction.

4.6.2. Visual stability assessment

The visual appearance of the formulations during storage at 40 °C is presented in Figures 69 to 71. All formulations showed visible changes during the first month of storage, which coincided with the initial decrease in pH observed throughout the stability study.

The S_MCT_LF_P formulation (Figure 69) exhibited the most pronounced visual change, transitioning from a transparent and homogeneous system to a turbid, milky appearance after one month of storage. In contrast, S_MCT_LF_NaDC (Figure 70) maintained its initial slightly opalescent appearance but gradually developed a yellowish coloration over time. Similarly, the PN_LF_P_SA formulation (Figure 71) evolved from a clear and transparent system to a turbid, slightly yellowish dispersion after one month of storage. Following these initial changes, the visual appearance of all formulations remained relatively stable throughout the remainder of the study. Although a gradual increase in

yellowish coloration was observed for both S_MCT_LF_NaDC and PN_LF_P_SA, no visible signs of phase separation, creaming, sedimentation, or precipitation were detected in any formulation during the storage period.

The visual modifications observed, together with the progressive reduction in pH, suggest that physicochemical changes occurred within the formulations under accelerated storage conditions. Nevertheless, the absence of macroscopic instability indicates that all systems maintained their physical integrity throughout the study period.

As this preliminary stability assessment relied solely on visual inspection and pH monitoring, additional analyses, including particle size determination, PDI, zeta potential, and CBD content evaluation, would be necessary to fully characterise the long-term physicochemical stability of the developed formulations.

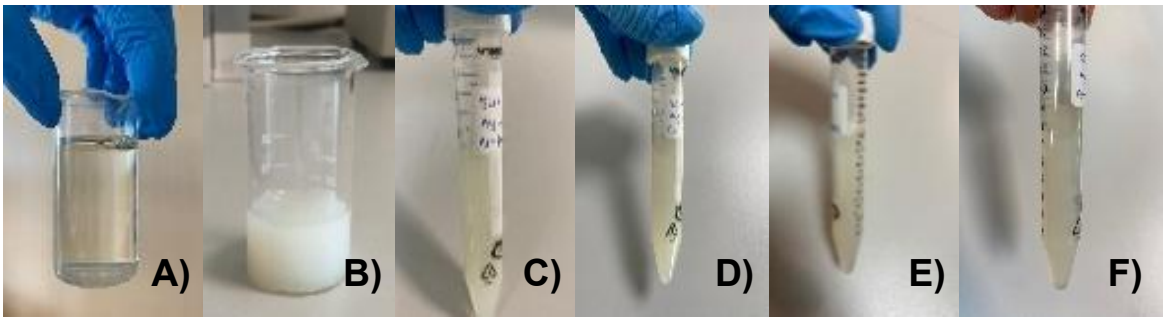

Figure 69. Visual assessment of the S_MCT_LF_P formulation during accelerated storage at 40 °C: A) Initial state; B) 1 month; C) 2 months; D) 3 months; E) 4 months and F) 5 months.

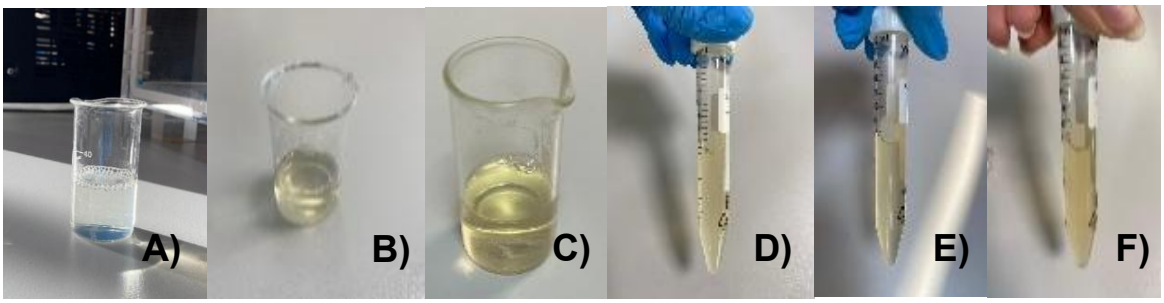

Figure 70. Visual assessment of the S_MCT_LF_NaDC formulation during accelerated storage at 40 °C: A) Initial state; B) 1 month; C) 2 months; D) 3 months; E) 4 months and F) 5 months of storage.

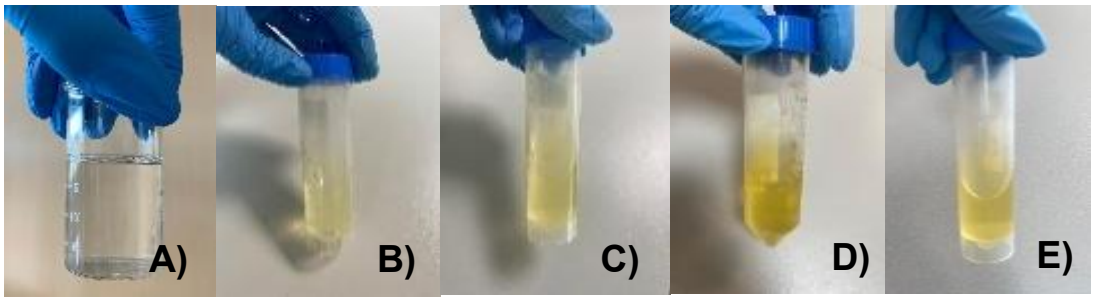

Figure 71. Visual assessment of the PN_LF_P_SA formulation during accelerated storage at 40 °C: A) Initial state; B) 1 month; C) 2 months; D) 3 months and E) 4 months.

5. CONCLUSIONS AND FUTURE PERSPECTIVES

A large number of formulations were developed and evaluated throughout this work to identify suitable nanosystems for the delivery of CBD. Although several formulations exhibited favourable physicochemical characteristics, it proved difficult to establish a single optimal formulation. Among the polymeric nanomicelles, particle sizes below 20 nm were achieved, with PDI values close to 0.200-0.250 and zeta potential values reaching approximately -13 mV after incorporation of sodium alginate. Formulations prepared with reduced Transcutol® concentrations reached zeta potential values close to -16 mV. In the SNEDDS systems, Labrasol®-based formulations containing MCT produced the smallest particles, with particle sizes around 19 to 21 nm and PDI values below 0.250. Encapsulation efficiencies above 98% were obtained for SNEDDS and one polymeric nanomicelles formulation, while TEM analysis confirmed the presence of predominantly spherical nanostructures, showing overall good agreement with DLS measurements.

Although several formulation variables were investigated, including surfactant type, oil phase, sodium alginate concentration, Transcutol® concentration and emulsification medium, no clear universal trend was observed. For example, Labrasol® generally produced smaller particles than Labrafil®, and sodium alginate contributed to more negative zeta potential values, but these effects were not always consistent across all systems. Likewise, reducing the amount of Transcutol® produced only subtle and formulation dependent changes. These observations suggest that the interactions between the excipients are complex and that the contribution of each individual parameter cannot be considered independently.

Biological evaluation demonstrated acceptable *in vitro* biocompatibility within the concentration ranges tested. Free CBD and polymeric nanomicelles produced a more pronounced reduction in Caco-2 viability at higher concentrations, whereas SH-SY5Y cells exhibited greater tolerance towards both free CBD and the nanoformulations. Nevertheless, the biological studies should be regarded as preliminary, as only a limited concentration range was evaluated for SNEDDS formulations, and a relatively small number of replicates was performed.

The results obtained provide preliminary evidence supporting the use of both polymeric nanomicelles and SNEDDS as potential CBD carriers; however, further studies are required before more definitive conclusions can be drawn.

Future work should focus on increasing the number of replicates in order to improve the robustness and reproducibility of the results. More extensive stability studies, including different environmental conditions and an increased number of formulations, would also be

valuable. In addition, *in vivo* pharmacokinetic studies would be necessary to determine whether the favourable physicochemical characteristics observed translate into improved bioavailability. Further optimisation of formulation composition, together with the evaluation of alternative excipients and combinations with other cannabinoids or terpenes, may also contribute to the development of more effective CBD delivery systems.

REFERENCES

1. American Psychological Association. Anxiety [Internet]. Washington, DC: American Psychological Association; 2018 [cited 2025 Oct 6]. Available from: https://dictionary.apa.org/anxiety.
2. National Institutes of Health. Understanding anxiety disorders [Internet]. Bethesda, MD: National Institutes of Health; 2016 [cited 2025 Oct 6]. Available from: https://newsinhealth.nih.gov/2016/03/understanding-anxiety-disorders.
3. Craske MG, Stein MB. Anxiety. Lancet. 2016;388(10063):3048-59.
4. Friedman MJ, Resick PA, Bryant RA, Strain J, Horowitz M, Spiegel D. Classification of trauma and stressor-related disorders in DSM-5. Depress Anxiety. 2011;28(9):737-49.
5. National Institute of Mental Health. Generalized anxiety disorder: what you need to know [Internet]. Bethesda, MD: National Institute of Mental Health; 2025 [cited 2025 Oct 6] Available from: https://www.nimh.nih.gov/health/publications/generalized-anxiety-disorder-gad
6. National Institute of Mental Health. Phobias and phobia-related disorders [Internet]. Bethesda, MD: National Institute of Mental Health; 2025 [cited 2025 Oct 6]. Available from: https://www.nimh.nih.gov/health/publications/phobias-and-phobia-related-disorders
7. National Institute of Mental Health. Social anxiety disorder: what you need to know [Internet]. Bethesda, MD: National Institute of Mental Health; 2025 [cited 2025 Oct 6]. Available from: https://www.nimh.nih.gov/health/publications/social-anxiety-disorder-more-than-just-shyness
8. National Institute of Mental Health. Post-traumatic stress disorder (PTSD) [Internet]. Bethesda, MD: National Institute of Mental Health; 2025 [cited 2025 Oct 6]. Available from: https://www.nimh.nih.gov/health/publications/post-traumatic-stress-disorder-ptsd
9. Gundugurti PR, Banda N, Yadlapalli SSR, Narala A, Thatikonda R, Kocherlakota C, et al. Evaluation of the efficacy, safety, and pharmacokinetics of nanodispersible cannabidiol oral solution (150 mg/mL) versus placebo in mild to moderate anxiety subjects: a double-blind multicenter randomized clinical trial. Asian J Psychiatr. 2024;97:104073.
10. Bandelow B, Werner AM, Kopp I, Rudolf S, Wiltink J, Beutel ME. The german guidelines for the treatment of anxiety disorders: first revision. Eur Arch Psychiatry Clin Neurosci. 2022;272(4):571-82.
11. Garakani A, Murrough JW, Freire RC, Thom RP, Larkin K, Buono FD, et al. Pharmacotherapy of anxiety disorders: current and emerging treatment options. Front Psychiatry. 2020;11:595584.

12. Antos Z, Zackiewicz K, Tomaszek N, Modzelewski S, Waszkiewicz N. Beyond pharmacology: a narrative review of alternative therapies for anxiety disorders. Diseases. 2024;12(9):216.
13. Lu HC, Mackie K. An introduction to the endogenous cannabinoid system. Biol Psychiatry. 2016;79(7):516-25.
14. Kaplan BLF, Dhanabalan UVA. Professional needs regarding cannabis: learning about the endocannabinoid system and cannabinoid pharmacology. Curr Opin Toxicol. 2026;45:100552.
15. Hasbi A, Madras BK, George SR. Endocannabinoid system and exogenous cannabinoids in depression and anxiety: a review. Brain Sci. 2023;13(2):325.
16. Tahir MN, Raz FS, Rondeau-Gagné S, Trant JF. The biosynthesis of the cannabinoids. J Cannabis Res. 2021;3(1):7.
17. Vlad RA, Hancu G, Ciurba A, Antonoaea P, Rédai EM, Todoran N, et al. Cannabidiol: therapeutic and legal aspects. Pharmazie. 2020;75(10):463-9.
18. Dawidowicz AL, Olszowy-Tomczyk M, Typek R. CBG, CBD, Δ9-THC, CBN, CBGA, CBDA and Δ9-THCA as antioxidant agents and their intervention abilities in antioxidant action. Fitoterapia. 2021;152:104915.
19. Nelson KM, Bisson J, Singh G, Graham JG, Chen SN, Friesen JB, et al. The essential medicinal chemistry of cannabidiol (CBD). J Med Chem. 2020;63(21):12137-55.
20. Martinez Naya N, Kelly J, Corna G, Golino M, Abbate A, Toldo S. Molecular and cellular mechanisms of action of cannabidiol. Molecules. 2023;28(16):5980.
21. Britch SC, Babalonis S, Walsh SL. Cannabidiol: pharmacology and therapeutic targets. Psychopharmacology (Berl). 2021;238(1):9-28.
22. Wright M, Di Ciano P, Brands B. Use of cannabidiol for the treatment of anxiety: a short synthesis of pre-clinical and clinical evidence. Cannabis Cannabinoid Res. 2020;5(3):191-6.
23. Guimarães FS, Chiaretti TM, Graeff FG, Zuardi AW. Antianxiety effect of cannabidiol in the elevated plus-maze. Psychopharmacology (Berl). 1990;100(4):558-9.
24. Larsen C, Shahinas J. Dosage, efficacy and safety of cannabidiol administration in adults: a systematic review of human trials. J Clin Med Res. 2020;12(3):129-41.
25. Ferber SG, Namdar D, Hen-Shoval D, Eger G, Koltai H, Shoval G, et al. The "entourage effect": terpenes coupled with cannabinoids for the treatment of mood disorders and anxiety disorders. Curr Neuropharmacol. 2020;18(2):87-96.
26. Crippa JA, Derenusson GN, Ferrari TB, Wichert-Ana L, Duran FL, Martin-Santos R, et al. Neural basis of anxiolytic effects of cannabidiol (CBD) in generalized social anxiety disorder: a preliminary report. J Psychopharmacol. 2011;25(1):121-30.

27. Millar SA, Stone NL, Bellman ZD, Yates AS, England TJ, O'Sullivan SE. A systematic review of cannabidiol dosing in clinical populations. Br J Clin Pharmacol. 2019;85(9):1888-900.
28. Galvez-Florez JF, Guillen-Burgos HF, Flórez-Puentes CA, Navarro CE, Moreno-Sanz G. Long-term treatment for unspecified anxiety disorders with cannabidiol: a retrospective case series from real-world evidence in colombia. Med Cannabis Cannabinoids. 2024;7(1):193-205.
29. Coelho CF, Vieira RP, Araújo-Junior OS, Lopes-Martins PSL, Dos Santos LG, Dias LD, et al. The impact of cannabidiol treatment on anxiety disorders: a systematic review of randomized controlled clinical trials. Life (Basel). 2024;14(11):1373.
30. Skelley JW, Deas CM, Curren Z, Ennis J. Use of cannabidiol in anxiety and anxiety-related disorders. J Am Pharm Assoc (2003). 2020;60(1):253-61.
31. Han K, Wang JY, Wang PY, Peng YC. Therapeutic potential of cannabidiol (CBD) in anxiety disorders: a systematic review and meta-analysis. Psychiatry Res. 2024;339:116049.
32. Simei JLQ, de Souza JDR, Lisboa JR, Guimarães FS, Crippa JAS. Cannabidiol in anxiety disorders: current and future perspectives. Int Rev Neurobiol. 2024;177:205-34.
33. Huestis MA, Solimini R, Pichini S, Pacifici R, Carlier J, Busardò FP. Cannabidiol adverse effects and toxicity. Curr Neuropharmacol. 2019;17(10):974-89.
34. Souza JDR, Pacheco JC, Rossi GN, de-Paulo BO, Zuardi AW, Guimarães FS, et al. Adverse effects of oral cannabidiol: an updated systematic review of randomized controlled trials (2020-2022). Pharmaceutics. 2022;14(12):2598.
35. O'Sullivan SE, Jensen SS, Kolli AR, Nikolajsen GN, Bruun HZ, Hoeng J. Strategies to improve cannabidiol bioavailability and drug delivery. Pharmaceuticals (Basel). 2024;17(2):244.
36. Moazen-Zadeh E, Chisholm A, Bachi K, Hurd YL. Pharmacokinetics of cannabidiol: a systematic review and meta-regression analysis. Cannabis Cannabinoid Res. 2024;9(4):939-66.
37. Kolli AR, Hoeng J. Cannabidiol bioavailability is nonmonotonic with a long terminal elimination half-life: a pharmacokinetic modeling-based analysis. Cannabis Cannabinoid Res. 2025;10(1):81-91.
38. Della Rocca G, Paoletti F, Conti MB, Galarini R, Chiaradia E, Sforna M, et al. Pharmacokinetics of cannabidiol following single oral and oral transmucosal administration in dogs. Front Vet Sci. 2023;9:1104152.
39. Millar SA, Maguire RF, Yates AS, O'Sullivan SE. Towards better delivery of cannabidiol (CBD). Pharmaceuticals (Basel). 2020;13(9):219.

40. Perumal S, Atchudan R, Lee W. A review of polymeric micelles and their applications. Polymers (Basel). 2022;14(12):2510.
41. Sosnik A, Shabo RB, Halamish HM. Cannabidiol-loaded mixed polymeric micelles of chitosan/poly(vinyl alcohol) and poly(methyl methacrylate) for trans-corneal delivery. Pharmaceutics. 2021;13(12):2142.
42. Cagel M, Tesan FC, Bernabeu E, Salgueiro MJ, Zubillaga MB, Moretton MA, et al. Polymeric mixed micelles as nanomedicines: achievements and perspectives. Eur J Pharm Biopharm. 2017;113:211-28.
43. Ghezzi M, Pescina S, Padula C, Santi P, Del Favero E, Cantù L, et al. Polymeric micelles in drug delivery: an insight of the techniques for their characterization and assessment in biorelevant conditions. J Control Release. 2021;332:312-36.
44. Kotta S, Aldawsari HM, Badr-Eldin SM, Nair AB, Yt K. Progress in polymeric micelles for drug delivery applications. Pharmaceutics. 2022;14(8):1636.
45. Bose A, Roy Burman D, Sikdar B, Patra P. Nanomicelles: types, properties and applications in drug delivery. IET Nanobiotechnol. 2021;15(1):19-27.
46. Li L, Zeng Y, Chen M, Liu G. Application of nanomicelles in enhancing bioavailability and biological efficacy of bioactive nutrients. Polymers (Basel). 2022;14(16):3278.
47. Tawfik SM, Azizov S, Elmasry MR, Sharipov M, Lee YI. Recent advances in nanomicelles delivery systems. Nanomaterials (Basel). 2020;11(1):70.
48. Buya AB, Beloqui A, Memvanga PB, Préat V. Self-nano-emulsifying drug-delivery systems: from the development to the current applications and challenges in oral drug delivery. Pharmaceutics. 2020;12(12):1194.
49. Rathore C, Hemrajani C, Sharma AK, Gupta PK, Jha NK, Aljabali AAA, et al. Self-nanoemulsifying drug delivery system (SNEDDS) mediated improved oral bioavailability of thymoquinone: optimization, characterization, pharmacokinetic, and hepatotoxicity studies. Drug Deliv Transl Res. 2023;13(1):292-307.
50. PHARCON Inc. SNEDDS [Internet]. 2026 [cited 2026 May 15]. Available from: https://pharcon.ca/snedds
51. Kok LY, Bannigan P, Sanaee F, Evans JC, Dunne M, Regenold M, et al. Development and pharmacokinetic evaluation of a self-nanoemulsifying drug delivery system for the oral delivery of cannabidiol. Eur J Pharm Sci. 2022;168:106058.
52. Paczkowska-Walendowska M, Trzaskoma P, Dziopa A, Moeini A, Soczawa M, Krasiński Z, et al. Innovative strategies to enhance the bioavailability of cannabidiol: nanotechnology and advanced delivery systems. Pharmaceuticals. 2025;18(11):1637.

53. Wu F, Ma Q, Tian G, Chen K, Yang R, Shen J. Formulation and evaluation of solid self-nanoemulsifying drug delivery system of cannabidiol for enhanced solubility and bioavailability. Pharmaceutics. 2025;17(3):340.
54. Lacerda M, Carona A, Castanheira S, Falcão A, Bicker J, Fortuna A. Pharmacokinetics of non-psychotropic phytocannabinoids. Pharmaceutics. 2025;17(2):236.
55. Crippa JA, Pereira Junior LC, Pereira LC, Zimmermann PM, Brum Junior L, Rechia LM, et al. Effect of two oral formulations of cannabidiol on responses to emotional stimuli in healthy human volunteers: pharmaceutical vehicle matters. Braz J Psychiatry. 2022;44(1):15-20.
56. Sandmeier M, Wong ET, Nikolajsen GN, Purwanti A, Lindner S, Bernkop-Schnürch A, et al. Oral formulations for cannabidiol: improved absolute oral bioavailability of biodegradable cannabidiol self-emulsifying drug delivery systems. Colloids Surf B Biointerfaces. 2025;255:114879.
57. Nie Y, Kong Y, Peng J, Sun J, Fan B. Enhanced oral bioavailability of cannabidiol by flexible zein nanoparticles: *in vitro* and pharmacokinetic studies. Front Nutr. 2024;11:1431620.
58. Assadpour E, Rezaei A, Das SS, Krishna Rao BV, Singh SK, Kharazmi MS, et al. Cannabidiol-loaded nanocarriers and their therapeutic applications. Pharmaceuticals (Basel). 2023;16(4):505.
59. Abidi AH, Alghamdi SS, Derefinko K. A critical review of cannabis in medicine and dentistry: a look back and the path forward. Clin Exp Dent Res. 2022;8(3):613-31.
60. Johnson DA, Funnell MP, Heaney LM, Cable TG, Wheeler PC, Bailey SJ, et al. Cannabidiol oil ingested as sublingual drops or within gelatin capsules shows similar pharmacokinetic profiles in healthy males. Cannabis Cannabinoid Res. 2024;9(5):e1423-e32.
61. Presidência do Conselho de Ministros. Decreto-Lei n.º 8/2019, de 15 de janeiro. Diário da República. 2019;1(10):184-91.
62. Infarmed - Autoridade Nacional do Medicamento e Produtos de Saúde, I.P. Infarmed aprova comercialização de três produtos à base de canábis [Internet]. Lisboa: Portal da Ordem dos Advogados; 2024 [cited 2026 Jun 10]. Available from: https://portal.oa.pt/comunicacao/imprensa/2024/3/14/infarmed-aprova-comercializacao-de-tres-produtos-a-base-de-canabis/
63. European Medicines Agency. EMA concludes review of anxiety medicine Stresam (etifoxine) [Internet]. Amsterdam: European Medicines Agency; 2022 [updated 24 March 2022; cited 2026 Jun 10]. Available from:

https://www.ema.europa.eu/en/documents/referral/etifoxine-containing-medicinal-products-article-31-referral-ema-concludes-review-anxiety-medicine-stresam-etifoxine_en.pdf

64. Chime SA, Kenechukwu FC, Attama AA. Nanoemulsions - advances in formulation, characterization and applications in drug delivery. Application of nanotechnology in drug delivery. London: InTech; 2014. p. 77-126.

65. Gaggero A, Marko V, Jeremic D, Tetyczka C, Caisse P, Afonso Urich JA. AQbD-based UPLC-ELSD method for quantifying medium chain triglycerides in Labrafac™ WL 1349 for nanoemulsion applications. Molecules. 2025;30(3):486.

66. Gattefossé. Labrafac Lipophile WL 1349 [Internet]. Gattefossé; [cited 2026 May 20]. Available from: https://www.gattefosse.com/pharmaceuticals/product-finder/labrafac-lipophile-wl-1349

67. Sutradhar KB, Amin ML. Nanoemulsions: increasing possibilities in drug delivery. Eur J Nanomed. 2013;5(2):97-110.

68. Gattefossé. Labrafil M 1944 CS [Internet]. Gattefossé; [cited 2026 May 21]. Available from: https://www.gattefosse.com/pharmaceuticals/product-finder/labrafil-m-1944-cs

69. Gattefossé. Labrasol ALF [Internet]. Gattefossé; [cited 2026 May 22]. Available from: https://www.gattefosse.com/pharmaceuticals/product-finder/labrasol-alf

70. McCartney F, Jannin V, Chevrier S, Boulghobra H, Hristov DR, Ritter N, et al. Labrasol® is an efficacious intestinal permeation enhancer across rat intestine: ex vivo and in vivo rat studies. J Control Release. 2019;310:115-26.

71. McCartney F, Jannin V, Brayden D. Investigation of Labrasol® ALF as an intestinal permeation enhancer: Ussing chambers and intestinal instillations2019.

72. Carter J, Kelly C, Jenkins M. Processing optimization of PEDOT:PSS and PEDOT:PSS/Tween 80 films. Polymer J. 2022;55:1-8.

73. Maher S, Geoghegan C, Brayden DJ. Safety of surfactant excipients in oral drug formulations. Adv Drug Deliv Rev. 2023;202:115086.

74. Sigma-Aldrich. TWEEN® 80 [Internet]. Sigma-Aldrich; [cited 2026 May 23]. Available from: https://www.sigmaaldrich.com/PT/en/product/sial/p1754

75. Gattefossé. Capryol 90 [Internet]. Gattefossé; [cited 2026 May 23]. Available from: https://www.gattefosse.com/pharmaceuticals/product-finder/capryol-90

76. National Center for Biotechnology Information. PubChem Compound Summary for CID 109307, Propylene glycol 1-caprylate [Internet]. 2026 [cited 2026 May 25]. Available from: https://pubchem.ncbi.nlm.nih.gov/compound/Propylene-glycol-1-caprylate

77. Osborne DW, Musakhanian J. Skin penetration and permeation properties of Transcutol®-neat or diluted mixtures. AAPS PharmSciTech. 2018;19(8):3512-33.

78. Ha ES, Lee SK, Choi DH, Jeong SH, Hwang SJ, Kim M-S. Application of diethylene glycol monoethyl ether in solubilization of poorly water-soluble drugs. J Pharm Investig. 2020;50(3):231-50.
79. Gattefossé. Transcutol® HP [Internet]. Gattefossé; [cited 2026 May 30]. Available from: https://www.gattefosse.com/pharmaceuticals/product-finder/transcutol-hp
80. Javadzadeh Y, Adibkia K, Hamishehkar H. Transcutol® (diethylene glycol monoethyl ether): a potential penetration enhancer 2015. p. 195-205.
81. Sullivan DW, Gad SC, Julien M. A review of the nonclinical safety of Transcutol®, a highly purified form of diethylene glycol monoethyl ether (DEGEE) used as a pharmaceutical excipient. Food and Chemical Toxicology. 2014;72:40-50.
82. National Center for Biotechnology Information. PubChem Compound Summary for CID 8146, Diethylene glycol monoethyl ether [Internet]. 2026 [cited 2026 Jun 4]. Available from: https://pubchem.ncbi.nlm.nih.gov/compound/Diethylene-Glycol-Monoethyl-Ether
83. Gattefossé. Transcutol® P [Brochure on the internet]. 2021 [cited 2026 August 6]. Available from: https://www.pharmaexcipients.com/wp-content/uploads/2021/01/Transcutol-P-Brochure.pdf
84. Kumari S, Chauhan S, Singh K, Umar A, Fouad H, Alissawi MS, et al. Volumetric, compressibility and viscometric approach to study the interactional behaviour of sodium cholate and sodium deoxycholate in aqueous glycyl glycine. Molecules. 2022;27(24):8998.
85. Perinelli DR, Cespi M, Lorusso N, Palmieri GF, Bonacucina G, Blasi P. Surfactant self-assembling and critical micelle concentration: one approach fits all? Langmuir. 2020;36(21):5745-53.
86. Wang L, Liu S, Xin X, Cao X, Yuan D, Liu X, et al. Mixed micelles formed by biological surfactant sodium deoxycholate and nonionic surfactants in aqueous solution. J Dispersion Sci Technol. 2020;41(3):330-7.
87. Merck S-A. Safety data sheet: sodium deoxycholate (SRE0046) [Internet]. 2025 [cited 2026 May 8]. Available from: https://www.sigmaaldrich.com/PT/en/sds/sigma/sre0046
88. Sigma-Aldrich. Sodium deoxycholate [Internet]. Sigma-Aldrich; [cited 2026 May 8]. Available from: https://www.sigmaaldrich.com/PT/en/product/mm/106504?mmredirect=1
89. National Center for Biotechnology Information. PubChem Compound Summary for CID 23668196, sodium deoxycholate [Internet]. 2026 [cited 2026 May 9]. Available from: https://pubchem.ncbi.nlm.nih.gov/compound/Sodium-deoxycholate
90. Wang Z, Wu T, Zhou W, Wei X, Zhao J. Surface properties and micellar molecular interaction in binary systems of a biosurfactant sodium deoxycholate (NaDC) with conventional surfactants. J Surfactants Deterg. 2011;14(3):391-400.

91. Palrasu M, Wright L, Patel M, Leech L, Branch S, Harrelson S, et al. Perspectives on challenges in cannabis drug delivery systems: where are we? Med Cannabis Cannabinoids. 2022;5(1):102-19.
92. Durán-Lobato M, Martín-Banderas L, Gonçalves LMD, Fernández-Arévalo M, Almeida AJ. Comparative study of chitosan- and PEG-coated lipid and PLGA nanoparticles as oral delivery systems for cannabinoids. J Nanopart Res. 2015;17:1-17.
93. Zhang Z, Tan S, Feng S-S. Vitamin E TPGS as a molecular biomaterial for drug delivery. Biomaterials. 2012;33(19):4889-906.
94. Yang C, Wu T, Qi Y, Zhang Z. Recent advances in the application of vitamin E TPGS for drug delivery. Theranostics. 2018;8(2):464-85.
95. Abu-Fayyad A, Kamal MM, Carroll JL, Dragoi A-M, Cody R, Cardelli J, et al. Development and in-vitro characterization of nanoemulsions loaded with paclitaxel/γ-tocotrienol lipid conjugates. Int J Pharm. 2018;536(1):146-57.
96. Kumbhar PS, Nadaf S, Manjappa AS, Jha NK, Shinde SS, Chopade SS, et al. D-α-tocopheryl polyethylene glycol succinate: a review of multifarious applications in nanomedicines. OpenNano. 2022;6:100036.
97. Mehata AK, Setia A, Vikas, Malik AK, Hassani R, Dailah HG, et al. Vitamin E TPGS-based nanomedicine, nanotheranostics, and targeted drug delivery: past, present, and future. Pharmaceutics. 2023;15(3):875.
98. Guo Y, Luo J, Tan S, Otieno BO, Zhang Z. The applications of Vitamin E TPGS in drug delivery. Eur J Pharm Sci. 2013;49(2):175-86.
99. Choukaife H, Doolaanea AA, Alfatama M. Alginate nanoformulation: influence of process and selected variables. Pharmaceuticals (Basel). 2020;13(11):300.
100. Merck (Sigma-Aldrich). Sodium alginate [Internet]. [cited 2026 May 11]. Available from: https://www.sigmaaldrich.com/PT/en/product/aldrich/w201502
101. American Chemical Society. Sodium alginate [Internet]. 2026 [cited 2026 May 12]. Available from: https://www.acs.org/molecule-of-the-week/archive/s/sodium-alginate.html
102. Frent OD, Vicas LG, Duteanu N, Morgovan CM, Jurca T, Pallag A, et al. Sodium alginate-natural microencapsulation material of polymeric microparticles. Int J Mol Sci. 2022;23(20):12108.
103. National Center for Biotechnology Information. Sodium alginate [Internet]. Bethesda (MD): National Library of Medicine (US); [cited 2026 May 15]. Available from: https://pubchem.ncbi.nlm.nih.gov/compound/Sodium-Alginate#section=Names-and-Identifiers

104. Balenzano G, Racaniello GF, Spennacchio A, Lopalco A, Iacobazzi RM, Lopedota AA, et al. Harnessing therapeutic deep eutectic solvents in self-emulsifying systems to improve CBD delivery. Int J Pharm. 2024;659:124267.
105. Sakho EHM, Allahyari E, Oluwafemi OS, Thomas S, Kalarikkal N Chapter 2 - Dynamic light scattering (DLS). In: Thomas S, Thomas R, Zachariah AK, Mishra RK, editors. Thermal and rheological measurement techniques for nanomaterials characterization. Elsevier; 2017. p. 37-49.
106. Stetefeld J, McKenna SA, Patel TR. Dynamic light scattering: a practical guide and applications in biomedical sciences. Biophys Rev. 2016;8(4):409-27.
107. Cho EJ, Holback H, Liu KC, Abouelmagd SA, Park J, Yeo Y. Nanoparticle characterization: state of the art, challenges, and emerging technologies. Mol Pharm. 2013;10(6):2093-110.
108. Bhattacharjee S. DLS and zeta potential – what they are and what they are not? J Control Release. 2016;235:337-51.
109. Clogston JD, Patri AK. Zeta potential measurement. In: McNeil SE, editor. Characterization of nanoparticles intended for drug delivery. Totowa (NJ): Humana Press; 2011. p. 63-70.
110. Winey M, Meehl JB, O'Toole ET, Giddings TH, Jr. Conventional transmission electron microscopy. Mol Biol Cell. 2014;25(3):319-23.
111. Eskandari M, Gostariani R, Asadi Asadabad M. Transmission electron microscopy of nanomaterials. In: Singh D, Condurache-Bota S, editors. Electron crystallography. London: IntechOpen; 2020.
112. Malatesta M. Transmission electron microscopy for nanomedicine: novel applications for long-established techniques. Eur J Histochem. 2016;60(4):2751.
113. Malatesta M. Transmission electron microscopy as a powerful tool to investigate the interaction of nanoparticles with subcellular structures. Int J Mol Sci. 2021;22(23):12858.
114. Fathi F, Ebrahimi SN, Salehi P, Safari A, Shahsavari Z, Hadian J, et al. Antimicrobial multi-component lipid-based nanoemulsion of Eucalyptus globulus and Mentha piperita as natural preservative. J Dispersion Sci Technol. 2023;44(8):1423-32.
115. Yordanov Y, Stefanova D, Spassova I, Kovacheva D, Tzankova V, Konstantinov S, et al. Formulation of nanomicelles loaded with cannabidiol as a platform for neuroprotective therapy. Pharmaceutics. 2022;14(12):2615.
116. Ghasemi M, Turnbull T, Sebastian S, Kempson I. The MTT assay: utility, limitations, pitfalls, and interpretation in bulk and single-cell analysis. Int J Mol Sci. 2021;22(23):13027.
117. Van Meerloo J, Kaspers G, Cloos J. Cell sensitivity assays: the MTT assay. Methods Mol Biol. 2011;731:237-45.

118. Jannin V, Musakhanian J, Marchaud D. Approaches for the development of solid and semi-solid lipid-based formulations. Adv Drug Deliv Rev. 2008;60(6):734-46.
119. Pouton CW, Porter CJH. Formulation of lipid-based delivery systems for oral administration: materials, methods and strategies. Adv Drug Deliv Rev. 2008;60(6):625-37.
120. Pavlović N, Goločorbin-Kon S, Đanić M, Stanimirov B, Al-Salami H, Stankov K, et al. Bile acids and their derivatives as potential modifiers of drug release and pharmacokinetic profiles. Front Pharmacol. 2018;9:1283.
121. Madenci D, Egelhaaf SU. Self-assembly in aqueous bile salt solutions. Curr Opin Colloid Interface Sci. 2010;15(1):109-15.
122. Prajapati V, Ghosh AK, Ray D, Aswal VK, Kuperkar KC, Bahadur P. Understanding molecular-level interactions between the Soluplus-bile salts mixed micellar system. J Phys Chem B. 2025;129(41):10914-27.
123. Lopez F, Samseth J, Mortensen K, Rosenqvist E, Rouch J. Micro- and macrostructural studies of sodium deoxycholate micellar complexes in aqueous solutions. Langmuir. 1996;12(26):6188-96.
124. Patel V, Bharatiya B, Ray D, Aswal VK, Bahadur P. Investigations on microstructural changes in pH responsive mixed micelles of Triton X-100 and bile salt. J Colloid Interface Sci. 2015;441:106-12.
125. Cárdenas-Noriega KA, Elizondo-Luévano JH, Chávez-Montes A, Rodríguez-Tovar LE, Franco-Molina MA, Zárate-Triviño DG, et al. Nanoencapsulated cannabidiol-cannabigerol using Eudragit L100: in vitro and in vivo evidence in murine colitis model. Drugs Drug Candidates. 2026;5(1):10.
126. Danaei M, Dehghankhold M, Ataei S, Hasanzadeh Davarani F, Javanmard R, Dokhani A, et al. Impact of particle size and polydispersity index on the clinical applications of lipidic nanocarrier systems. Pharmaceutics. 2018;10(2):57.
127. Ow V, Lin Q, Wong JHM, Sim B, Tan YL, Leow Y, et al. Understanding the interplay between pH and charges for theranostic nanomaterials. Nanoscale. 2025;17(12):6960-80.
128. Choi SJ, McClements DJ. Nanoemulsions as delivery systems for lipophilic nutraceuticals: strategies for improving their formulation, stability, functionality and bioavailability. Food Sci Biotechnol. 2020;29(2):149-68.
129. Kulig D, Zimoch-Korzycka A, Jarmoluk A, Marycz K. Study on alginate-chitosan complex formed with different polymers ratio. Polymers. 2016;8(5):167.
130. Niculescu AG, Grumezescu AM. Applications of chitosan-alginate-based nanoparticles: an up-to-date review. Nanomaterials (Basel). 2022;12(2):289.
131. Constantinides PP. Lipid microemulsions for improving drug dissolution and oral absorption: physical and biopharmaceutical aspects. Pharm Res. 1995;12(11):1561-72.

132. Kawakami K, Yoshikawa T, Moroto Y, Kanaoka E, Takahashi K, Nishihara Y, et al. Microemulsion formulation for enhanced absorption of poorly soluble drugs: I. Prescription design. J Control Release. 2002;81(1):65-74.
133. Klein S. The use of biorelevant dissolution media to forecast the in vivo performance of a drug. AAPS J. 2010;12(3):397-406.
134. Pouton CW. Formulation of self-emulsifying drug delivery systems. Adv Drug Deliv Rev. 1997;25(1):47-58.
135. Mota WS, Severino P, Kadian V, Rao R, Zielińska A, Silva AM, et al. Nanometrology: particle sizing and influence on the toxicological profile. Front Nanotechnol. 2025;7:1479464.
136. Taha IE, ElSohly MA, Radwan MM, Elkanayati RM, Wanas A, Joshi PH, et al. Enhancement of cannabidiol oral bioavailability through the development of nanostructured lipid carriers: In vitro and in vivo evaluation studies. Drug Deliv Transl Res. 2025;15(8):2722-32.
137. Alhadid A, Luca SV, Nasrallah S, Minceva M. Experimental investigation and thermodynamic modeling of cannabidiol solubility in plant oils and hydrophobic eutectic systems. J Mol Liq. 2023;372:121172.
138. Rapoport N. Ultrasound-mediated micellar drug delivery. Int J Hyperthermia. 2012;28(4):374-85.
139. Kulthe SS, Choudhari YM, Inamdar NN, Mourya V. Polymeric micelles: authoritative aspects for drug delivery. Des Monomers Polym. 2012;15(5):465-521.
140. Montes-de-Oca-Saucedo CR, Perales-Martínez JE, Arellano-Barrientos JC, Rodríguez-Tovar LE, Nevárez-Garza AM, Garza-Arredondo AJ, et al. Targeting human cancer cells with cannabidiol (CBD): apoptotic cytotoxicity in HeLa, MDA-MB-231, and Caco-2 lines. Int J Mol Sci. 2025;26(24):12136.
141. Silva AM, Martins-Gomes C, Coutinho TE, Fangueiro JF, Sanchez-Lopez E, Pashirova TN, et al. Soft cationic nanoparticles for drug delivery: production and cytotoxicity of solid lipid nanoparticles (SLNs). Appl Sci. 2019;9(20):4438.
142. Mattson MP. Hormesis defined. Ageing Res Rev. 2008;7(1):1-7.